Investigation of patients diagnosed with *mut* methylmalonic aciduria

by

Jordan Chu

Department of Human Genetics

McGill University

Montreal. Quebec Canada

December 2016

A thesis submitted to McGill University in partial fulfillment of the requirements of the degree

of

Masters of Science

Abstract

Methylmalonic aciduria is caused by mutations affecting the mitochondrial enzyme methylmalonyl-CoA mutase, the synthesis of its cofactor, adenosylcobalamin, and certain other steps in propionyl-CoA metabolism. Biallelic mutations in the *MUT* gene, which encodes methylmalonyl-CoA mutase, are responsible for the *mut* form of methylmalonic aciduria. Patients with this disorder present symptoms of metabolic acidosis, failure to thrive, recurrent vomiting, hypotonia, lethargy, and dehydration in the newborn period. Nearly 330 *MUT* gene mutations are known to cause *mut* methylmalonic aciduria. In this study, a next generation sequencing based gene panel recently developed at Baylor Miraca Genetics Laboratories was used to analyze 53 patients that had been diagnosed with *mut* methylmalonic aciduria by somatic cell complementation analysis. A total of 54 different mutations in *MUT* were identified in 48 of 53 (91%) patients. Of these, 16 mutations were novel, including the largest insertion mutation in the *MUT* gene to date. Phenotypic rescue studies and analysis of cDNA were used to confirm that the large insertion was responsible for the MCM deficiency observed in the patient's fibroblasts. No *MUT* gene mutations were detected in 5 of 53 (9%) patients. Review of the cellular complementation data used to initially diagnosis these patients showed the results to be equivocal, putting the initial *mut* diagnosis into question. One patient was found to carry two novel mutations in the *SUCLG1* gene which are likely responsible for the patient's phenotype. Another patient was found to carry a novel heterozygous variant in *SUCLG2*. Deficiency of *SUCLG2* was investigated in cells from this patient as a novel cause of human disease. In conclusion, combination of gene panel analysis and somatic cell studies provided optimal diagnoses for this cohort of patients.

Résume

L'acidurie méthylmalonique est causée par des mutations affectant l'enzyme mitochondriale méthylmalonyl-CoA mutase, la synthèse de son cofacteur, l'adénosylcobalamine, et certaines autres étapes du métabolisme du propionyl-CoA. Les mutations biallélіques dans le gène *MUT*, qui code pour la méthylmalonyl-CoA mutase, sont responsables de la forme *mut* de l'acidurie méthylmalonique. Les patients avec cette maladie présentent des symptômes d'acidose métabolique, d'échec de croissance, de vomissements récurrents, d'hypotonie, de léthargie, et de déshydratation au cours de la période néonatale. Près de 330 mutations du gène *MUT* sont connu de provoquer l'acidurie méthylmalonique *mut*. Dans cette étude, un panel de gènes basé sur le séquençage de la prochaine génération récemment développé chez Baylor Miraca Genetics Laboratories, a été utilisé pour analyser 53 patients qui avaient été diagnostiqués avec l'acidurie méthylmalonique *mut* par l'analyse de complémentation de cellules somatiques. En total, 54 mutations différentes ont été identifiées en 48 des 53 patients (91%). Parmi ceux-ci, 16 mutations étaient nouvelles, y compris la plus grande mutation d'insertion dans le gène *MUT* à jour. Le sauvetage phénotypique et l'analyse de l'ADNc ont été utilisés pour confirmer que l'insertion majeure était responsable de la carence en MCM observée dans les fibroblastes du patient. Aucune mutation du gène *MUT* n'a été détectée chez 5 des 53 patients (9%). Un réexamen des données de complémentation cellulaire utilisées pour diagnostiquer initialement ces patients a montré que les résultats étaient équivoques, remettant en cause le diagnostic initial. Un patient s'est avéré porter deux nouvelles mutations dans le gène *SUCLG1* qui sont probablement responsables du phénotype du patient. Un autre patient a été trouvé à porter un nouveau variant hétérozygote dans *SUCLG2*. La carence en *SUCLG2* a été étudiée dans les cellules de ce patient comme une nouvelle cause de maladie humaine. En conclusion, la combinaison de l'analyse d'un

panel de gènes et des études de cellules somatiques a fourni des diagnostics optimaux pour cette cohorte de patients.

Table of Contents

List of Figures

List of Tables

List of Abbreviations

µg: microgram
µmol: micromole
ABCC1: ATP-binding cassette subfamily C member 1
ABCD4: ATP-binding cassette subfamily D member 4
aCGH: microarray-based genomic hybridization
AdoCbl: adenosylcobalamin
ADP: adenosine diphosphate
AMN: amnionless
ATP: adenosine triphosphate
ATR: cobalamin adenosyltransferase
bp: basepair
CD320: transcobalamin receptor
cDNA: complementary DNA
ChIP-Seq: chromatin immunoprecipitation sequencing
CLYBL: citrate lyase beta-like protein
cm: centimeter
CNCbl: cyanocobalamin
CNV: copy number variant
CoA: coenzyme A
Cob(I)alamin: oxidation state of Co atom in cobalamin is +1
Cob(II)alamin: oxidation state of Co atom in cobalamin is +2
CRF: chronic renal failure
CRM: cross-reacting material
CUBN: cubilin
DNA: deoxyribonucleic acid
EMEM: Eagle's minimum essential medium
ExAc: Exome Aggregation Consortium Database
FUT2: fucosyltransferase-2
g: gram
GDP: guanosine diphosphate
GTP: guanosine triphosphate
hr: hour
HC: haptocorrin
HCFC1: host cell factor 1
holoTC: holotranscobalamin
hTert: human telomerase
HRP: horseradish peroxidase
IF: intrinsic factor

IGS: Imerslund-Gräsbeck Syndrome
kb: kilobase
L: litre
LMBD1: methylmalonic aciduria and homocystinuria *cblF* type protein
MCEE: methylmalonyl-CoA epimerase
MCM: methylmalonyl-CoA mutase
MeCbl: methylcobalamin
mg: milligram
mL: millilitre
mm: millimeter
mM: millimolar
MMA: isolated methylmalonic aciduria
MMACHC: methylmalonic aciduria and homocystinuria *cblC* type protein
MMADHC: methylmalonic aciduria and homocystinuria *cblD* type protein
mRNA: messenger RNA
MS: methionine synthase
MSR: methionine synthase reductase
mtDNA: mitochondrial DNA
N: normal
NDPK: nucleoside diphosphate kinase
NGS: next generation sequencing
nmol: nanomole
PA: propionic acidemia
PBS: phosphate buffered saline
PCC: propionyl-CoA carboxylase
PCR: polymerase chain reaction
*ps*MCM: *Propionibacterium shermanii* methylmalonyl-CoA mutase
PVDF: polyvinylidine fluoride
RNA: ribonucleic acid
RNAi: RNA interference
RT-PCR: reverse transcription polymerase chain reaction
SD: standard deviation
SDS-PAGE: sodium dodecyl sulphate polyacrylamide gel electrophoresis
SIFT: sorting intolerant from tolerant
SNP: single-nucleotide polymorphism
SUCL: succinyl-CoA synthetase
SUCLA2: succinyl-CoA synthetase ADP-forming beta subunit
SUCLG1: succinyl-CoA synthetase alpha subunit
SUCLG2: succinyl-CoA synthetase GDP-forming beta subunit
TC: transcobalamin

TCA: trichloroacetic acid
THAP11: THAP domain containing 11
UTR: untranslated region
ZNF143: zinc finger protein 143

Acknowledgements

Above all else, I would like to thank my supervisor, Dr. David Rosenblatt, for his endless support, encouragement, and advice over the past two and a half years. His kindness and sense of humor have made my experience as a graduate student an absolute pleasure. It has truly been an honor to learn from him and his generosity as a mentor will not be forgotten.

I would also like to thank Dr. David Watkins for his company and friendship throughout my time in the lab. His help and insight have been invaluable over the past two and a half years.

I would like to thank my supervisory committee, namely Drs. Pierre Moffatt and Eric Shoubridge, for their time and advice. Their feedback during my graduate studies has been greatly appreciated.

I would like to thank Gail Dunbar for teaching me everything there is to know about cell culture. I also want to thank Leah Ladores and Keo Phommarihn for providing the many cell lines.

This work would not have been possible without our collaborators at Baylor College of Medicine, namely Dr. Xia Tian, Dr. Yanming Feng, Stella Chen, Remington Fenter, Dr. Victor W. Zhang, Dr. Jing Wang, and Dr. Lee-Jun Wong. I also want to thank all of the families for their contributions to the study, as well as the referring physicians for providing clinical information.

I would like to thank all of my lab-mates that I have had the pleasure of working alongside over the past two and a half years. I want to thank Wayne Mah and, especially, Mihaela Pupavac, for showing me the ropes and for being fantastic company in the lab. I also want to thank Zvi Cramer, Lina Sobhy Abdrabo, Courtney Ells, Armin Changizi, and everyone else who passed through the lab for making the past two and a half years such a wonderful experience.

I want to thank all of my family: Mom, Dad, Michael, Wincy, and everyone else for all of their encouragement, support, and love. I wouldn't be where I am today if it wasn't for you.

And finally, I want to express my appreciation for my girlfriend Lauren for loving and motivating me, and for constantly making life easier and happier.

CHAPTER 1

Introduction to cobalamin and propionyl-CoA metabolism

1.0 Introduction

The aim of the thesis presented herein is to investigate patients who have been diagnosed with *mut* methylmalonic aciduria by somatic cell complementation analysis. Methylmalonic aciduria (MMA) can be caused by genetic defects affecting either the absorption and metabolism of cobalamin or the processing of propionyl-CoA into the Krebs cycle. Accordingly, in order to address the many different causes of MMA, the introduction chapter will discuss both the inborn errors of cobalamin metabolism and absorption as well as inherited disorders affecting propionyl-CoA metabolism.

1.1. Cobalamin structure

Cobalamin (vitamin B_{12}) is a structurally complex water-soluble compound that is essential in human beings for intermediary cellular metabolism. The vitamin consists of a planar corrin ring bound to a central cobalt atom. Four of the 6 coordination sites are provided by the corrin ring (Figure 1). A fifth coordination site is provided by a 5,6-dimethylbenzamidizole base in the lower axial position that is also covalently bound to the corrin ring. Depending on whether or not the 5,6-dimethylbenzamidizole base is bound to the central cobalt atom, cobalamin can be in either a “base-on” or “base-off” configuration. Multiple different compounds may afford the sixth coordination site in the upper axial position. In cyanocobalamin (CNCbl), the synthetic form of cobalamin used pharmaceutically, a cyanide group occupies this position. A hydroxyl

group occupies this coordination site in hydroxocobalamin, the natural form of cobalamin produced by bacteria. The upper-axial ligand also distinguishes 5'-deoxyadenosylcobalamin (AdoCbl) and methylcobalamin (MeCbl), the two cobalamin derivatives that are active in human metabolism.

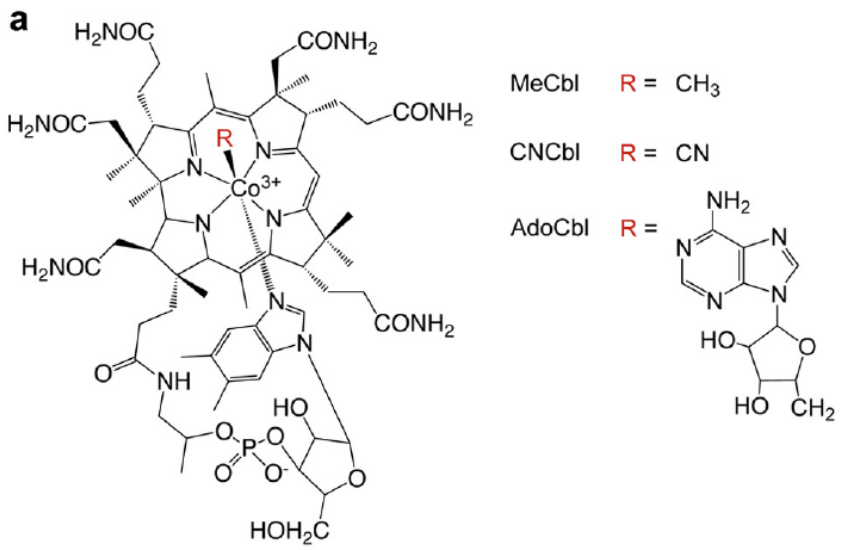

Figure 1. Cobalamin structure (from Gherasim et al. 2013b). This research was originally published in the Journal of Biological Chemistry. Gherasim et al. Navigating the B_{12} Road: Assimilation, Delivery, and Disorders of Cobalamin. Journal of Biological Chemistry. 2013; 288:13186-93. © the American Society for Biochemistry and Molecular Biology. Cobalamin consists of a planar corrin ring bound to a central cobalt atom. Multiple different compounds (R-groups), which distinguish the different derivatives of cobalamin, can bind to the central cobalt.

1.2. Cobalamin biosynthesis

De novo biosynthesis of cobalamin is a highly complex reaction that requires approximately 30 enzymes and is seen only in certain bacteria and archaea (Warren et al. 2002). There are two known pathways for the synthesis of cobalamin: the anaerobic pathway and the aerobic pathway. The anaerobic route does not require oxygen and is characterized by the insertion of the cobalt atom early in synthesis (Frank et al. 2005). On the contrary, the aerobic route requires oxygen and chelation of cobalt into the corrin ring occurs late in the pathway (Heldt et al. 2005).

1.3. Dietary cobalamin requirement

Cobalamin is synthesized by certain bacteria and migrates up the food chain where it is absorbed into the tissue of higher predatory animals (Watanabe 2007). As human beings cannot synthesize cobalamin, they must acquire the vitamin from dietary sources to maintain normal cellular function. Food products of animal origin, such as meat and dairy, are considered to be the primary dietary source of cobalamin. The recommended daily intake of cobalamin for adults is 2.4µg, increasing to 2.6µg during pregnancy and 2.8µg for breastfeeding females (Institute of Medicine (US) Standing Committee on the Scientific Evaluation of Dietary Reference Intakes and its Panel on Folate, Other B Vitamins 1998). As it is assumed that only 50% of cobalamin is absorbed into the body, this recommendation ensures absorption of 1µg per day (Stabler and Allen 2004).

1.4. Dietary cobalamin deficiency

Dietary cobalamin deficiency is a common worldwide phenomenon and is especially prevalent in vegetarians and elderly people. Though the symptoms of deficiency are subtle, an adequate level of cobalamin intake is necessary to prevent megaloblastic anemia and neurological damage (O'Leary and Samman 2010). Additionally, cobalamin deficiency is associated with hyperhomocysteinemia which may put people at greater risk for vascular disease and cognitive impairment (Selhub 2008). Breast-fed infants of cobalamin-deficient mothers are at risk for severe clinical manifestations including MMA, developmental abnormalities, hypotonia, failure to thrive, and anemia (Stabler and Allen 2004; Guez et al. 2012). Treatment with intramuscular cobalamin results in a rapid reversal of symptoms in most deficient infants. However, if diagnosis and treatment is delayed, impaired brain development can lead to permanent developmental abnormalities (Dror and Allen 2008).

1.5. Cobalamin Function

All human cells require derivatives of cobalamin for two intracellular reactions. MeCbl is a cofactor for the cytoplasmic enzyme methionine synthase (MS) which is involved in methionine biosynthesis. MS catalyzes the methyl transfer from methyltetrahydrofolate to homocysteine to form methionine and tetrahydrofolate in a process that uses MeCbl as an intermediate carrier. AdoCbl is a cofactor for the mitochondrial enzyme methylmalonyl-CoA mutase (MCM) which is responsible for isomerizing L-methylmalonyl-CoA to succinyl-CoA, a key reaction in propionyl-CoA metabolism.

1.6. Cobalamin absorption and metabolism

1.6.1. Cobalamin absorption

The process of cobalamin absorption is a selective series of events that involves several different proteins (Figure 2). Cobalamin is bound to protein in food and must be released from these proteins to be absorbed. Pepsin and hydrochloric acid secreted by the gastric mucosa facilitate cleavage of these proteins from cobalamin. Free cobalamin is then able to bind haptocorrin (HC), a cobalamin-binding glycoprotein secreted by the salivary glands, and pass into the duodenum. Pancreatic proteases cleave HC into two or three fragments and cobalamin is released, allowing it to bind intrinsic factor (IF). IF has two different cobalamin-binding domains that cooperatively interact to bind cobalamin (Fedosov et al. 2005). Unlike HC which binds both cobalamin and compounds similar in structure to cobalamin, IF has high specificity for cobalamin and discriminates cobalamin analogues (Fedosov et al. 2007). It has been speculated that the high specificity of IF for cobalamin allows the selective absorption of true cobalamin, while the less-specific HC is able to sequester cobalamin analogues in the plasma and prevent them from associating with the cobalamin-dependent enzymes, MS and MCM (Wuerges et al. 2007).

The IF-cobalamin complex is absorbed in the distal ileum through endocytosis mediated by the specific receptor cubam. Cubam is a large complex that is comprised of the proteins amnionless (AMN) and cubilin (CUBN). CUBN, which has no transmembrane domains, is essential to the recognition and binding of the IF-cobalamin complex. AMN contains a single transmembrane domain that anchors cubam to the plasma membrane and is believed to direct internalization of the complex (Fyfe et al. 2004). IF is subsequently degraded by lysosomal enzymes and free cobalamin is exported across the basolateral membrane in a process that

appears to involve the ATP-binding cassette drug transporter ABCC1 (also known as multidrug resistance protein [MRP1]). *ABCC1*-knockout mice show accumulation of cobalamin in the distal intestine and decreased cobalamin concentrations in the liver, kidney, and plasma (Beedholm-Ebsen et al. 2010), supporting the notion that ABCC1 mediates cellular export of cobalamin into the blood. However, it is speculated that alternative cobalamin efflux processes are able to compensate for deficiencies in *ABCC1* as (1) these mice do not have any metabolic abnormalities, and (2) no cobalamin-deficient patients have been found to have mutations in *ABCC1* (Shah et al. 2011).

Absorbed cobalamin appears in circulation bound to cobalamin-binding proteins. Approximately 70 - 80% of cobalamin in circulation is bound to HC and unavailable for cellular uptake, with the exception of absorption into hepatocytes. For this reason, the validity of using total serum cobalamin as a measure of cobalamin status has been questioned. The remainder of circulating cobalamin is bound to transcobalamin (TC), which facilitates the delivery of cobalamin to tissues. Measurement of holotranscobalamin (holoTC) concentrations, the fraction of cobalamin bound to TC, appears to be a more reliable indicator of cobalamin status (Nexo et al. 2002; Refsum et al. 2006). Furthermore, assessment of both holoTC and TC concentrations can be used to determine saturation levels of TC, which may be a slightly better indicator of cobalamin status than holoTC concentrations alone (Bor et al. 2004).

There have been several genome-wide association studies investigating genetic factors that affect circulating cobalamin levels (Tanaka et al. 2009; Lin et al. 2012; Grarup et al. 2013). Significant associations have been identified in many of the genes known to be involved in cobalamin absorption and metabolism, including *MUT, CD320, ABCD4, MMAA, MMACHC, TCN2, CUBN,* and *TCN1* (Lin et al. 2012; Grarup et al. 2013). Surprisingly, the *FUT2* gene,

encoding fucosyltransferase-2, has been consistently found to have the most significant associations with cobalamin status (Lin et al. 2012; Grarup et al. 2013). The relationship between *FUT2* and serum cobalamin is discussed in section 1.9.1. Strong associations between the rs4128112 premature stop polymorphism in the *CLYBL* gene, encoding citrase lyase beta-like protein, and serum cobalamin levels have also been unexpectedly identified in multiple populations (Lin et al. 2012; Grarup et al. 2013). The *CLYBL* gene product has no obvious mechanistic link to cobalamin status, but has been found to synthesize malate from glyoxylate and acetyl-CoA and β-methylmalate from glyoxylate and propionyl-CoA (Strittmatter et al. 2014). The rs4128112 polymorphism results in a truncated *CLYBL* transcript that escapes nonsense-mediated decay (Grarup et al. 2013) and individuals with this polymorphism exhibit reduced levels of circulating cobalamin (Lin et al. 2012). Men homozygous for this polymorphism have 3-fold reduced levels of circulating cobalamin while heterozygotes present with an intermediate phenotype (Lin et al. 2012). More research is needed to elucidate the role of the *CLYBL* gene product in maintaining homeostasis of circulating cobalamin.

1.6.2. Cellular cobalamin uptake

Cellular uptake of TC-bound cobalamin from the plasma involves the transmembrane protein CD320. Endocytosis of the TC-cobalamin complex results in the complex being released into the cell in a clathrin-coated vesicle (Takahashi et al. 1980). Intracellular concentrations of cobalamin are regulated by modulating expression levels of CD320 at the plasma membrane in a cell-cycle dependent manner. Expression and activity of CD320 is highest in actively-dividing cells and lowest in quiescent cells (Hall et al. 1987). It has been suggested that the physiological purpose of this regulatory process is to meet the increased cobalamin requirement of DNA synthesis in proliferating cells (Quadros 2010). Other receptors involved in cellular uptake of

cobalamin have been described in the liver and kidney. HC-bound cobalamin can be taken up by hepatocytes via the asialoglycoprotein receptor (Burger et al. 1975), but the physiological relevance of this phenomenon is not fully understood. Megalin, a TC-cobalamin receptor found on the apical membrane of kidney proximal tubule cells, facilitates reabsorption of filtered cobalamin and prevents urinary loss of the vitamin (Moestrup et al. 1996).

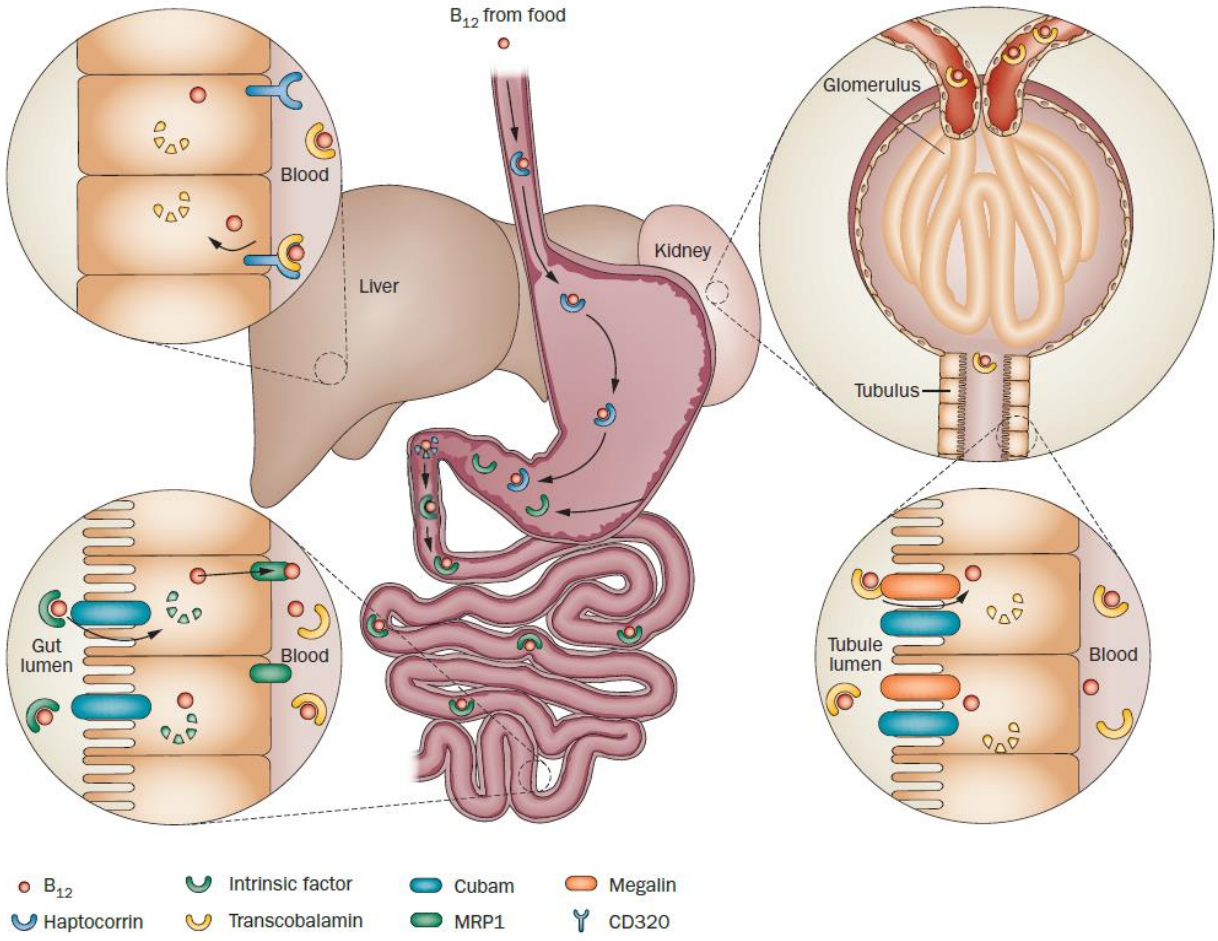

Figure 2. Cobalamin absorption (adapted from Nielsen et al. 2012 with permission). Cobalamin is freed from proteins in food by pepsin secreted by the gastric mucosa. Free cobalamin is then able to bind haptocorrin and pass into the duodenum, where pancreatic proteases release cobalamin from haptocorrin. Cobalamin subsequently binds intrinsic factor and

is absorbed in the distal ileum through endocytosis mediated by the receptor cubam. Inside the cell, cobalamin is released from intrinsic factor by lysosomal enzymes and free cobalamin is exported across the basolateral membrane through a process involving ABCC1 (also known as multidrug resistance protein [MRP1]). Cobalamin associates with transcobalamin in the blood which facilitates cellular uptake of cobalamin. Cellular absorption of the cobalamin-transcobalamin complex is mediated by transcobalamin receptor (CD320) in most human tissue. Megalin, a receptor on the apical membrane of proximal tubule cells, facilitates reabsorption of cobalamin from glomerular filtrate.

1.6.3. Cellular cobalamin metabolism

Various enzymes are involved in intracellular processing of cobalamin (Figure 3). Once internalized, the TC-cobalamin-CD320 complex is transported to the lysosomes where resident hydrolases release cobalamin from the complex and CD320 is recycled back to the plasma membrane. Two lysosomal membrane proteins, LMBD1 (LMBR1 domain containing 1) and ABCD4 (ATP-binding cassette subfamily D member 4), are required for cobalamin to be transported out of the lysosome and into the cytosol (Rutsch et al. 2009; Coelho et al. 2012). The precise role that LMBD1 and ABCD4 each play in the lysosomal export of cobalamin is unclear. Functional studies have demonstrated that cells deficient in LMBD1 and ABCD4 exhibit similar phenotypes and complement one another, suggesting that they act synergistically. It has recently been shown that ABCD4 interacts with LMBD1 at the endoplasmic reticulum (Kawaguchi et al. 2016). Furthermore, ABCD4 appears to be dependent on the lysosomal targeting sequence of LMBD1 to translocate to the lysosome. Knockout of the gene encoding LMBD1, *LMBRD1*, results in reduced expression of ABCD4 at the lysosomal membrane (Kawaguchi et al. 2016). Considering efflux of cobalamin from mammalian epithelial cells via ABCC1 and import of

cobalamin in bacteria via the ABC transporter BtuCD-F are both ATP-driven processes (Borths et al. 2005; Beedholm-Ebsen et al. 2010), it may be true that cobalamin transport from the lysosome to the cytosol is as well. Kawaguchi et al. 2016 postulate that the ATP-driven ABCD4 is the true cobalamin transporter and LMBD1 acts as a cofactor based on these observations.

Upon exiting the lysosome, cobalamin is processed into its coenzyme derivatives, AdoCbl and MeCbl. The MMACHC (methylmalonic aciduria and homocystinuria *cblC* type) protein interacts with cobalamins with various upper-axial ligands, converting them to a common intermediate that can be used for synthesis of AdoCbl and MeCbl. When bound to alkylcobalamins such as AdoCbl and MeCbl, MMACHC catalyzes a dealkylation reaction and when bound to CNCbl, MMACHC eliminates the cyanide group through a decyanation reaction (Hannibal et al. 2009). Recently, numerous transcription factors including THAP11 (THAP domain containing 11), HCFC1 (host cell factor 1), and ZNF143 (zinc finger protein 143) have been identified as modulators of *MMACHC* expression (Yu et al. 2013; Pupavac et al. 2016b). HCFC1 acts as a scaffold protein that facilitates the regulatory roles of the THAP11 and ZNF143 proteins (Michaud et al. 2013). Binding of the THAP11-HCFC1-ZNF143 complex to DNA appears to be directed by the ACTACA submotif shared by both ZNF143 and THAP11 (Vinckevicius et al. 2015). Chromatin immunoprecipitation sequencing (ChIP-Seq) studies in mouse embryonic stem cells have identified binding sites of the THAP11-HCFC1-ZNF143 complex near multiple genes involved in cobalamin metabolism including *ABCD4*, *MTR*, *SUCLG1*, and *MMACHC* (Dejosez et al. 2010). Mutations affecting the *HCFC1* and *ZNF143* genes have been shown to result in clinically-significant dysregulation of MMACHC protein levels (Yu et al. 2013; Pupavac et al. 2016b).

Distribution of cobalamin to either the mitochondria or the cytoplasm for synthesis of AdoCbl or MeCbl, respectively, is facilitated by the MMADHC (methylmalonic aciduria and homocystinuria *cblD* type) protein. Although MMADHC contains a predicted cobalamin-binding domain, the protein does not directly bind cobalamin. Instead, MMADHC forms a complex with MMACHC and likely assists in the delivery of cobalamin to downstream targets (Deme et al. 2012). Subcellular localization experiments have found that MMADHC localizes to both the cytoplasm and the mitochondria, consistent with the hypothesis that MMADHC modulates a branch point in cobalamin processing (Mah et al. 2013).

1.6.4. MeCbl synthesis

Cobalamin that stays in the cytoplasm for MeCbl synthesis is delivered to MS, though the precise roles of MMACHC and MMADHC in this process are not known. MS catalyzes a methyl transfer from methyltetrahydrofolate to homocysteine to form methionine and tetrahydrofolate in a two-step reaction. First, the methyl group from MeCbl is transferred to homocysteine, forming methionine and cob(I)alamin. Next, the methyl group from methyltetrahydrofolate is transferred to cob(I)alamin to re-form MeCbl and form tetrahydrofolate (Matthews et al. 2008). During this reaction, cob(I)alamin will occasionally be oxidized to its inactive cob(II)alamin form. Methionine synthase reductase, encoded by the *MTRR* gene, is essential to maintaining MS activity by reducing cob(II)alamin back to its active state (Leclerc et al. 1999).

1.6.5. AdoCbl synthesis

Two mitochondrial proteins, encoded by the *MMAA* and *MMAB* genes, are essential for synthesis of AdoCbl and its subsequent delivery to MCM. ATR-dependent cobalamin adenosyltransferase (ATR), encoded by the *MMAB* gene, is responsible for the generation of

AdoCbl from cob(II)alamin. Cob(II)alamin binds ATR in the "base-off" configuration, which favors reduction to the cob(I)alamin state by 100-fold compared to cob(II)alamin in the "base-on" configuration (Yamanishi et al. 2005). The ATR-coupled protein that catalyzes this reduction remains to be identified. ATR subsequently catalyzes adenosylation of cob(I)alamin to form AdoCbl. ATR is also directly involved in the transfer of AdoCbl to MCM in a process that is believed to be dependent on the *MMAA* gene product (Padovani et al. 2008). While the precise function of human MMAA is not known, studies on its bacterial ortholog, MeaB, suggest roles in chaperoning AdoCbl to MCM and protecting MCM from oxidative inactivation (Padovani and Banerjee 2006). It has also been hypothesized that MeaB functions to discriminate cob(II)alamin during docking of AdoCbl to MCM, thus promoting correct assembly of the MCM apoenzyme (Banerjee et al. 2009). MCM catalyzes the conversion of L-methylmalonyl-CoA to succinyl-CoA, an essential step in propionyl-CoA metabolism.

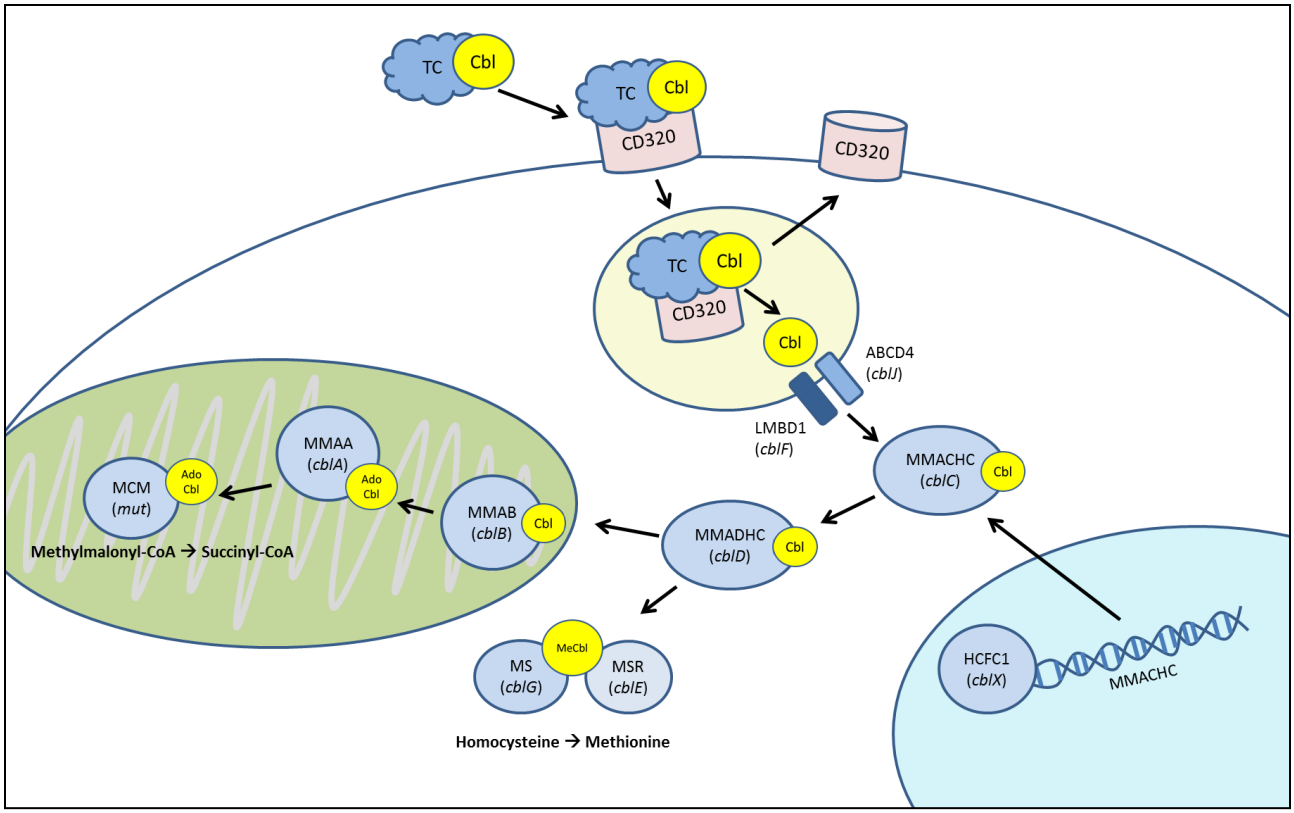

Figure 3. Intracellular processing of cobalamin. Cobalamin (Cbl) enters the cell bound to transcobalamin (TC) through endocytosis mediated by the transcobalamin receptor (CD320). Cobalamin then enters the lysosome where it dissociates from TC and exits into the cytoplasm via a process mediated by ABCD4 and LMBD1. MeCbl is required in the cytoplasm for the activity of MS, which synthesizes methionine from homocysteine. AdoCbl is required in the mitochondria for the activity of MCM, which catalyzes the isomerization of methylmalonyl-CoA to succinyl-CoA. The inborn errors are listed in brackets underneath the name of the underlying gene product.

1.7. Cobalamin-dependent propionyl-CoA metabolism

Propionyl-CoA is a common intermediate produced during the catabolism of certain branched-chain amino acids (isoleucine, threonine, and valine), methionine, odd-chain fatty acids, and cholesterol. In the cobalamin-dependent pathway of propionyl-CoA metabolism, propionyl-CoA is channeled into the Kreb's cycle intermediate succinyl-CoA through a process involving multiple nuclear-encoded mitochondrial enzymes (Figure 4). Propionyl-CoA carboxylase (PCC) is responsible for converting propionyl-CoA to D-methylmalonyl-CoA. PCC is a heterodimeric mitochondrial protein consisting of an α-subunit, encoded by the *PCCA* gene, and a β-subunit, encoded by the *PCCB* gene. Methylmalonyl-CoA epimerase (racemase) (MCEE) catalyzes the second enzymatic reaction in cobalamin-dependent propionyl-CoA metabolism. The *MCEE* gene was originally hypothesized to be involved in the propionyl-CoA metabolic pathway based upon the finding that *MCEE* and *MUT* reside in the same operon in prokaryotic genomes, suggesting that they function in a coordinated manner. Biochemical analyses confirmed this hypothesis, demonstrating that MCEE is involved in the interconversion of D- to L-methylmalonyl-CoA (Bobik and Rasche 2001). However, knockdown of *MCEE* by siRNA in HeLa cells led to only a mild reduction in propionyl-CoA metabolic activity, suggesting nonenzymatic conversion of D- to L-methylmalonyl-CoA may contribute to epimerization (Dobson et al. 2006). The L-isomer of methylmalonyl-CoA binds cobalamin-dependent MCM which catalyzes its rearrangement to succinyl-CoA. MCM is encoded by the *MUT* gene and will be discussed extensively in section 1.11.3.4. In the Krebs cycle, succinyl-CoA synthetase (SUCL) catalyzes the reversible synthesis of succinate from succinyl-CoA. The reverse reaction produces succinyl-CoA for heme synthesis and activation of ketone bodies. SUCL functions as a heterodimer consisting of an α-subunit encoded by *SUCLG1* and a β-

subunit encoded by either the ADP-forming *SUCLA2* gene or the GDP-forming *SUCLG2* gene (Johnson et al. 1998). Localization studies in human brains have identified exclusive expression of SUCLA2 in neurons in the cerebral cortex (Dobolyi et al. 2015b), while SUCLG2 appears to be expressed in the vasculature of the brain (Dobolyi et al. 2015a). Expression of both SUCLA2 and SUCLG2 was entirely absent in glial cells, suggesting the participation of alternate pathways such as the GABA shunt and ketone body metabolism in these cells (Dobolyi et al. 2015a).

1.8. Cobalamin-independent propionyl-CoA metabolism

Certain organisms that do not depend on cobalamin, such as plants and *Candida albicans*, utilize a β-oxidation-like pathway to prevent the toxic accumulation of propionyl-CoA (Otzen et al. 2014). Recently, a metabolic pathway involved in the degradation of propionyl-CoA that is not dependent on cobalamin has been characterized in *C. elegans* (Watson et al. 2016). It has been hypothesized that this alternate pathway provides *C. elegans* with the ability to metabolize propionyl-CoA in accordance with cobalamin availability. Watson et al. have shown that under conditions simulating dietary cobalamin deficiency, or in genetic conditions that mimic the disorders of propionyl-CoA metabolism, *C. elegans* respond to elevated levels of propionyl-CoA by transcriptional activation of a cobalamin-independent propionate shunt (Figure 4). Furthermore, they show that cobalamin transcriptionally represses the genes involved in this pathway (Watson et al. 2014). These findings suggest that *C. elegans* are able to adapt to cobalamin-depleted or cobalamin-rich conditions through metabolic rewiring of propionyl-CoA utilization.

Five genes in *C. elegans*, namely acyl-CoA dehydrogenase (*acdh-1*), enoyl-CoA hydratase 6 (*ech-6*), hydroxacyl-CoA hydrolase (F09F7.4 or *hach-1*), 3-hydroxypropionate-oxoacid transhydrogenase (Y38F1A.6 or *hphd-1*), and aldehyde dehydrogenase (*alh-8*), appear to be involved in cobalamin-independent metabolism of propionyl-CoA (Figure 4) (Watson et al. 2016). The acyl-CoA dehydrogenase *acdh-1* was determined to be a component of the alternate propionate pathway after it was found that a cross between Δ*pcca-1* (the *C. elegans* ortholog of human *PCCA*) and Δ*acdh-1* mutants produced no viable double homozygous knockout offspring. *Acdh-1* is believed to catalyze the first step in the alternate propionate pathway, converting propionyl-CoA into the highly reactive acrylyl-CoA. The human gene encoding short/branched-chain acyl-CoA dehydrogenase, *ACADSB,* is homologous to *C. elegans acdh-1*. Mutations in the human *ACADSB* gene are associated with acyl-CoA dehydrogenase deficiency, a disorder of isoleucine metabolism (Van Calcar et al. 2013).

A synthetic lethality screen in *C. elegans* found that RNA interference (RNAi) knockdowns of *ech-6, hach-1*, and *acdh-1* in Δ*ppc-1* mutants produced no viable offspring, suggesting that *ech-6* and *hach-1* may also be involved in the alternate pathway (Watson et al. 2016). Acrylyl-CoA is predicted to be the substrate of *ech-6* and knockdown of *ech-6*, and to a lesser degree *hach-1*, results in accumulation of acrylyl-CoA (or its derivative acrylate). Interestingly, recent metabolomics studies have shown that patients with mutations in *ECHS1* and *HIBCH*, the human homologs of *ech-6* and *hach-1*, have elevated levels of acrylyl-CoA (Peters et al. 2015).

Hphd-1 and *alh-8* have been suggested to catalyze the fourth and fifth reactions of the alternate propionate pathway in *C. elegans*, respectively (Watson et al. 2016). Both genes were identified with bioinformatics tools that integrate various datasets to predict functional metabolic

networks. The human ortholog of *hphd-1*, *ADHFE1,* is known to metabolize a structural analog of 3-hydroxypropionate (3-HP), β-hydroxybutyrate (Lyon et al. 2009). 3-HP is a known clinical biomarker of methylmalonic and propionic acidurias in newborns (Manoli et al. 1993) but the mechanism driving this association has not been previously characterized. The existence of an alternate propionate pathway in human beings, homologous to the one described in *C. elegans*, may explain this phenomenon. *Alh-8* is homologous to the human *ALDH6A1* (aldehyde dehydrogenase 6 family member A1) gene. *ALDH6A1* is known to decarboxylate methylmalonic semialdehyde (Marcadier et al. 2013), a metabolite that is similar in structure to malonic semialdehyde. In the fifth reaction of the alternate propionate pathway, malonic semialdehyde is converted to acetyl-CoA which can incorporate into the Krebs cycle. All five human homologs of the *C. elegans* alternate propionate pathway genes are co-expressed in mouse and human tissue (Watson et al. 2016). Furthermore, human liver carcinoma cells upregulate the *ADHFE1, HIBCH, ECHS1¸ and ALDH6A1* genes in response to propionate supplementation (Watson et al. 2016), adding support to the notion that a cobalamin-independent pathway of propionyl-CoA metabolism exists in humans. Further research is needed to evaluate the existence of a human cobalamin-independent pathway and, if it does exist, its significance in healthy and disease states. It is possible that inherited defects in the cobalamin-dependent pathway are partially compensated by upregulation of the cobalamin-independent pathway. This could explain why mutations affecting genes in the cobalamin-dependent pathway do not result in embryonic lethality. Furthermore, therapies that harness alternate metabolic pathways can be used to benefit patients with inborn errors of metabolism. For instance, sodium phenylbutyrate is used to treat children with inborn errors affecting the urea cycle (Batshaw et al. 2001). These compounds divert nitrogen from urea synthesis to alternate excretory pathways, preventing toxic

accumulation of ammonia and glutamine. It is possible that therapies enhancing the alternate propionyl-CoA metabolic pathway would be beneficial to patients with disorders affecting the conventional pathway, such as in propionic and methylmalonic acidurias.

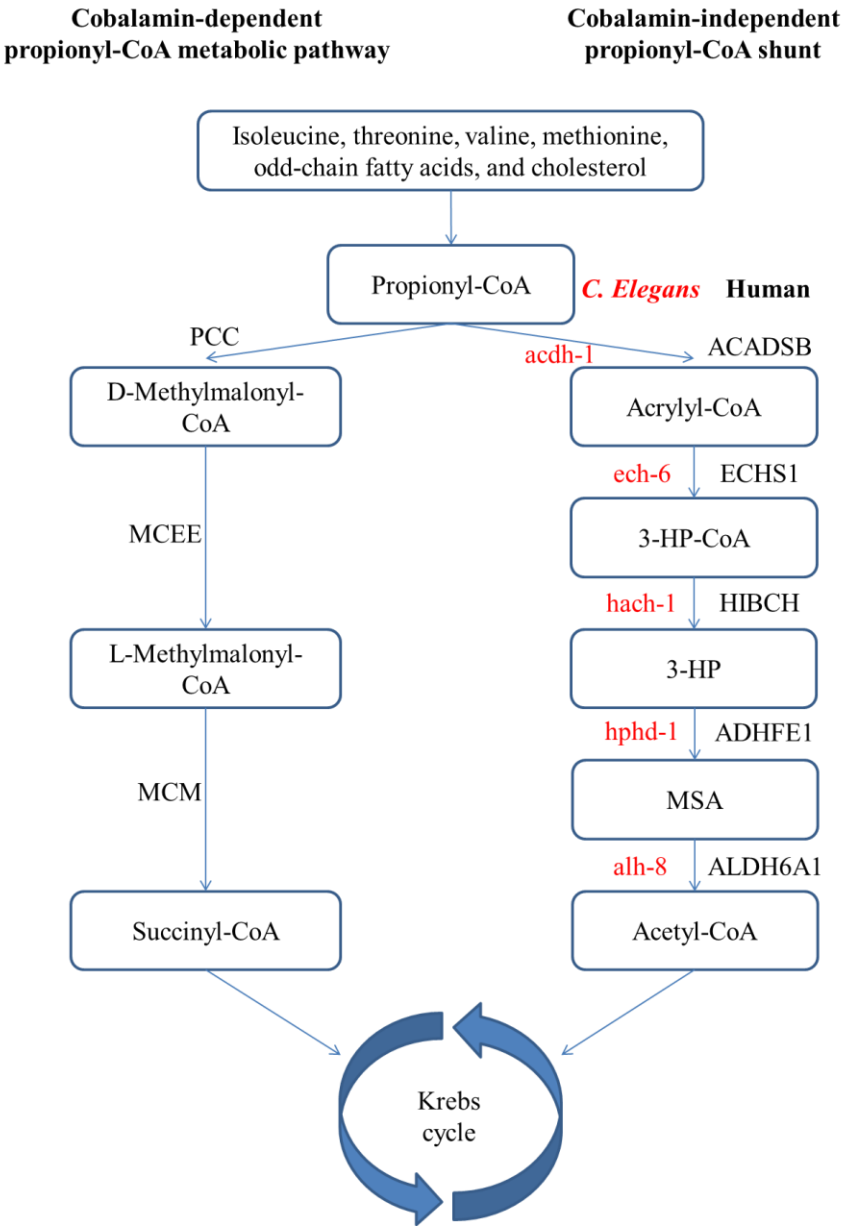

Figure 4. Propionyl-CoA metabolic pathways in *C. elegans* and humans. The known cobalamin-dependent propionyl-CoA metabolic pathway (left) in humans is mediated by the enzymes PCC, MCEE, and MCM. The cobalamin-independent shunt (red) proposed in *C. elegans* involves the genes *acdh-1, ech-6, hach-1, hphd-1,* and *alh-8*. The human orthologs of these genes are shown (right).

1.9. Inherited disorders of cobalamin absorption

1.9.1. Intrinsic factor deficiency

Inherited IF deficiency is an autosomal recessive disorder that is characterized by mutations in the IF-encoding gene, *GIF*. Pathogenic mutations may lead to increased susceptibility of IF to pepsin hydrolysis, low functional IF expression in gastric juice, or reduced affinity for the cubam receptor (Gordon et al. 2004). Patients with inherited IF deficiency have low serum cobalamin and typically present with pernicious anemia. Clinical manifestations of these patients may also include pancytopenia, peripheral neuropathy, splenomegaly, hepatomegaly, and early death (Ferrand et al. 2015). Symptoms often appear between ages 1 and 5 years, although onset in early adulthood has been reported (Carmel 1983). Gastric IF deficiency has also been observed in patients with single heterozygous mutations in *GIF* who carry the *FUT2* secretor variant (Chery et al. 2013). Individuals who are homozygous for the *FUT2* rs601338 polymorphism (p.W143*) have no secretion of H-type antigens (non-secretor variant), the precursor to histo-blood group antigens. Individuals who carry the 143W allele secrete H-type antigens (secretor variant) into body fluids, including the saliva and gastric mucosa. The allelic frequency of the rs601338 variant is 0.3894 and approximately 20% of Caucasians are homozygous for the *FUT2* non-secretor phenotype (Lek et al. 2016), which is strongly associated with high plasma cobalamin levels (Hazra et al. 2009; Lin et al. 2012). Cobalamin deficiency in patients with single heterozygous mutations in *GIF* who carry the *FUT2* secretor variant appears to be caused by impaired IF secretion from the parietal cells into the gastric juice (Chery et al. 2013), however the mechanism underlying this observation is incompletely understood.

1.9.2. Imerslund-Gräsbeck Syndrome

Imerslund-Gräsbeck Syndrome (IGS), also known as megaloblastic anemia 1, is caused by defects in the IF-cobalamin receptor, cubam, The two subunits of the cubam receptor are encoded by the *AMN* and *CUBN* genes and biallelic mutations in both of these genes have been implicated in IGS (Fyfe et al. 2004). Patients with this disorder have defective enterocyte absorption of cobalamin which leads to deficiency once fetal cobalamin storage in the liver is depleted. IGS is notably characterized by megaloblastic anemia and may also include neurological impairment and cobalamin-resistant proteinuria (Gräsbeck 2006). Proteinuria is found in approximately half of IGS patients and is believed to be a result of impaired renal reabsorption of proteins, including apolipoprotein A-I, albumin, and transferrin, through the cubam receptor (Kozyraki et al. 1999; Birn et al. 2000; Zhai et al. 2000). The lack of proteinuria in some patients can be explained by mutations exclusively affecting the IF-cobalamin binding ability of the cubam receptor (Kristiansen et al. 2000).

1.9.3. Haptocorrin Deficiency

HC deficiency is poorly understood and few cases have been reported in the literature. This is likely a result of difficulty in distinguishing HC deficiency from true cobalamin deficiency. As HC does not facilitate cellular uptake of cobalamin, cobalamin metabolism does not seem to be compromised in HC deficiency and patients are clinically unaffected (Carmel et al. 2009). Both mild and severe forms of the deficiency are known. Patients with mild HC deficiency have reduced levels of circulating HC, while patients with severe HC deficiency have undetectable levels of circulating HC (Carmel et al. 2009). HC-deficient patients have low serum cobalamin levels but are otherwise asymptomatic. A study of HC deficiency in patients with low

serum cobalamin of an unknown cause found that 15% of patients had mild HC deficiency, while 0.6% had severe HC deficiency (Carmel 2003).

1.9.4. Transcobalamin deficiency

TC facilitates transfer of cobalamin from the blood to inside the cell. Inherited TC deficiency is associated with mutations in the *TCN2* gene and appears in infancy with symptoms including failure to thrive, anemia, hypotonia, and diarrhea (Trakadis et al. 2014). Patients also tend to present with homocystinuria and MMA. Low serum cobalamin levels are usually not reported in TC deficient patients since the majority of serum cobalamin is HC-bound. While some patients have an inactive form of TC that is unable to mediate cellular uptake of cobalamin, the majority of patients have no detectable TC (Teplitsky et al. 2003). TC deficiency is treated with cobalamin supplementation with the purpose of maintaining high serum cobalamin concentrations in patients. Early diagnosis and onset of aggressive treatment appear to favor optimal outcomes in patients (Schiff et al. 2010; Trakadis et al. 2014).

1.9.5. Transcobalamin receptor deficiency

Several patients with decreased cellular uptake of cobalamin have been found to have a 3 base-pair deletion (p.E88del) in the *CD320* gene, which encodes the membrane receptor for TC (Quadros et al. 2010). These patients have been found to have moderately elevated levels of methylmalonic acid and most have homocystinuria as well. Though cellular uptake of cobalamin is reduced by 50% in patients' fibroblasts (Quadros and Sequeira 2013), patients have normal synthesis of cobalamin derivatives and normal activity of MCM and MS. Furthermore, patients with the *CD320* defect do not appear to be clinically affected. A study investigating the association between *CD320* polymorphisms and neural tube defects in an Irish population found

that 1% of the population were homozygous for the p.E211del change (Pangilinan et al. 2010). Two variants in *CD320,* rs2336573 and rs9426, have been found to be associated with a 6-fold increased risk of neural tube defects (Pangilinan et al. 2010). Knockout of the *CD320* gene in mice did not lead to systemic cobalamin deficiency, suggesting alternative mechanisms for cellular cobalamin uptake (Lai et al. 2013).

1.10. Inherited disorders of cobalamin metabolism

Considering the substantial clinical and biochemical heterogeneity of patients with disorders affecting cobalamin metabolism, complementation analysis has value in classifying patients into genetically distinct groups. Initially, four complementation groups (*cblA, cblB, cblC,* and *mut*) were identified (Gravel et al. 1975). Research on the inborn errors of cellular cobalamin metabolism has since identified 6 additional complementation classes (*cblD, cblE, cblF*, *cblG, cblJ,* and *ZNF143* deficiency). All of the underlying genes associated with the 10 complementation groups are believed to have been identified. In recent years it has been shown that deficiencies in non-classical genes (such as that observed in *cblX* disease) are responsible for a small portion of the *cblC* complementation group. It may be true that other complementation classes are similarly genetically heterogeneous.

In somatic cell complementation analysis, cells from different patients are fused and enzymatic activity is assessed in the hybrid cultures. Cell lines deficient in different genes exhibit complementation in fused cultures. Incorporation of label from [^{14}C]propionate, a measure of MCM activity, and incorporation of label from [^{14}C]methyltetrahydrofolate, a measure of MS activity, are used to measure cellular complementation (Froese and Gravel 2010).

All of the inborn errors of cobalamin metabolism are inherited in an autosomal recessive manner, with the exception of the X-linked *cblX* disorder.

1.10.1. Combined methylmalonic aciduria and homocystinuria

1.10.1.1 *cblF*

Patients belonging to the *cblF* complementation group have defects in the *LMBRD1* gene leading to loss of LMBD1 function. The majority of *cblF* patients carry the c.1056delG frameshift mutation in *LMBRD1* (Rutsch et al. 2009). Cells from affected individuals have an accumulation of free cobalamin in the lysosome, consistent with defective efflux of cobalamin across the lysosomal membrane. As a result, synthesis of both AdoCbl and MeCbl is inadequate and activity of both cobalamin-dependent enzymes is low. Patients with the *cblF* disorder have elevations in both methylmalonic acid and homocysteine. Clinical findings tend to be variable and may include failure to thrive, developmental delay, anemia, neutropenia, facial abnormalities, and congenital heart defects (Rutsch et al. 2009; Gailus et al. 2010).

1.10.1.2. *cblJ*

The *cblJ* disorder is associated with mutations affecting the *ABCD4* gene and is characterized by lysosomal trapping of free cobalamin, similar to the *cblF* disease. Although only a few *cblJ* patients have been identified, the clinical and cellular phenotypes show variability between patients (Coelho et al. 2012; Kim et al. 2012). Studies of cultured *cblJ* fibroblasts show severely reduced synthesis of both cobalamin cofactors in all patients. Some patients demonstrate deficient activity of MCM and MS, however a *cblJ* patient with decreased synthesis of cobalamin derivatives and normal activity of both cobalamin-dependent enzymes has been described (Kim et al. 2012). Analogous to the *cblF* disorder, there is a dramatic

decrease in enzyme-bound cobalamin and increase in free cobalamin (Coelho et al. 2012). Onset of symptoms in both the newborn period (Coelho et al. 2012) and early childhood (Kim et al. 2012) has been reported. These manifestations include macrocytic anemia, MMA, and hyperhomocysteinemia. The symptoms of the neonatal-onset patients also included poor feeding, hypotonia, and heart defects (Coelho et al. 2012). Progressive hyperpigmentation has been reported in patients who presented with symptoms in childhood (Kim et al. 2012; Takeichi et al. 2015).

1.10.1.3. *cblC*

MMA and homocystinuria, *cblC* type, is the most common inborn error of cobalamin metabolism. The disorder is secondary to mutations in the *MMACHC* gene, the product of which is involved in the processing of cobalamin for cofactor synthesis. Defects in the MMACHC protein result in abnormal synthesis of MeCbl and AdoCbl leading to reduced activity of both cobalamin-dependent enzymes. Patients are characterized by combined MMA and homocystinuria which can lead to a wide array of symptoms including failure to thrive, feeding difficulties, and hematological, neurological, ophthalmological, and dermatological abnormalities (Lerner-Ellis et al. 2009). Both early and late onset subtypes of *cblC* disease exist, which tend to differ in their severity of symptoms and outcome following treatment (Rosenblatt et al. 1997). Patients that are most severely affected typically present in the first year of life and have prominent neurological and hematological impairments. Those who present after 4 years of age tend to have less severe pathologies and a more favourable response to treatment (Rosenblatt et al. 1997).

1.10.1.4. *cblX*

The *cblX* disorder is an X-linked inborn error of cobalamin metabolism that is associated with mutations affecting the Kelch domain of the *HCFC1* gene (Yu et al. 2013). C*blX* disease presents as a phenocopy of the *cblC* disorder and fibroblasts from *cblX* patients do not complement fibroblasts from *cblC* patients. The disorder was initially discovered in a male patient who had been designated to the *cblC* complementation group but had no identifiable mutations in *MMACHC* (Yu et al. 2013). Exome sequencing identified a missense mutation affecting the N-terminal Kelch domain of the *HCFC1* gene. *HCFC1* mutations were identified in 14 additional male patients who had been assigned to the *cblC* complementation class but were negative for *MMACHC* mutations (Yu et al. 2013). Decreased levels of *MMACHC* mRNA and protein were detected in patients' cells, consistent with a regulatory role of *HCFC1* in *MMACHC* expression. Severe neurological symptoms including intractable epilepsy and cognitive impairment has been observed in all affected patients. The biochemical phenotype of *cblX* disease appears to be more variable than early-onset *cblC* disease as numerous *cblX* patients have normal levels of plasma homocysteine.

1.10.1.5. *cblD*

Patients belonging to the *cblD* complementation group may present with MMA or homocystinuria, in either isolation or combination (Suormala et al. 2004). In *cblD*-variant 1, mutations affecting a conserved C-terminus region (p.D246-L259) of the *MMADHC* gene result in deficiency of MeCbl synthesis and isolated homocystinuria. Mutations located across the C-terminus (p.Y140-R250) appear to be associated with combined MMA and homocystinuria. The *cblD*-variant 2 disorder is caused by mutations in the N-terminus of the *MMADHC* gene leading

to defective synthesis of AdoCbl cofactor and isolated MMA (Jusufi et al. 2014). Clinical manifestations of the *cblD* disorder vary greatly between patients depending on the underlying genetic defect and may include neurological impairment, metabolic acidosis, muscle weakness, vomiting, developmental delay, and megaloblastic anemia (Miousse et al. 2009).

1.10.2. Isolated homocystinuria

1.10.2.1. *cblE*

Pathogenic mutations affecting the *MTRR* gene, encoding MSR, lead to reduced MS activity and are responsible for the *cblE* inborn error (Wilson et al. 1999). MSR is required for reactivation of the MS protein. This disorder is characterized by isolated homocystinuria and presents early in life with complications including megaloblastic anemia, failure to thrive, and neurological impairment (Huemer et al. 2015). The most frequent mutation leading to the *cblE* disorder is a deep intronic mutation (c.903+469T>C) that results in inclusion of a pseudoexon via creation of an exonic splicing enhancer site (Homolova et al. 2010).

1.10.2.2. *cblG*

Mutations in the *MTR* gene leading to defective MS apoenzyme and reduced synthesis of methionine from homocysteine are implicated in the *cblG* complementation class. Affected patients are characterized by isolated homocystinuria and typically present with megaloblastic anemia, cognitive impairment, developmental delay, mental retardation, and decreased visual acuity (Huemer et al. 2015). The *cblG* clinical phenotype is nearly indistinguishable from that of the *cblE* disorder, however muscular hypotonia seems to be more frequently reported in *cblG* patients (Huemer et al. 2015). A digenic inheritance pattern involving single heterozygous mutations in the *MTR* and *LMBRD1* genes has been suggested in a single patient with cobalamin

deficiency (Farwell Gonzalez et al. 2015), though more evidence is needed to evaluate this assertion.

1.10.3. Isolated methylmalonic aciduria

Isolated MMA is characterized by elevated levels of methylmalonic acid in blood and urine and often manifests in the early stages of life. The incidence of this condition is estimated to be between 1 in 50,000 and 1 in 100,000 births (Chace et al. 2001; Shigematsu et al. 2002). MMA can be caused by a complete (*mut*^{0}) or partial (*mut*$^{-}$) deficiency of MCM, a defect in the synthesis of its cofactor, adenosylcobalamin, a deficiency in the MCEE enzyme, or a deficiency in the Krebs cycle enzyme SUCL. Onset of clinical manifestations ranges from during the neonatal period to adulthood. The severity of symptoms is variable and dependent on the underlying genetic defect (Hörster et al. 2007), however neonatal presentation is typically associated with a severe prognosis (Fenton et al. 2001). Neonatal symptoms of MMA can include encephalomyopathy, lethargy, vomiting, hypotonia, respiratory distress, ketoacidosis, neutropenia, thrombocytopenia, and hyperammonemia (Manoli et al. 1993; O'Shea et al. 2012). If left untreated, recurrent metabolic crises can lead to overwhelming illness that may result in multiorgan failure, coma, and early death. Long-term complications of chronic MMA can include chronic renal failure (CRF), developmental delay, neurological deficit, psychomotor retardation, and failure to thrive (Manoli et al. 1993; Cosson et al. 2009; O'Shea et al. 2012). Metabolic crises can lead to acute injury to the globus pallidus and produce a severe movement disorder in some patients (Baker et al. 2015). Patients with the *mut*$^{-}$ and *cblA* forms of MMA tend to have milder clinical phenotypes than patients diagnosed with the *mut*^{0} and *cblB* disorders (Hörster et al. 2007). The *mut*^{0} and *cblB* disorders are generally characterized by higher mortality, neurological impairment, and greater excretion of methylmalonic acid (Matsui et al.

1983; Hörster et al. 2007; Nizon et al. 2013). Presence of hyperammonemia in affected patients has been associated with lower IQ scores, suggesting that hyperammonemia may be a determinant of neurological impairment in MMA (O'Shea et al. 2012). While overall survival of this disorder has improved in recent decades, the long-term outcome remains unfavourable due to a lack of therapeutic advancements (Manoli et al. 1993; van der Meer et al. 1994; Hörster et al. 2007).

1.10.3.1. *cblA*

In the *cblA* type of MMA, mutations in the *MMAA* gene disrupt synthesis of AdoCbl and subsequently lead to impaired function of MCM (Dobson et al. 2002). Cells from *cblA* patients have a reduced ability to synthesize AdoCbl from exogenous CNCbl. The common c.433C>T (p.R145*) mutation in *MMAA* is associated with European ancestry and accounts for nearly 50% of pathogenic alleles (Lerner-Ellis et al. 2004). Patients affected with *cblA* tend to present during the newborn period or early-childhood with severe, life-threatening metabolic acidosis secondary to elevated levels of methylmalonic acid (Manoli et al. 1993). All *cblA*-affected individuals respond to hydroxocobalamin therapy. Significant reductions in plasma methylmalonic acid concentration is observed in these patients following cobalamin treatment (Hörster et al. 2007).

1.10.3.2. *cblB*

The *cblB* disorder is a severe form of isolated MMA that is associated with pathogenic mutations affecting the *MMAB* gene leading to dysfunctional ATR protein. Functional analyses of *cblB*-causing mutations have identified mutant genotypes that lead to reduced ATR affinity for substrate and AdoCbl (Lofgren and Banerjee 2011), as well as mutations leading to complete and partial loss of enzymatic activity (Zhang et al. 2006; Jorge-Finnigan et al. 2010). Both early-

and late-onset forms have been described. In the severe early-onset disease, patients suffer from symptoms of neonatal ketoacidosis, failure to thrive, and encephalomyopathy. The late-onset form is usually diagnosed in infancy and has a milder phenotype with less pronounced neurological impairment (Hörster et al. 2007). Mitochondrial dysfunction has been described in fibroblasts derived from *cblB* patients (Brasil et al. 2015), which exhibit increased levels of reactive oxygen species and reduced energy production. It is possible that therapy aiming to restore mitochondrial function would be clinically beneficial to *cblB* patients.

1.11. Disorders of propionyl-CoA metabolism

1.11.1. Propionic acidemia

Propionic acidemia (PA) is a metabolic disorder that is characterized by inherited defects in the PCC enzyme, secondary to mutations affecting either the *PCCA* or *PCCB* loci. PA is characterized by the toxic accumulation of propionic acid in the blood. The severe, neonatal-onset form of PA is the most common form of the disease. Affected infants present with symptoms of poor feeding, vomiting, lethargy, metabolic acidosis, and early death (Deodato et al. 2006). Late-onset PA is characterized by chronic vomiting, failure to thrive, hypotonia, and in some instances, cardiomyopathy. Longevity of PA can lead to progressive neurological impairment and movement disorders (Carrillo-Carrasco and Venditti 1993). In general, null alleles are associated with severe forms of PA while missense variants are associated with milder clinical presentations (Carrillo-Carrasco and Venditti 1993), although exceptions have been described (Muro et al. 2001).

1.11.2. *MCEE* deficiency

Biallelic mutations affecting the *MCEE* gene have been described as a very rare cause of persistent mild MMA. Deficiency in *MCEE* was initially reported in 2 patients who were homozygous for a p.R43* nonsense mutation (Bikker et al. 2006; Dobson et al. 2006). Both severely affected patients and asymptomatic individuals with mutations in *MCEE* have been reported (Gradinger et al. 2007). It appears as though the presence of MMA in these patients does not consistently translate to a symptomatic phenotype. The *MCEE* gene product is involved in the isomerization of D- to L-methylmalonyl-CoA, the form used by MCM. It may be true that non-enzymatic conversion of D- to L-methylmalonyl-CoA contributes to flux through the propionyl-CoA metabolic pathway. Such a phenomenon could explain why some individuals with mutations in *MCEE* are asymptomatic.

1.11.3. *mut* MMA

The *mut* type of MMA is caused by a defect in the cobalamin-dependent enzyme MCM and accounts for 60% of cases of isolated MMA (Manoli et al. 1993). Patients affected with *mut* MMA typically present with acute metabolic distress in the neonatal period. Symptoms are often characterized by failure to thrive, recurrent vomiting, mild microcephaly, lethargy, hypotonia, dehydration, respiratory distress, hyperammonemia, and ketoacidosis (Hörster et al. 2007). Affected patients display periods of relative health intersected with intermittent acute metabolic crises that may lead to death (Manoli et al. 1993). Early enzymatic studies on MCM activity in fibroblasts derived from *mut* patients identified two cellular subtypes of the disorder (Willard and Rosenberg 1977). Cell lines with virtually undetectable MCM activity, at both the basal level and under high concentrations of AdoCbl, were designated mut^0. Cells that had measurable

activity of MCM, ranging from 1-50% of wild-type, and showed a robustly elevated K_m for AdoCbl were designated *mut*$^-$ (Rosenberg 1980). Immunochemical studies found highly variable levels of cross-reacting material (CRM) in fibroblasts from *mut* patients (Kolhouse et al. 1981; Fenton et al. 1987), underscoring the diversity of pathogenic mutations affecting the *MUT* locus. Detectable CRM in fibroblasts belonging to the *mut*$^-$ subgroup were found to range from 20% to 100% of control levels and CRM values in fibroblasts from *mut*^{0} patients ranged from virtually undetectable to 40% of control (Kolhouse et al. 1981). Fibroblasts from both *mut*^{0} and *mut*$^-$ patients have decreased ability to incorporate [^{14}C]propionate into acid-precipitable protein, indicating defective metabolism of propionyl-CoA. Supplementation of hydroxocobalamin to *mut*$^-$ cell cultures ameliorates [^{14}C]propionate incorporation towards the reference range, while *mut*^{0} cultures are nonresponsive. Approximately 78% of *mut* patients belong to the *mut*^{0} subtype while the remaining 22% are *mut*$^-$ (Manoli et al. 1993). The *mut* subtype is ultimately determined by the underlying genetic defect and mutations in *MUT* are typically classified as either *mut*^{0}- or *mut*$^-$ -associated. However, *mut*$^-$ mutations that result in very low residual enzymatic activity can make the *mut*^{0} and *mut*$^-$ phenotypes difficult to distinguish (Janata et al. 1997). Diagnosis of *mut* MMA often requires genetic analysis of the *MUT* gene and/or somatic cell studies. Fibroblasts from *mut* patients typically exhibit reduced [^{14}C]propionate incorporation and normal or slightly reduced synthesis of AdoCbl (Worgan et al. 2006). Somatic cell complementation analysis allows the *mut* disorder to be distinguished from the other forms of MMA, however the process is complicated by the existence of interallelic complementation within the *mut* phenotype (Raff et al. 1991).

1.11.3.1. Clinical manifestations

The *mut*^{0} disease is the most adverse form of isolated MMA. Patients affected by the *mut*^{0} disorder typically present with a severe clinical phenotype that manifests in the neonatal stage (Cosson et al. 2009). Approximately 75% of *mut*^{0} patients develop symptoms within the first week of life, while approximately 37% of *mut*$^-$ patients present within the first month (Hörster et al. 2007). The median age of onset in *mut*^{0} and *mut*$^-$ patients has been estimated to be 5 and 75 days, respectively (Hörster et al. 2007). Patients belonging to the *mut*^{0} enzymatic subtype tend to have the highest mortality, incidence of failure to thrive, and mean levels of urinary methylmalonic acid excretion. Anorexia and feeding difficulties are also reported more often in *mut*^{0} than *mut*$^-$ patients (Hörster et al. 2007). Chronic renal failure (CRF) is commonly identified in *mut*^{0} patients, affecting over half of patients (Hörster et al. 2007; Cosson et al. 2009). Estimations of the occurrence of CRF in *mut*$^-$ patients have been inconsistent. Hörster et al. 2007 found that 0/9 *mut*$^-$ patients with long term follow-up had CRF, while 2/3 *mut*$^-$ patients assessed in Cosson et al. 2009 did have CRF, albeit less severe than what is typically observed in the *mut*^{0} phenotype. Interestingly, it has been found that the occurrence of CRF correlates well with monthly excretion levels of methylmalonic acid, suggesting MMA levels may be a predictor of CRF (Hörster et al. 2007). The incidence of neurological impairment in the *mut*^{0} patient population is high, however data measuring the incidence of neurological disease in *mut*$^-$ patients varies, with one study describing a high frequency (Hörster et al. 2007) while another has reported no incidence at all (Cosson et al. 2009). *Mut*^{0}-affected patients generally have a worse cognitive outcome than *mut*$^-$ patients (Manoli et al. 1993). Seizures, mental retardation, and movement disorders comprise the major complications, as well as persistent basal ganglia lesions in *mut*^{0} patients. It should be noted that a minority of *mut*^{0} patients with no neurological disease

have been reported (Hörster et al. 2007; Cosson et al. 2009). This may reflect certain patients being more receptive to therapeutic intervention or genetic factors in these individuals that improve the natural history of the disease.

1.11.3.2. Mouse models

In order to study therapy and manifestations of chronic illness, there have been multiple efforts to create a mouse model that recapitulates human *mut* MMA. The first attempt at creating a knockout mouse model resulted in neonatal lethality in all homozygous knockout pups (Peters et al. 2003). Recently, Forny et al. 2016b have generated two mouse models, based upon the p.M700K human missense mutation, that appear to exhibit the key phenotypic features of *mut* MMA. Mice homozygous for the p.M700K mutation (KI/KI) as well as compound heterozygotes associated with a knockout allele (KI/KO) survive the neonatal period, exhibit failure to thrive, and have elevated levels of methylmalonic acid. The $mut^{Ki/Ko}$ mice have more pronounced metabolic defects and lower MCM activity than $mut^{Ki/Ki}$ mice, consistent with gene dosage. Treatment with hydroxocobalamin alleviated the symptoms of metabolic crises that were induced by a high protein diet in the $mut^{Ki/Ki}$ mice. Hydroxocobalamin therapy was less effective in the $mut^{Ki/Ko}$ mice.

1.11.3.3. Treatment

Treatment of *mut* MMA primarily consists of carnitine supplementation, dietary interventions, and management of symptoms (Baumgartner et al. 2014). Pharmacological doses of hydroxocobalamin are often given to *mut* patients with the intention of overloading the patients' cells with cobalamin cofactor to stimulate any residual enzymatic activity and alleviate

the toxic accumulation of metabolites. However, most patients, especially those belonging to the *mut*^{0} subtype, do not respond to this treatment (Hörster et al. 2007). *In vitro* responsiveness to cobalamin does not appear to reliably predict *in vivo* responsiveness to hydroxocobalamin therapy. When treatment is entirely ineffective, transplantation of liver, kidney, or both may be advocated. However, neurological injury resulting from metabolic stroke has been reported in patients several years following liver and combined liver-kidney transplantation (Chakrapani et al. 2002; Kaplan et al. 2006). More data is needed to assess the long-term effect of isolated kidney transplantation, but early evidence suggests a more promising outcome. Renal transplantation appears to have an immediate effect in *mut* patients, reducing plasma and urinary methylmalonic acid levels and improving overall renal function (Brassier et al. 2013). Complete cessation of acute metabolic decompensations following kidney transplantation has been observed in many patients, as well as dramatic improvement in survival (Lubrano et al. 2007; Mc Guire et al. 2008; Brassier et al. 2013; Niemi et al. 2015). The short-term effect of kidney transplantation on neurological status also appears to be favourable, with patients either maintaining or improving cognitive ability (Niemi et al. 2015). However, data evaluating the long-term impact of kidney transplantation on neurological development is lacking.

1.11.3.4. The human *MUT* gene

The human *MUT* gene is located on chromosome 6p12.3 and spans 35kb of genomic DNA (Nham et al. 1990). Its mRNA product consists of 13 exons encoding 750 amino acids which comprise the immature enzyme (Jansen et al. 1989). The structure of MCM has been extensively studied in the prokaryotic organism *Propionibacterium shermanii* (Francalanci et al. 1986; Marsh et al. 1989). The α-subunit of *P. shermanii* MCM (*ps*MCM) has 65% amino acid sequence homology with human MCM and X-ray crystallography has revealed significant

conservation of domain architecture between human MCM and *ps*MCM (Thomä and Leadlay 1996; Froese et al. 2010). However, the human and bacterial enzymes differ in that human MCM functions as a homodimer composed of two identical subunits, each with catalytic activity, (Jansen et al. 1989) while *ps*MCM has a heterodimeric configuration comprising a catalytic α-subunit and a non-catalytic β-subunit (Marsh et al. 1989). Each subunit of the human MCM apoenzyme has the capacity to bind one molecule of AdoCbl.

The first 32 amino acid residues of the human *MUT* open reading frame constitute the mitochondrial leader sequence and are cleaved upon MCM entering the mitochondria. An N-terminal extended segment (residues 33-87) facilitates subunit interaction and precedes the two functional domains of the enzyme. The N-terminal $(\beta\alpha)_8$ -TIM barrel domain (residues 88-422) is involved in binding of methylmalonyl-CoA (Thomä and Leadlay 1996) and the C-terminal $(\beta\alpha)_5$ -Rossmann domain (residues 578-750) contains the AdoCbl-binding site. A 155 amino acid linker region (residues 423-577) connects the N- and C-terminal functional domains.

1.11.3.5. Spectrum of pathogenic *MUT* mutations

Three hundred and twenty six pathogenic mutations in the *MUT* gene are currently known (Chu et al. 2016; Forny et al. 2016a). The majority of mutations in *MUT* are rare, private mutations that have only been identified in a single family. However, ethnicity-specific recurrent mutations are known, including the p.G94V, p.G623R, and p.G717V mutations in black patients (Worgan et al. 2006), the p.E117* mutation in Japanese patients (Ogasawara et al. 1994), the p.N219Y mutation in Caucasian patients (Acquaviva et al. 2001), the p.V227Nfs*2 mutation in Spanish patients (Martínez et al. 2005), the p.G94R, p.R108C, and p.N341Kfs*20 mutations in North American Hispanic patients (Worgan et al. 2006), and the p.D244Lfs*39, p.G427D, and

p.G544* mutations in Asian patients (Liu et al. 2012). The highest number of *MUT* mutations are missense mutations, many of which lead to protein instability (Forny et al. 2016a). Though disease-causing mutations spanning the entire coding region have been identified, variation favours the N-terminal TIM barrel domain and, to a lesser extent, the C-terminal AdoCbl-binding domain. Mutations located in the former tend to be associated with a mut^0 phenotype and mutations affecting the latter are often associated with a mut^- phenotype (Acquaviva et al. 2005), although exceptions are known (Janata et al. 1997). It has been suggested that mut^- mutations have a dominant effect on the biochemical phenotype of the cell and that patients who are compound heterozygous for a mut^--associated mutation and a mut^0-associated mutation will exhibit a mut^- phenotype (Acquaviva et al. 2005). The greater occurrence of the mut^0 phenotype corresponds with the high frequency of mutations affecting the N-terminal binding domain. The N-terminal extended segment and linker regions have relatively low frequencies of mutations (Chu et al. 2016; Forny et al. 2016a). Some residues located in the N-terminal extended segment have been shown to participate in interallelic complementation (Ledley and Rosenblatt 1997). No disease-causing mutations have been identified in exon 1 of *MUT*, which is entirely untranslated and consists of only 36 base pairs. Further research is needed to elucidate the biological role of this exon, which is conserved in species ranging from bacteria to humans.

1.11.4. Succinate-CoA ligase deficiency

Mitochondrial DNA (mtDNA) depletion syndromes are caused by defects in enzymes involved in replication of mtDNA, a process that is essential to maintaining mitochondrial integrity. These disorders are characterized by reduced levels of mtDNA below a clinically-necessary threshold (Van Hove et al. 2010). Deficiency in the enzyme SUCL, secondary to mutations in either *SUCLG1* or *SUCLA2*, is associated with mtDNA depletion syndrome

presenting with encephalomyopathy. Mild MMA is also often observed in affected patients (Carrozzo et al. 2007). The causal link between SUCL deficiency and mtDNA depletion is not understood, but may be due to interaction between SUCL and the mitochondrial isoform of nucleoside diphosphate kinase (NDPK), which is involved in mtDNA replication (Kowluru et al. 2002). *SUCLA2* mutations result in a Leigh-like syndrome that can include symptoms of severe hypotonia, muscular atrophy, seizures, and developmental delay (Carrozzo et al. 2007). Mutations affecting *SUCLG1* cause a severe phenotype often leading to fatal infantile lactic acidosis in the early weeks of life (Valayannopoulos et al. 2010). Sensorineural hearing loss has also been described in *SUCLG1* deficiency (Van Hove et al. 2010). Patients with *SUCLA2* mutations have significantly better survival than those with *SUCLG1* mutations (Carrozzo et al. 2016). Though *SUCLG1* deficiency tends to be more severe than *SUCLA2* deficiency, *SUCLG1*-deficient patients with clinical phenotypes indistinguishable from *SUCLA2* deficiency have been reported. It has been suggested that the severe clinical phenotype is secondary to complete absence of functional SUCLG1, while patients with residual SUCLG1 protein can have a *SUCLA2* deficiency-like phenotype (Rouzier et al. 2010). It is possible that deficiency of *SUCLG1* is more severe than that of *SUCLA2* because the SUCLG1-SUCLG2 complex is not compromised in *SUCLA2* deficiency. However, the necessity of *SUCLG2* to mitochondrial homeostasis is unknown and mutations in *SUCLG2* have not been associated with a human disease. Nevertheless, knockdown of *SUCLG2* in human fibroblasts results in mtDNA depletion, growth impairment, and reduced mitochondrial NDPK and cytochrome c oxidase activities (Miller et al. 2011), suggesting a role for *SUCLG2* in maintaining mitochondrial integrity. Transgenic mice lacking either one *SUCLA2* allele or one *SUCLG2* allele present with mtDNA depletion, consistent with human deficiency of SUCL (Kacso et al. 2016). Interestingly, *SUCLA2*

heterozygous mice have increased levels of cardiac SUCLG2 expression and GTP-dependent activity. *SUCLG2* heterozygous mice do not have a similar compensatory response in SUCLA2 expression.

1.12 Diagnosis of *mut* MMA

1.12.1. Somatic cell studies

Patients are referred to the Vitamin B_{12} Clinical Research Laboratory at McGill University for diagnosis of the inborn errors of cobalamin metabolism through somatic cell studies. The diagnostic protocol for patient fibroblasts includes assessment of MS and MCM activity, as well as assessment of synthesis of cobalamin cofactors from [^{57}Co]CNCbl (Figure 5). Assessment of MS activity is achieved by measuring the ability of cells to incorporate label from [^{14}C]methyltetrahydrofoloate into acid-precipitable protein and MCM activity is determined by measuring incorporation of label from [^{14}C]propionate. Cells that exhibit deficient activity for either side of the pathway are studied with somatic cell complementation analysis in order to identify the genetic locus associated with the patient's disease. For instance, fibroblasts derived from patients with *mut* MMA exhibit complementation when fused with cells from *cblA* and *cblB* patients, but typically do not complement cells from other *mut* patients. Interallelic complementation is an exception to this rule, whereby cells from certain *mut* patients show complementation with other cells belonging to the *mut* complementation class. It is believed that this phenomenon is secondary to a compensatory interaction between the *MUT* mutations of the two cell lines. For instance, it has been hypothesized that some *mut* fibroblasts which have an unimpaired ability to bind cobalamin can provide cobalamin-binding activity to *mut* cells that have genetic defects affecting binding of cobalamin (Raff et al. 1991).

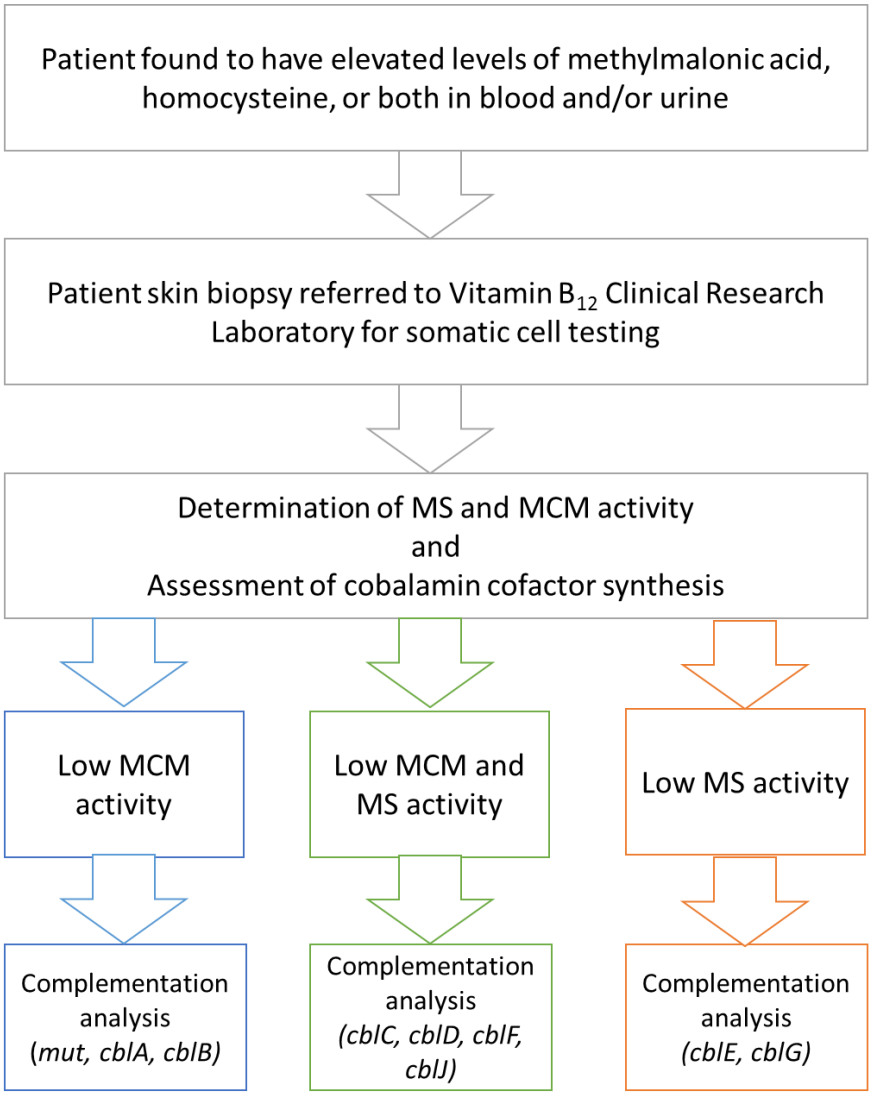

Figure 5. Diagnostic process for patient cells referred to the Vitamin B_{12} Clinical Research Laboratory. Fibroblasts from patients with suspected inborn errors of cobalamin metabolism are referred to the Vitamin B_{12} Clinical Research Laboratory for somatic cell studies. MS and MCM activity are measured through [^{14}C]methyltetrahydrofolate and [^{14}C]propionate incorporation assays, respectively. Synthesis of cobalamin derivatives from [^{57}Co]CNCbl is also determined. Cells with deficient activity of cobalamin-dependent enzymes are subjected to somatic cell complementation analysis for specific diagnosis.

1.12.2. Next generation sequencing

In light of the increasing availability of next generation sequencing (NGS), gene panels and whole exome analysis are frequently being used clinically to facilitate diagnosis of rare disorders. These approaches allow rapid molecular analysis of many genes at once and can accelerate diagnosis. There are currently numerous NGS-based gene panels available as clinical tests which offer sequencing of MMA-related genes. The comprehensiveness of these panels varies greatly as the number of genes assessed can range from only a few genes to over 20. In recent years, these panels have often been used as a first-tier diagnostic test for MMA and the role of somatic cell studies in the diagnostic process has become less clear.

Rationale and objectives of study

Genetic testing and somatic cell complementation analysis are two common means of diagnosing the inborn errors of cobalamin metabolism. However, the relative efficacies of each test have not been directly compared. The aim of the present study was to identify the underlying genetic defect of patients who had been diagnosed with *mut* MMA by somatic cell complementation analysis. In this study, a cohort of 53 complementation-confirmed *mut* patients were studied with a NGS-based gene panel in order to (1) validate the diagnoses made by somatic cell studies, and (2) identify the genetic defects responsible for the patients' phenotypes. This work has been published in Chu et al. Mol Genet Metab 118(4):264-271, 2016. Follow-up studies, not presented in the above manuscript, involved the investigation of deficiency in *SUCLG2* in one patient as a novel cause of human disease.

CHAPTER 2

Materials and methods

2.1. Patients and cell culture

Mycoplasma-negative primary fibroblast lines derived from patients were obtained from the Repository for Mutant Human Cell Strains of the Montreal Children's Hospital (http://www.cellbank.mcgill.ca). All cell lines were referred to the Vitamin B_{12} Clinical Research Laboratory (Department of Medical Genetics, McGill University Health Centre) to rule out an inborn error of cobalamin metabolism. Fifty three patients diagnosed with *mut* MMA by somatic cell complementation analysis were investigated in this study. Patient fibroblasts were designated to be either mut^0 or mut^- depending upon cellular responsiveness to supplemental hydroxocobalamin, as measured by [1-C^{14}]propionate incorporation analysis. Cells from 44 patients showed no response to hydroxocobalamin supplementation in culture and these patients were classified mut^0. The remaining 9 patients were found to belong to the mut^- subtype based upon stimulation of [1-C^{14}]propionate incorporation following addition of exogenous hydroxocobalamin. Cells were cultured in Eagle's minimum essential medium (EMEM) containing Earle's salts, L-glutamine, and high glucose (Wisent Inc, Saint-Jean-Baptiste, Quebec), supplemented with non-essential amino acids, 0.11g/L sodium pyruvate, 0.01g/L ferric nitrate, 5% fetal bovine serum (Wisent Inc, Saint-Jean-Baptiste, Quebec), and 5% bovine calf serum (Wisent Inc, Saint-Jean-Baptiste, Quebec). Cell cultures were routinely fed twice a week and incubated at 37ºC in 5% CO_2.

2.2. DNA extraction

Genomic DNA was extracted from patient fibroblasts using the FlexiGene DNA kit (Qiagen, Canada) according the manufacturer's instructions. Concentration and purity of DNA were assessed using the BioDrop µLITE spectrophotometer and extracts were stored at -20^{o}C.

2.3. Gene panel analysis

Genomic DNA from all 53 patients was analyzed with the "Cobalamin Metabolism Panel and Severe MTHFR Deficiency by Massively Parallel Sequencing" clinical test developed at Baylor Miraca Genetics Laboratories. This NGS-based panel is comprised of MUT and 20 other genes associated with cobalamin metabolism. Three additional genes (AMN, CUBN, and SLC46A1) that are not currently included in the clinical test were analyzed in this study. Target sequences of all 24 genes (Table 1) were enriched using custom designed NimbleGen SeqCap probe hybridization (Roche NimbleGen Inc., Madison, WI, USA). The captured sequences include all exons and 20bp of their flanking intronic regions. DNA template libraries were prepared according to the manufacturer's recommendation. Equal molar ratios of 10 indexed samples were pooled to be loaded onto each lane of the flow cells for sequencing on a HiSeq2000 (Illumina, San Diego, CA, USA) with 100 cycle single-end reads. Raw data in base call files (.bcl format) were converted to qseq files before demultiplexing with CAVAv1.7 software (Illumina Inc., San Diego, CA, USA). Demultiplexed data were processed further by NextGENe soft- ware for alignment (SoftGenetics, State College, PA, USA). Average depth of coverage of the NGS analysis was 500–1000×. All exons were covered at sufficient depth. The coverage-based depth analysis using NGS data has been previously reported (Feng et al. 2015).

Table 1: Genes tested by the NGS-based cobalamin metabolism panel

Gene	Gene Name	GenBank Accession
ABCD4	ATP-binding cassette, subfamily D, member 4	NM_005050.3
ACSF3	Acyl-CoA synthetase family, member 3	NM_174917.4
AMN	Amnionless	NM_030943.3
CBS	Cystathionine beta-synthase	NM_000071.2
CD320	Transcobalamin receptor	NM_016579.3
CUBN	Cubilin	NM_001081.3
GIF	Gastric intrinsic factor	NM_005142.2
HCFC1	Host cell factor C1	NM_005334.2
IVD	Isovalery-CoA dehydrogenase	NM_002225.3
LMBRD1	LMBR1 domain-containing protein 1	NM_018368.3
MCEE	Methylmalonyl-CoA epimerase	NM_032601.3
MMAA	Methylmalonic aciduria, cblA type	NM_172250.2
MMAB	Methylmalonic aciduria, cblB type	NM_052845.3
MMACHC	Methylmalonic aciduria and homocystinuria, cblC type	NM_015506.2
MMADHC	Methylmalonic aciduria and homocystinuria, cblD type	NM_015702.2
MTHFR	5,10-methylenetetrahydrofolate reductase	NM_005957.4
MTR	Methionine synthase	NM_000254.2
MTRR	Methionine synthase reductase	NM_002454.2
MUT	Methylmalonyl-CoA mutase	NM_000255.3
SLC46A1	Solute carrier family 46 (folate transporter), member 1	NM_080669.5
SUCLA2	Succinate-CoA ligase, ADP-forming, beta subunit	NM_003850.2
SUCLG1	Succinate-CoA ligase, alpha subunit	NM_003849.3
SUCLG2	Succinate-CoA ligase, beta subunit	NM_001177599.1
TCN2	Transcobalamin II	NM_000355.3

2.4. Immortalization

To facilitate additional functional analyses, immortalized cell lines were derived from primary fibroblasts from patients WG3654, WG3499, WG3126, and MCH23 through retroviral transduction of the *E7* gene of human papillomavirus and the human telomerase (*hTert*) gene. Viral supernatant was collected from the packaging cells PA317 E7 and PA317 hTert and supplemented with 4µg/mL polybrene. Patient fibroblasts were exposed to the retroviral solution overnight and detoxified the following day.

2.5. Retroviral transduction

Phenotypic correction studies were conducted on immortalized cells from WG3654, WG3499, and WG3126 to confirm that the mutations identified in these patients were responsible for the patients' phenotypes. Retroviral pBABE-*MUT* and pBABE-*SUCLG2* (NM_003848) vectors were generated from cloning pDONR-*MUT* (GeneCopoeia, Rockville MD, USA) and pShuttle^{TM}-*SUCLG2* (GeneCopoeia, Rockville MD, USA) constructs into pBABE plasmids using Gateway® Technology (Life Technologies, Burlington, ON). The pBABE-*MUT* retroviral vector was transfected into a Phoenix amphoteric cell line using the HEPES-buffered saline/Ca3(PO4)2 protocol (https://web.stanford.edu/group/nolan/_OldWebsite/protocols/pro_helper_dep.html). The viral supernatant was collected and used to infect immortalized fibroblasts from WG3654, WG3499, a *cblJ* patient, a *mut* patient with known mutations, and a healthy control. Patient cells were exposed to the viral supernatant in the presence of 4µg/mL polybrene for 24 hours. To select for cells that successfully incorporated the vector, cultures were incubated in media containing

1µg/mL puromycin for up to 1 week. The pBABE-*SUCLG2* construct was transduced into immortalized fibroblasts from WG3126 using the same protocol.

2.6. [1-C^{14}]propionate incorporation

[1-C^{14}]propionate incorporation was measured in transduced and untransduced cell lines to assess correction. Patient cells were plated in triplicate at 400,000 cells per 35mm culture dish and incubated in Puck's saline solution containing 100µmol/L [1-C^{14}]propionic acid and 15% fetal bovine serum for 18 hours at 37^{o}C. Cultures were washed three times with phosphate-buffered saline (PBS) and subsequently washed with 5% trichloroacetic acid (TCA) three times with 15 minute incubations at 4^{o}C between washes. TCA-precipitable macromolecules were then dissolved in 0.2N NaOH and incubated at 37^{o}C for 3 hours. Radioactivity was determined using liquid scintillation counting and protein concentrations were quantified using the Lowry method (Lowry et al. 1951).

2.7. cDNA analysis

Total RNA was extracted from cultured fibroblasts from patients WG3654, WG3499, WG3126, and MCH23 using TRI reagent (Sigma-Aldrich, Oakville, Ontario) according to the manufacturer's protocol. RNA concentration was determined with the BioDrop µLITE spectrophotometer and quality was assessed with electrophoresis on a 1% agarose gel. RNA extracts were stored at -80^{o}C. The Superscript III First Strand Synthesis system for RT-PCR was used to create cDNA according to the manufacturer's recommendations. PCR amplification of 3 overlapping segments which encompass the entire *MUT* open reading frame was performed on

cDNA derived from WG3654 and WG3499 to elucidate the effects of the *MUT* gene mutations identified in these patients. PCR amplification of 4 overlapping segments was used to analyze *SUCLG2* cDNA from WG3126 to confirm the heterozygous c.273A>T variant identified by the panel and to search for a second genetic defect in *SUCLG2*. Amplification of *GAPDH* cDNA was used as a positive control. RT-PCR primer pairs for *MUT, SUCLG2,* and *GAPDH* are listed in Table 2 and were generated by Alpha DNA (Montreal, Quebec). Sanger sequencing of PCR products was performed at the McGill University and Genome Quebec Innovation Centre.

Table 2. RT-PCR primers

Amplification product	Forward Primer (5'→ 3')	Reverse Primer (5'→ 3')	Annealing temperature (°C)
MUT segment 1	CGGGGGACGCAGAAGTGCAG	GGCATCAGCCCTGCTTCCTG	65
MUT segment 2	AACCCT CGACTTCGTGGTGATG	CAATCTGCCTGTTTCGCACT GAA	65
MUT segment 3	ATGTGCTGCCCGAAGACAAG C	CAAGCACCTGAACGGCAGCC T	65
SUCLG2 segment 1	CGTGCCGAGTTTCCTGTTTA	ATCTGCAGCCTGGCTTTTC	55
SUCLG2 segment 2	GGAATAAAGGACAGCCAAGC	TGAACCATCCCTTTTTACGG	55
SUCLG2 segment 3	GAAGGAACCAACGTCCAAGA	AGCTTCCACTCCCAAAATCA	55
SUCLG2 segment 4	GTGATTTTGGGAGTGGAAGC	TCCCACAACAAAATTGGACA	55
GAPDH	GAAAGCCTGCCGGTGACTAA	GCCCAATACGACCAAATCAGAG	65

2.8. Western blot

Western blot analysis was used to quantify *SUCLG2* protein abundance in fibroblasts from WG3126. Cell pellets from one 75 cm^2 flask were resuspended in 1mL of extraction buffer containing 100mM potassium phosphate (pH 7.3), 35mM β-mercaptoethanol, and cOmplete™

protease inhibitor cocktail (Sigma-Aldrich, Oakville, Ontario). Cells were lysed by sonicating 5 times for 10 seconds with 1 minute between pulses. Protein concentrations were determined using the Lowry method (Ramirez et al. 2010). Equal amounts of total protein extracts from WG3126 and a control cell line were loaded onto a 10% polyacrylamide gel and separated by sodium dodecyl sulfate polyacrylamide gel electrophoresis (SDS-PAGE). Samples were subsequently transferred to a polyvinylidine fluoride (PVDF) membrane (BioRad, California, USA). For detection of SUCLG2 protein, the membrane was exposed to the rabbit anti-SUCLG2 polyclonal primary antibody NBP1-32521 (Novus Biologicals, Oakville, Ontario) at 1:1000 dilution followed by exposure to the secondary antibody goat anti-rabbit IgG (H+L)-horseradish peroxidase (HRP) conjugate (BioRad, California, USA) at 1:10,000. For detection of β-actin, the membrane was exposed to the primary antibody β-actin (13E5) rabbit mAB (New England BioLabs, Massachusetts, USA) at 1:1000 followed by exposure to the secondary antibody goat anti-rabbit IgG (H+L)-HRP conjugate (BioRad, California, USA) at 1:10,000. The Pierce^{TM} ECL Western Blotting Substrate (ThermoFisher Scientific, Illinois, USA) was added to the membrane according to the manufacturer's instructions and HRP-activity was detected using the Omega Lum^{TM} C Imaging System (Aplegen). Image analysis was performed with ImageJ software.

CHAPTER 3

Results

3.1. Sequencing findings

Homozygous or multiple heterozygous mutations in the *MUT* gene were identified in 48/53 (91%) patients. Twenty-nine patients had two or more heterozygous mutations in *MUT* (Table 3) and 19 were homozygotes (Table 4). In total, 54 different mutations in *MUT* were identified, spanning the entire coding region. Thirty-eight of the identified *MUT* mutations have been reported previously in the literature and 16 were novel. The novel mutations consisted of 1 initiation site mutation (c.2T>C; p.M1?), 1 missense mutation (c.566A>T; p.N189I, 2 nonsense mutations (c.1975C>T; p.Q659* and c.129G>A; p.W43*), 2 mutations located in splicing junctions (c.753+3A>G and c.754-2A>G), 8 small insertions, deletions, and duplications (c.795_796insT; p.M266Yfs*7, c.1240delG; p.E414Kfs*17, c.1061delCinsGGA; p.S354Wfs*20, c.631_633delGAG; p.E211del, c.29dupT; p.L10Ffs*39, c.1065_1068dupATGG; p.S357Mfs*5, c.1181dupT; p.L394Ffs*30, and c.55dupG; p.V19Gfs*30), and two copy number variants (CNVs) (c.146_147ins279 and a deletion encompassing exon 13). The 279bp insertion (c.146_147ins279) consists of a 183bp segment that aligns to the 3' untranslated region (UTR) of the alpha enolase (*ENO1)* gene on chromosome 1 and a ~96bp polyA repeat (Figure 6).

Table 3. Patients with heterozygous mutations in *MUT*

	WG #	Ethnicity	Age at biopsy	*mut* class	Prop. Inc	Prop. Inc + OHCbl	Gene	Mutation	Protein change	Protein Domain
1	3468	NR	13 months	mut^-	2.4	4.7	*MUT*	c.1A>G	p.M1?	MLS
							MUT	c.2150G>T	p.G717V	Cbl
2	3572	Palestinian	1 month	mut^0	1.5	1.5	*MUT*	**c.2T>C**	p.M1?	MLS
							MUT	c.1630_1631delGGinsTA	p.G544*	Link
							CD320	c.658G>A	p.G220R	
3	3427	Irish/Scottish /Polish	19 years	mut^0	1.2	1.2	*MUT*	**c.29dupT**	p.L10Ffs*39	MLS
							MUT	c.1658delT	p.V553Gfs*17	Link
4	3512	Black	2 years	mut^-	2.1	3.1	*MUT*	c.91C>T	p.R31*	MLS
							MUT	c.323G>A	p.R108H	TIM
							TCN2	c.89T>G	p.L30R	
5	3650	Korean	1 year 9 months	mut^0	0.7	0.7	*MUT*	c.91C>T	p.R31*	MLS
							MUT	c.349G>T	p.E117*	TIM
6	3473	White	2 months	mut^-	1.1	3.0	*MUT*	**c.129G>A**	p.W43*	NES
							MUT	c.299A>G	p.Y100C	TIM
7	3654	White	10 days	mut^0	0.4	0.5	*MUT*	**c.146_147ins279**	mRNA not detected	NES
							MUT	c.372_374dupGGA	p.K124_D125insE	TIM
8	3337	White/ Mexican	12 days	mut^0	0.8	1.0	*MUT*	c.322C>T	p.R108C	TIM
							MUT	c.654A>C	p.Q218H	TIM
9	3863	Hispanic	46 days	mut^0	0.8	1.2	*MUT*	c.322C>T	p.R108C	TIM
							MUT	c.654A>C	p.Q218H	TIM
10	3529	Northern European/ Filipino	6 days	mut^0	1.4	1.5	*MUT*	c.322C>T	p.R108C	TIM
							MUT	c.682C>T	p.R228*	TIM
11	3679	White/ Hispanic	6 years	mut^-	2.6	7.0	*MUT*	**c.566A>T**	p.N189I	TIM
							MUT	c.655A>T	p.N219Y	TIM
12	2700	NR	6 years	mut^-	0.5	1.3	*MUT*	c.556A>G	p.M186V	TIM
							MUT	c.1106G>A	p.R369H	TIM
13	3495	English/Irish	21 years	mut^0	1.5	1.5	*MUT*	c.572C>A	p.A191E	TIM
							MUT	c.682C>T	p.R228*	TIM
14	4055	White/ Australian	3 months	mut^0	0.5	0.5	*MUT*	c.572C>A	p.A191E	TIM
							MUT	c.682C>T	p.R228*	TIM
15	3869	White	3 weeks	mut^0	0.5	0.7	*MUT*	c.572C>A	p.A191E	TIM
							MUT	**c.754-2A>G**	Splice	N/A
16	3972	Lao/Thai/ Mexican/ Portugese	5 days	mut^0	0.6	0.5	*MUT*	c.581C>T	p.P194L	TIM
							MUT	c.682C>T	p.R228*	TIM
17	3499	Black	6 years	mut^0	0.6	0.6	*MUT*	**c.631_633delGAG**	p.E211del	TIM
							MUT	c.682C>T	p.R228*	TIM

							MCEE	c.428G>A	p.R143H	TIM
18	3374	French Canadian	2 months	*mut*^{0}	0.7	0.7	*MUT*	c.655A>T	p.N219Y	TIM
							MUT	**c.1240delG**	p.E414Kfs*17	TIM
19	3556	White	1 month	*mut*^{0}	1.2	1.0	*MUT*	c.655A>T	p.N219Y	TIM
							MUT	c.1332+1delG	Splice	N/A
20	3520	White	5 days	*mut*^{0}	2.1	1.9	*MUT*	c.682C>T	p.R228*	TIM
							MUT	c.1106G>A	p.R369H	TIM
21	3965	White	2 months	*mut*^{0}	0.6	0.6	*MUT*	c.682C>T	p.R228*	TIM
							MUT	c.1287C>G	p.Y429*	Link
22	3329	Korean	28 months	*mut*^{0}	0.8	0.8	*MUT*	c.682C>T	p.R228*	TIM
							MUT	c.1481T>A	p.L494*	Link
23	4169	French Canadian	3 months	*mut*^{0}	1.4	1.3	*MUT*	**c.753+3A>G**	Splice	N/A
							MUT	c.1332+1delG	Splice	N/A
24	3637	NR	NR	*mut*^{0}	0.4	0.4	*MUT*	**c.795_796insT**	p.M266Yfs*7	TIM
							MUT	c.1207C>T	p.R403*	TIM
25	3602	White	25 years	*mut*^{0}	1.3	1.2	*MUT*	c.935G>T	p.G312V	TIM
							MUT	c.1909G>A	p.G637R	Cbl
26	3760	Hispanic	7 years	*mut*$^-$	4.5	7.2	*MUT*	c.970G>A	p.A324T	TIM
							MUT	c.1846C>T	p.P649L	Cbl
27	3669	Afghani	3 weeks	*mut*^{0}	0.4	0.4	*MUT*	**c.1061delCinsGGA**	p.S354Wfs*20	TIM
							MUT	**c.1065_1068dupATGG**	p.S357Mfs*5	TIM
28	3310	European	1 year, 1 month	*mut*^{0}	1.1	1.2	*MUT*	**c.1181dupT**	p.L394Ffs*30	TIM
							MUT	**c.1975C>T**	p.Q659*	Cbl
29	3707	Chinese	3 months	*mut*^{0}	0.3	0.6	*MUT*	c.1280G>A	p.G427D	Link
							MUT	**Exon 13 deletion**		Cbl
							TCN2	c.509G>A	p.R170Q	

Novel mutations are in **bold** font. DNA nucleotide +1 is the A of the ATG translation initiation codon in the reference sequence (*MUT*: NM_000255.3, *TCN2*: NM_000355.3, *CD320*: NM_016579.3, *MCEE*: NM_032601.3). Prop. Inc. = [^{14}C]-labeled propionate incorporation; values are given in nmol/mg protein/18h (reference [mean ± SD]: 13.1 ± 4.1, n=217; *mut*: 0.9 ± 0.7, n=190). Prop. Inc + OHCbl = [^{14}C]-labeled propionate incorporation with hydroxocobalamin supplementation. FS = translational frameshift. NR = no record. N/A = not applicable. MLS = mitochondrial leader sequence. NES = N-terminal extended segment. Link = Linker region. TIM = N-terminal $(\beta\alpha)_8$ TIM barrel domain. Cbl = C-terminal $(\beta\alpha)_5$ cobalamin-binding Rossmann domain. Tables are ordered by the location of the mutations, starting with the most 5' mutation.

Follow-up analyses were performed to confirm the identified CNVs. The existence of the c.146_147ins279 mutation identified in WG3654 was confirmed with PCR using primers designed to specifically amplify the insertion-containing allele (Figure 6). No such amplification product was obtained when template DNA from a healthy control was used in the PCR reaction. The large deletion encompassing exon 13 was initially detected in WG3707 through depth-analysis of the NGS data. Microarray-based genomic hybridization (aCGH) confirmed the presence of the deletion in this patient's DNA.

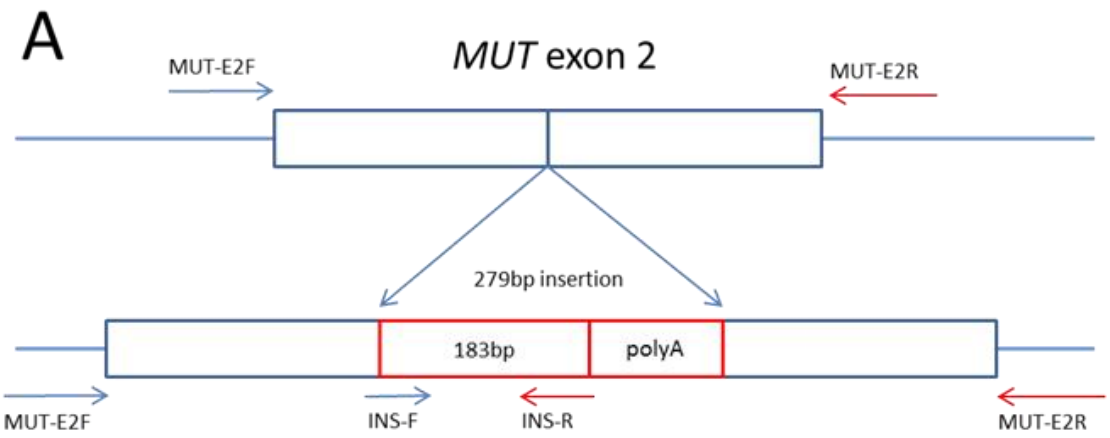

B

Lane	Sample	Primer pair
A	Control	MUT-E2F/INS-R
B	WG3654	MUT-E2F/INS-R
C	Control	INS-F/MUT-E2R
D	WG3654	INS-F/MUT-E2R
E	Control	MUT-E2F/MUT-E2R
F	WG3654	MUT-E2F/MUT-E2R
NTC	N/A	N/A

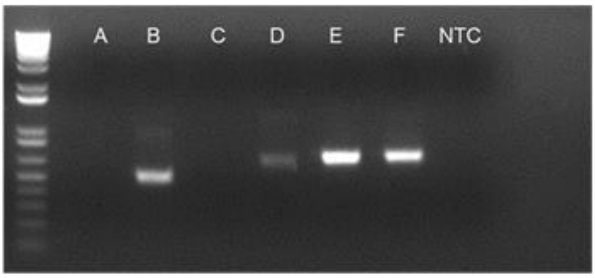

Figure 6. Allele-specific PCR amplification of c.146_147ins279 mutation in WG3654. A: Schematic of the c.146_147ins279 mutation identified in WG3654. Forward (blue) and reverse (red) primers are shown as arrows. The schematic is not to scale. B: PCR amplification of DNA from WG3654 using primers designed to specifically amplify the allele carrying the c.146_147ins279 mutation. NTC = no template control. N/A = not applicable.

Nineteen patients were found to have homozygous mutations in *MUT* (Table 4). As the NGS panel is able to detect CNVs, hemizygosity resulting from a major deletion affecting the second allele could be ruled out in these patients. A total of 17 different homozygous mutations were seen, including a novel c.55dupG mutation in WG3794 that was associated with a *mut*^{0} biochemical phenotype. Eleven of the homozygous mutations were missense mutations, 3 were nonsense mutations, and 3 were indels leading to translational frameshift and a premature

termination codon. The high incidence of homozygosity in this cohort of patients is partially explained by the prevalence of recurrent mutations. Hispanic patients WG3336, WG3361, and WG3742 were found to have the common c.322C>T (p.R108C) Hispanic mutation. WG3439 was found to have the common c.1280G>A (p.G427D) Asian mutation and WG3397 was found to have the recurrent c.2150G>T (p.G717V) black mutation. Parental consanguinity was documented in 4 patients (WG3784, WG3325, WG3721, and WG3482). In the remaining 10 patients who were found to have homozygous non-recurrent mutations, the status of parental consanguinity was not reported.

Table 4. Patients with homozygous mutations in *MUT*

	WG#	Ethnicity	Age at biopsy	*mut* class	Prop. Inc	Prop. Inc + OHCbl	Gene	Mutation	Protein change	Protein Domain
30	3794	Pakistani	6 weeks	*mut*^{0}	0.8	0.7	*MUT*	**c.55dupG**	p.V19Gfs*39	MLS
31[a]	3784	Indian	2 months	*mut*$^-$	0.7	1.9	*MUT*	c.257C>T	p.P86L	NES
32[a]	3325	Arab	10 years	*mut*^{0}	1.0	1.0	*MUT*	c.278G>A	p.R93H	TIM
33	3336	Hispanic	9 months	*mut*^{0}	1.0	1.3	*MUT*	c.322C>T	p.R108C	TIM
34	3361	White/Hispanic	3.5 weeks	*mut*^{0}	1.6	1.8	*MUT*	c.322C>T	p.R108C	TIM
35	3742	Hispanic	5 years	*mut*^{0}	0.5	0.7	*MUT*	c.322C>T	p.R108C	TIM
36[a]	3721	Hispanic	14 months	*mut*^{0}	0.7	0.8	*MUT*	c.406G>T	p.V136F	TIM
37	4027	Moroccan	18 months	*mut*^{0}	0.5	0.5	*MUT*	c.683G>A	p.R228Q	TIM
38	3426	German/Polish	9 years	*mut*^{0}	0.5	0.5	*MUT*	c.1106G>A	p.R369H	TIM
39[b]	3439	Asian	1 year	*mut*^{0}	1.4	1.5	*MUT*	c.1280G>A	p.G427D	Link
40[a]	3482	Middle Eastern	NR	*mut*^{0}	1.8	1.6	*MUT*	c.1420C>T	p.R474*	Link
41	3664	Pakistani	6 months	*mut*^{0}	0.6	0.6	*MUT*	c.1560G>C	p.K520N	Link
42	3705	Hmong	1 year, 7 months	*mut*$^-$	4.5	9.0	*MUT* *CUBN* *CUBN*	c.1663G>A c.3500G>T (het) c.6211A>G (het)	p.A555T p.G1167V p.I2071V	Link
43	3547	Lebanese	20 years	*mut*^{0}	1.4	1.1	*MUT*	c.1741C>T	p.R581*	Cbl
44	3820	Arab	13 years	*mut*^{0}	0.8	1.1	*MUT*	c.1871A>G	p.Q624R	Cbl
45	3599	Hispanic	1 month	*mut*^{0}	1.5	1.6	*MUT*	c.1891delG	p.A631Qfs*17	Cbl
46	3564	White	1 year	*mut*^{0}	1.0	0.9	*MUT*	c.1962_1963delTC	p.P654Pfs*2	Cbl
47[b]	3397	Barbadian	2 years, 7 months	*mut*$^-$	0.4	1.3	*MUT*	c.2150G>T	p.G717V	Cbl
48	3447	Indian	8 months	*mut*^{0}	1.1	1.1	*MUT*	c.2179C>T	p.R727*	Cbl

Novel mutations are in **bold** font. DNA nucleotide +1 is the A of the ATG translation initiation codon in the reference sequence (*MUT*: NM_000255.3, *CUBN*: NM_001081.3). Prop. Inc. = [^{14}C]-labeled propionate incorporation; values are given in nmol/mg protein/18h (reference [mean ± SD]: 13.1 ± 4.1, n=217; *mut*: 0.9 ± 0.7, n=190). Prop. Inc + OHCbl = [^{14}C]-labeled propionate incorporation with hydroxocobalamin supplementation. FS = translational frameshift. Het = heterozygous. MLS = mitochondrial leader sequence. NR = no record. NES = N-terminal extended segment. Link = Linker region. TIM = N-terminal $(\beta\alpha)_8$ TIM barrel domain. Cbl = C-terminal $(\beta\alpha)_5$ cobalamin-binding Rossmann domain.

[a]Documented consanguinity

[b]Reportedly non-consanguineous

No mutations in *MUT* were identified in 5/53 (9%) patients (Table 5). In WG2324 and WG2468, no mutations were detected in any of the genes on the panel. Two novel heterozygous variants (c.433G>A; p.E145K and c.511A>C; p.N171H) in *SUCLG1* were identified in WG2319. A novel heterozygous variant (c.273A>T; p.R91S) in *SUCLG2* was identified in WG3126 and a novel heterozygous variant in *HCFC1* was identified in WG3023.

Table 5. Patients with no mutations in *MUT*

#	WG#	Ethnicity	Age at biopsy	Initial Diagnosis	Prop. Inc	Prop. Inc + OHCbl	Gene	Mutation	Protein change
49	2324	White	13 years	*mut*^{0}	3.1	3.4	N/A	N/A	N/A
50	2468	German/Dutch	5 months	*mut*^{0}	3.0	2.8	N/A	N/A	N/A
51	2319	Irish/Italian	3 weeks	*mut*^{0}	1.0	0.9	*SUCLG1* *SUCLG1*	**c.433G>A** (het) **c.511A>C** (het)	p.E145K p.N171H
52	3126	White	3 months	*mut*^{0}	2.0	2.3	*SUCLG2*	**c.273A>T** (het)	p.R91S
53	3023 (female)	Arab/Turkish	4 months	*mut*^{0}	1.0	0.8	*HCFC1*	**c.4475C>T** (het)	p.P1492L

Novel variants are in **bold** font. DNA nucleotide +1 is the A of the ATG translation initiation codon in the reference sequence (*SUCLG1*: NM_003849.3, *SUCLG2*: NM_001177599.1, *HCFC1*: NM_005334.2). Prop. Inc. = [^{14}C]-labeled propionate incorporation; values are given in nmol/mg protein/18h (reference [mean ± SD]: 13.1 ± 4.1, n=217; *mut*: 0.9 ± 0.7, n=190). Prop. Inc + OHCbl = [^{14}C]-labeled propionate incorporation with hydroxocobalamin supplementation. Het = heterozygous. N/A = not applicable.

3.2. Functional analysis

Additional functional analyses were conducted on 3 patients (WG3499, WG3654, and WG3126) who had atypical sequencing findings.

3.2.1. WG3499

WG3499 was found to be heterozygous for the novel c.631_633delGAG (p.E211del) change and the c.628C>T (p.R228*) mutation. RT-PCR amplification of the *MUT* open reading frame identified loss of heterozygosity for the p.E211del mutation as well as common polymorphisms (data not shown), suggesting that the p.R228* leads to nonsense mediated decay of the transcript. A heterozygous c.428G>A (p.R143H) variant in the *MCEE* gene was also identified in this patient. Retroviral transduction of the wild-type *MUT* gene was used to confirm that a deficiency in MCM was responsible for the patient's phenotype (Figure 7). Propionate incorporation of untransduced fibroblasts was 1.4nmol/mg protein/18hr (reference [mean ± SD]: 13.1 ± 4.1, n=217; mut: 0.9 ± 0.7, n=190). Propionate incorporation of transduced cells was within the reference range at 12.5nmol/mg protein/18hr. These findings suggest correction of the MCM deficiency following transduction.

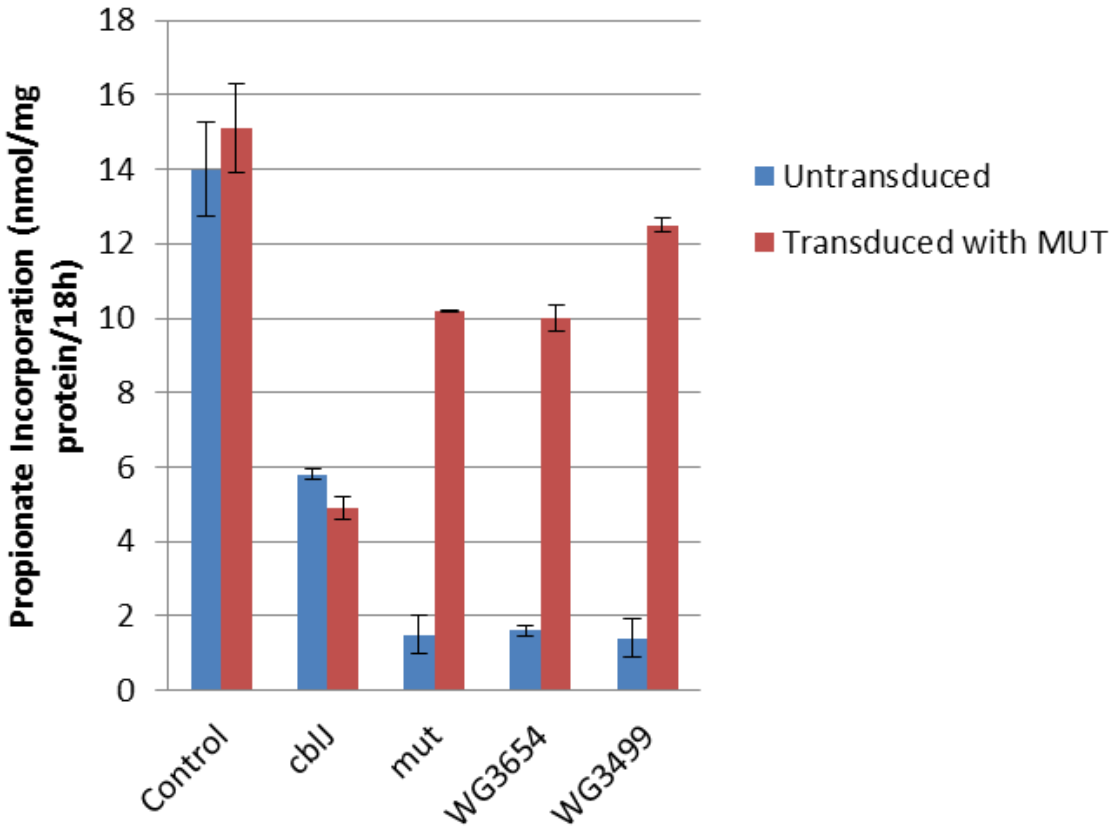

Figure 7. Phenotypic rescue studies for WG3654 and WG3499. Propionate incorporation in fibroblasts from WG3654 and WG3499, a *cblJ* patient, a *mut* patient with known mutations, and a healthy individual following retroviral transduction with the wild-type *MUT* gene. Propionate incorporation; reference [mean ± SD]: 13.1 ± 4.1, n=217; *mut* patients: 0.9 ±0.7, n = 190.

3.2.2. WG3654

WG3654 was found to be compound heterozygous for the c.146_147ins279 and c.372_374dupGGA (p.K124_D125insE) mutations in *MUT*. RT-PCR amplification of the *MUT* open reading frame identified loss of heterozygosity for the c.372_374dupGGA mutation and 3 common polymorphisms (c.636G>A, c.1595G>A, and c.2011A>G), suggesting that the c.146_147ins279 mutation results in an unstable transcript (Figure 8). Retroviral transduction of

the wild-type *MUT* gene into immortalized fibroblasts from WG3654 was used to confirm that the identified mutations in *MUT* were associated with the patient's cellular phenotype. Propionate incorporation of untransduced and transduced cells was found to be 1.6 and 10.0nmol/mg protein/18hr (Figure 7), respectively, suggesting transduction of the wild-type *MUT* gene rescued the deficiency of MCM.

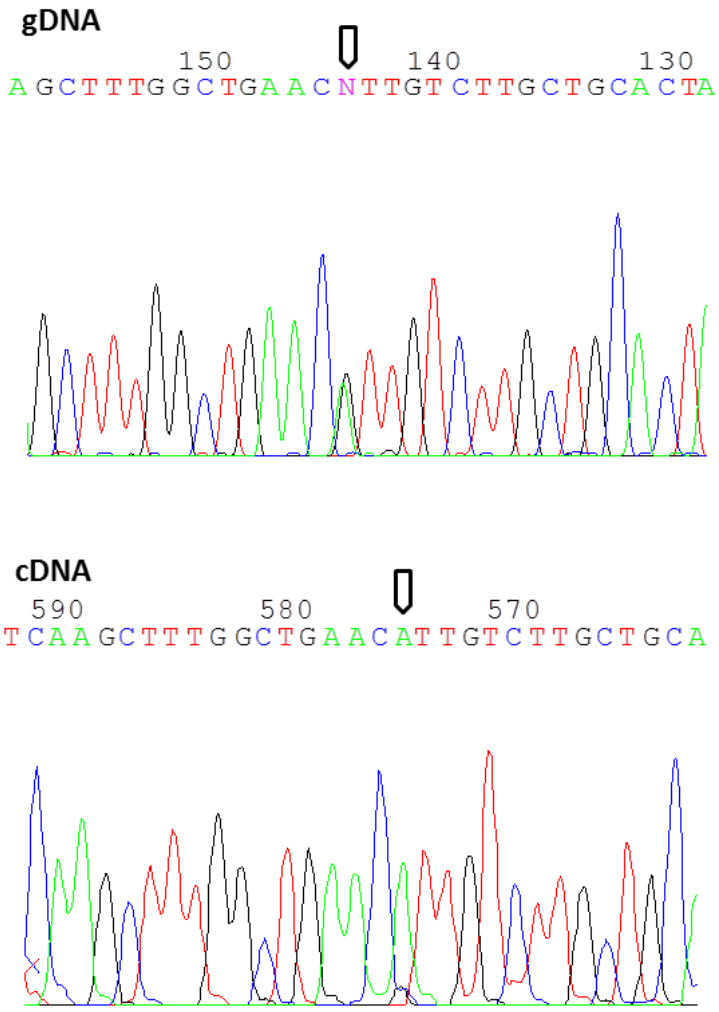

Figure 8. Analysis of cDNA from WG3654. Sanger sequencing of gDNA (top) and cDNA (bottom) from WG3654 identified loss of heterozygosity for the c.1595G>A common polymorphism (arrows).

3.2.3. WG3126

A single novel heterozygous c.273A>T (p.R91S) variant in *SUCLG2* was identified in WG3126. Review of the somatic cell complementation data that was initially used to diagnosis this patient was subsequently found to be unclear, putting the initial *mut* diagnosis into question. Retroviral transduction of the wild-type *SUCLG2* gene was used to assess whether a deficiency in *SUCLG2* was responsible for the patient's deficiency in propionyl-CoA metabolism. Propionate incorporation of untransduced and *SUCLG2*-transduced WG3126 fibroblasts was 2.5 and 5.3nmol/mg protein/18hr, suggesting partial correction of the defect in propionyl-CoA metabolism (Figure 9). RT-PCR amplification of the *SUCLG2* transcript revealed expression of both alleles and confirmed the existence of the c.273A>T variant. No splicing defects, deletions, or insertions were detected in the cDNA. Western blot analysis revealed significantly reduced levels of SUCLG2 protein abundance (Figure 10). The relative intensity of SUCLG2 protein to β-actin levels was 0.11 in WG3126 fibroblasts and 0.91 in control fibroblasts (Figure 10).

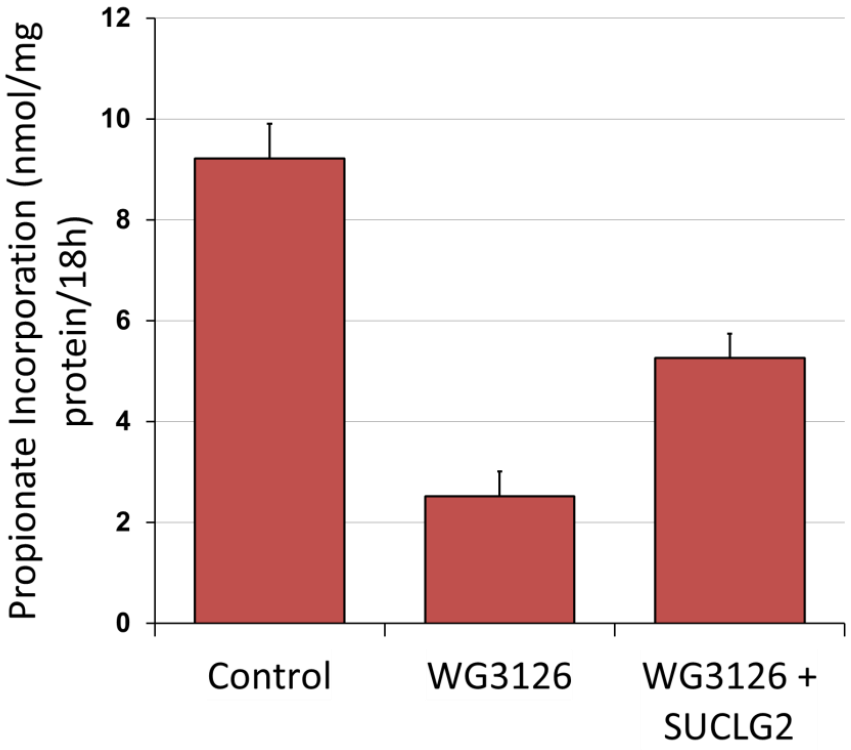

Figure 9. SUCLG2 correction studies for WG3126. Propionate incorporation was assessed in fibroblasts from WG3126 following retroviral transduction with the wild-type *SUCLG2* open reading frame. Propionate incorporation; reference [mean ± SD]: 13.1 ± 4.1, n=217.

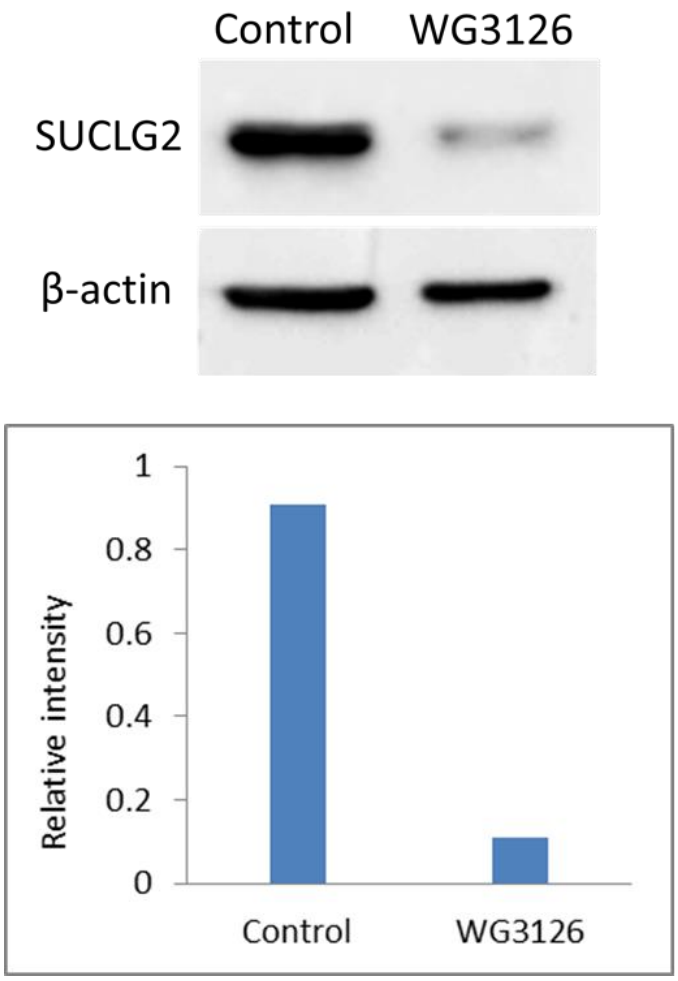

Figure 10. SUCLG2 western blot analysis for WG3126. Equal amounts of total protein extracts from a healthy individual and WG3126 were subjected to SDS-PAGE and subsequently transferred to a PVDF membrane. The membrane was then exposed to anti-SUCLG2 and anti-β-actin antibodies (top). The relative SUCLG2:β-actin intensities are shown (bottom).

CHAPTER 4

Discussion

In this study, 53 patients who had been diagnosed with *mut* MMA by somatic cell complementation analysis were studied using a NGS-based gene panel comprising the genes involved in cobalamin metabolism and absorption. Heterozygous mutations in *MUT* were identified in 29 patients, homozygous mutations were identified in 19 patients, and the remaining 5 patients were found to have no mutations in *MUT*.

4.1. Novel mutations

A total of 54 different *MUT* gene mutations were detected in this study, including 16 which have not been previously reported in the literature (Figure 11). All of the novel mutations, except for the c.1240delG and c.753-3A>G mutations, have not been reported in the Exome Aggregation Consortium (ExAc) database. The c.1240delG and c.753-3A>G mutations have each been documented as singletons in the database (allele frequency = 0.000008). These findings suggests that the novel mutations identified in this study are very rare changes, consistent with the observation that many *MUT* gene mutations are private mutations that exist in a single family. Fourteen of the 16 novel mutations were associated with a mut^0 phenotype.

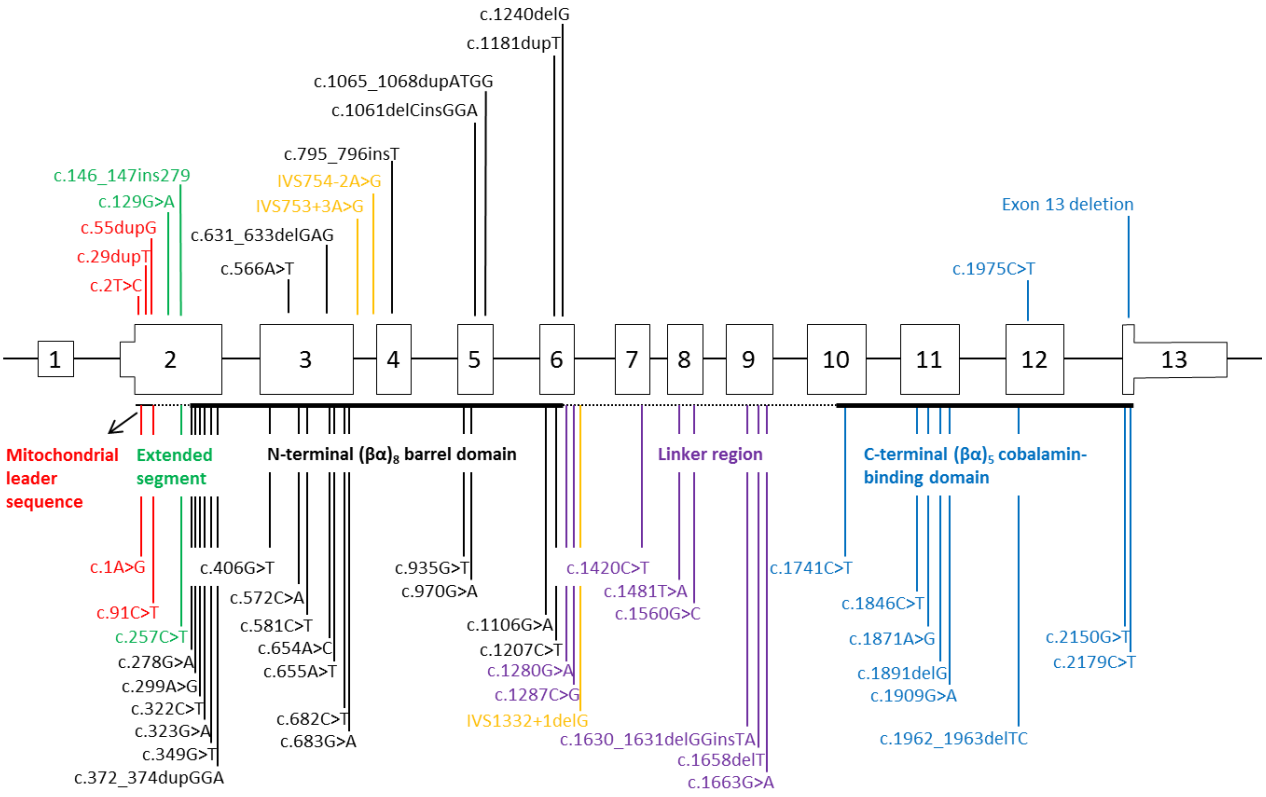

Figure 11. Distribution of identified *MUT* gene mutations. The mutations identified in the mitochondrial leader sequence (red), the N-terminal extended segment (green), the N-terminal $(\beta\alpha)_8$ barrel domain (black), splicing junctions (gold), the linker region (purple), and the C-terminal $(\beta\alpha)_5$ cobalamin-binding domain are depicted. Mutations that have been previously reported in the literature are shown below the schematic and novel mutations are depicted above.

4.1.1. Missense mutation

A novel c.566A>T (p.N189I) missense variant was identified in the heterozygous state in WG3679. This patient was diagnosed as *mut*$^-$ based on the finding that fibroblasts from this patient exhibited a robust response to hydroxocobalamin in culture. WG3679 was also found to be heterozygous for the common c.655A>T (p.N219Y) Caucasian mutation, which has been previously associated with a *mut*^{0} biochemical phenotype by transfection studies (Acquaviva et

al. 2001).. These findings suggest that the p.N189I mutation is associated with a *mut*$^-$ phenotype, consistent with the notion that *mut*$^-$ mutations have a dominant effect over *mut*^{0} mutations. The p.N189I mutation affects the N-terminal $(\beta\alpha)_8$ barrel domain and results in the substitution of an isoleucine residue for an asparagine. This change represents an alteration to the polarity of the original amino acid and is predicted to be disease-causing by three damage-prediction algorithms (SIFT, PolyPhen2, and Mutation Taster). The observation that the p.N189I mutation is associated with a *mut*$^-$ phenotype appears to be an exception to the general trend that mutations affecting the N-terminal $(\beta\alpha)_8$ barrel domain are associated with a *mut*^{0} phenotype.

4.1.2. Initiation site mutation

The novel c.2T>C (p.M1?) mutation was identified in the heterozygous state in the *mut*^{0} patient WG3572, who was also found to be heterozygous for the c.1630_1631delGGinsTA (p.G544*) mutation. The p.M1? mutation results in elimination of the transcription start site and is predicted to be damaging by prediction algorithms. As the nearest in-frame AUG initiation codon is 78 amino acids downstream of the p.M1? mutation, any peptide produced with this codon serving as the new initiation site would lack the mitochondrial leader sequence in its entirety. Mutations that abolish the mitochondrial leader sequence have been shown to be deleterious to MCM function and are associated with a *mut*^{0} phenotype (Ledley et al. 1990).

4.1.3. Nonsense mutations

Two novel mutations –c.1975C>T (p.Q659*) and c.129G>A (p.W43*) – that directly introduce a premature termination codon were identified in this study. The p.Q659* mutation was found in the heterozygous state in the *mut*^{0} patient WG3310, who was also found to carry a novel c.1181dupT (p.L394Ffs*30) mutation. If the transcript carrying the p.Q659* mutation

escapes nonsense mediated decay, it is possible that the allele carrying this mutation produces a truncated protein that lacks the cobalamin-binding domain. The heterozygous p.W43* mutation was found in WG3473. WG3473 was diagnosed as *mut*$^{-}$ given that the patient's cells demonstrate a mild response to cobalamin in culture. This patient was also found to carry the heterozygous c.299A>C (p.Y100C) mutation which has been previously associated with the *mut*$^{-}$ phenotype (Lempp et al. 2007). As such, in this instance it is not possible to determine whether the p.W43* mutation is associated a *mut*^{0} or *mut*$^{-}$ phenotype. However, given that the premature stop codon is introduced early in the transcript, it is likely that the mutated allele results in complete loss of MCM function and is associated with *mut*^{0}.

4.1.4. Consensus splice-site mutations

Two novel mutations affecting nucleotides in consensus splice site sequences were identified. WG4169 was found to be heterozygous for the c.753+3A>G mutation, which is predicted to abolish the 5' donor site of intron 3 by the Berkeley Drosophila Genome Project Splice Site Prediction tool (www.fruitfly.org/seq_tools/splice.html). The c.754-2A>G mutation, identified as a heterozygous change in WG3869, is predicted to eliminate the 3' acceptor site of intron 3. Both mutations were identified in *mut*^{0} patients.

4.1.5. Small insertions, deletions, and duplications

Eight novel indels, consisting of one small insertion (c.795_796insT), three small deletions (c.1240delG, c.1061_1062delCT, and c.631_633delGAG), and four small duplications (c.29dupT, c.1065_1068dupATGG, c.1181dupT, and c.55dupG) were identified in this study and all were associated with a *mut*^{0} phenotype. Only the c.631_633delGAG mutation leads to an in-

frame protein change. The remaining novel indels are out-of-frame alterations that result in translational frameshift and a premature termination codon.

The novel c.631_633delGAG (p.E211del) mutation was identified as a heterozygous change in WG3499. This patient was diagnosed as *mut*^{0} and was also found to carry a heterozygous c.682C>T (p.R228X) nonsense mutation. The p.E211del mutation results in the deletion of a glutamic acid residue from the N-terminal TIM barrel domain and is predicted to be disease-causing. PCR amplification of cDNA from WG3499 revealed loss of heterozygosity for the p.E211del mutation and the c.636G>A, c.1595G>A, and c.2011A>G common polymorphisms, suggesting that the allele carrying the p.R228X mutation is subjected to nonsense mediated decay. These findings also indicate that the p.R228X and p.E211del mutations are in *trans* configuration. Retroviral transduction of the wild-type *MUT* gene into immortalized WG3499 fibroblasts led to correction of propionate incorporation to within the reference range. These findings suggest that a deficiency in MCM, secondary to the p.E211del and p.R228X mutations in *MUT*, is responsible for the patient's MMA. A heterozygous c.428G>A (p.R143H) variant in the *MCEE* gene was also identified in this patient. However, given that transduction of *MUT* leads to complete rescue of propionyl-CoA metabolism, it is unlikely that this variant is associated with the patient's phenotype. Furthermore, the allelic frequency of the c.428G>A *MCEE* variant is 0.02 in the ExAc database. This frequency is considerably higher than those typical of MMA-causing mutations.

4.1.6. CNVs

A novel large deletion encompassing all of exon 13 was identified in the heterozygous state in WG3707, who was diagnosed as *mut*^{0} and also found to carry the heterozygous

c.1280G>A (p.G427D) mutation. This large deletion was initially detected by depth analysis of the NGS data. It was found that the normalized mean coverage of exon 13 was approximately half that of all other exons. Analysis through aCGH confirmed the presence of the deletion. The precise breakpoints of the deletion were not identified in this study. However, the copy number of a marker located approximately 400kb downstream of the *MUT* gene did not deviate from the reference value, indicating that the deletion does not extend beyond this marker.

WG3654 was found to carry a novel large c.146_147ins279 insertion in the heterozygous state as well as a heterozygous c.372_374dupGGA (p.K124_D125insE) mutation. The latter mutation has not been previously reported in the literature, however it has been documented in the ClinVar database as a "likely pathogenic" variant. The c.146_147ins279 insertion is the largest known insertion mutation in the *MUT* gene to date. This 279bp insertion is comprised of an 183bp segment that aligns to the 3'UTR of the *ENO1* gene on chromosome 1 (8861004-8861186) and a ~96bp polyA repeat. Allele-specific PCR confirmed the presence of the insertion in the DNA of WG3654. RT-PCR revealed loss of heterozygosity for the c.372_374dupGGA mutation and the c.636G>A, c.1595G>A, and c.2011A>G common polymorphisms, suggesting that instability of the insertion-containing allele results in monoallelic expression of the allele carrying the c.372_374dupGGA mutation. These findings also provide evidence that the identified mutations are in *trans.* Retroviral transduction of the wild-type *MUT* gene into immortalized fibroblasts from WG3654 led to full correction of propionate incorporation, suggesting that the 279bp insertion and the c.372_374dupGGA mutation are causative of the patient's phenotype.

4.2. Patients with no mutations in *MUT*

No *MUT* gene mutations were identified in 5/53 (94%) patients (Table 5). A subsequent review of the somatic cell complementation findings used to diagnose these patients found the data to be equivocal. All 5 patients were initially diagnosed as "atypical *mut*" patients based on the observation that their clinical presentations were inconsistent with what is typically associated with *mut* MMA. In light of the atypical clinical phenotypes, unclear complementation studies, and absence of *MUT* mutations in these patients, it is likely that these patients were misdiagnosed with *mut* MMA.

4.2.1. WG2324 and WG2468

Gene panel analysis did not detect mutations in any of the genes studied for patients WG2324 and WG2468. WG2324 is a Caucasian female that had moderate mental retardation and a history of nonspecific neonatal problems. Organic acids were normal. A skin biopsy was taken at 13 years and propionate incorporation was assessed to be 3.1nmol/mg protein/18h (reference [mean ± SD]: 13.1 ± 4.1, n=217; mut patients: 0.9 ± 0.7, n=187), which did not improve following hydroxocobalamin supplementation. The patient's clinical phenotype did not include elevated levels of methylmalonic acid and is not consistent with that of previously described *mut* patients. WG2468 experienced symptoms of developmental delay, failure to thrive, abnormal posturing, and crystals in urine. Elevated fat metabolites were detected in urine which is not typical for patients with *mut* MMA. Biopsy was taken at 5 months of age and propionate incorporation was found to be 3.0nmol/mg protein/18h and did not increase with hydroxocobalamin supplementation. It is unlikely that WG2324 and WG2468 have *mut* MMA as their clinical phenotypes are inconsistent with the *mut* phenotype and the complementation data

for these patients was eventually found to be inconclusive. Propionate incorporation was determined to be low for both patients, suggesting that the patients have non-*MUT* defects affecting propionyl-CoA metabolism. As sequencing analysis was negative for all of the genes examined, no alternative explanation of the patients' symptoms and biochemical phenotypes is offered. These patients may have mutations in genes that are not currently associated with cobalamin or propionyl-CoA metabolism, such as those involved in the proposed cobalamin-independent propionyl-CoA metabolic pathway (Figure 4).

4.2.2. WG2319

Two novel heterozygous variants (c.433G>A [p.E145K] and c.511A>C [p.N171H]) in the *SUCLG1* gene were identified in WG2319. Both variants are predicted to be damaging by prediction algorithms. Mutations in *SUCLG1* are associated with a deficiency in SUCL activity leading to mtDNA depletion, encephalomyopathy, and mild MMA. Baseline propionate incorporation for WG2319 was 1.0nmol/mg protein/18h and was not stimulated by hydroxocobalamin supplementation, consistent with both mut^0 patients and patients with *SULG1* mutations. Somatic cell complementation analysis was difficult to interpret as, interestingly, the patient's fibroblasts did not robustly complement *cblA* and *cblB* fibroblasts. The patient presented with severe metabolic acidosis, mildly elevated levels of MMA, and elevated levels of lactic acid in the early stages of life, consistent with the clinical presentations of previously-published patients with *SUCLG1* mutations (Ostergaard et al. 2007). Elevations of lactic acid are not usually seen in *mut* patients. The patient also exhibited sensorineural hearing loss which is not typical for *mut* MMA but has been described previously in a patient with mutations in *SUCLG1* (Van Hove et al. 2010). In light of these findings, the identified variants in *SUCLG1* appear to be responsible for the patient's disease.

4.2.3. WG3023

A single novel heterozygous c.4475C>T (p.P1492L) variant in the *HCFC1* gene was identified in the female patient WG3023. The clinical presentation of this patient comprised MMA, developmental delay, and infantile spasms. Mutations in *HCFC1* are associated with the *cblX* disorder, which is an X-linked disorder that presents as a cellular phenocopy of the *cblC* disorder (Yu et al. 2013). The *cblX* disorder typically consists of decreased synthesis of both cobalamin cofactors and no female *cblX* patient has been reported to date. The c.4475C>T variant identified in this patient alters a proline residue in the acidic domain of the protein while all other *HCFC1* mutations identified in *cblX* patients affect the N-terminal Kelch domain. Synthesis of cobalamin derivatives was found to be normal in fibroblasts from WG3023, inconsistent with the *cblX* phenotype. The patient's baseline level of propionate incorporation was 1.0 nmol/mg protein/18h and did not improve following hydroxocobalamin supplementation, suggesting a defect in propionyl-CoA metabolism. The cellular and genetic findings in this patient do not suggest a deficiency in either *MUT* or *HCFC1* and it is unlikely that the identified variant in *HCFC1* contributes to the patient's phenotype. It is possible that this patient has a deficiency in a gene not currently known to be involved in propionyl-CoA or cobalamin metabolism.

4.2.4. WG3126

WG3126 was found to have a novel heterozygous variant (c.273A>T, p.R91S) in *SUCLG2.* The clinical presentation of this patient included MMA and sudden infant death syndrome. Propionate incorporation was found to be 2.0nmol/mg protein/18hr and did not increase following cobalamin supplementation. Considering mutations in *SUCLG2* have not

been associated with a human disease, the relevance of this variant to the patient's phenotype warranted further investigation. Retroviral transduction of the wild-type *SUCLG2* open reading frame into fibroblasts from WG3126 resulted in 2-fold correction of propionate incorporation towards the reference range, suggesting that a deficiency in *SUCLG2* contributes to the patient's phenotype. RT-PCR amplification of *SUCLG2* cDNA revealed no splicing defects and SNP-analysis confirmed that transcripts from both alleles were being expressed. Western blot analysis of total protein extracts from WG3126 revealed significantly reduced SUCLG2 protein levels (12%) compared to control. This level of SUCLG2 protein abundance is unexpectedly low even if it is assumed that the heterozygous p.R91S change produces an unstable protein. Overall, these findings suggest that an unidentified second genetic defect, such as a regulatory or epigenetic mutation, may be responsible for the patient's decreased levels of SUCLG2 protein. It may be true that mutations in *SUCLG2* are associated with the patient's MMA, although more evidence is needed to support this claim.

4.3. Spectrum of *MUT* gene mutations

In this study, *MUT* gene mutations spanning the entire open reading frame were identified. At least one mutation was detected in each coding exon. No mutations were detected in exon 1, which is entirely untranslated and has an unknown function. To date, no mutations have been reported in exon 1 which is only 36 nucleotides in length. Further research is needed to determine the physiological role of this exon, which is conserved in a wide array of species ranging from humans to bacteria. The phase of mutations was not determined for most patients due to inaccessibility of parental DNA. However, as these patients have been diagnosed as *mut*

by somatic cell complementation analysis and their clinical presentations are consistent with *mut* MMA, it is expected that the identified mutations are pathogenic and in *trans* configuration.

Nearly half of the identified *MUT* gene mutations (25/54; 46%) were localized to the N-terminal TIM barrel domain and 10 (19%) were identified in the C-terminal cobalamin-binding domain. As mutations affecting the TIM barrel domain and the cobalamin-binding domain are generally associated with the mut^0 and mut^- phenotypes, respectively, this uneven distribution of mutations is consistent with the high proportion of mut^0 patients included in this study. Five mutations (9%) were identified in the mitochondrial leader sequence, 3 (6%) were identified in the N-terminal extended segment, and 3 (6%) were identified in splicing junctions. The remaining 8 (15%) mutations affect the linker region. The distribution of *MUT* gene mutations identified in this study, which favours the TIM barrel and cobalamin-binding domains, is consistent with that of previous molecular analyses of *mut* patients (Forny et al. 2016a) as well as with the overall distribution of known mutations (Froese and Gravel 2010).

4.4. Somatic cell complementation analysis vs. NGS

Complementation analysis and NGS-based gene panel analysis are both common clinical tests that are used for achieving diagnosis of inherited MMA. In this study, *MUT* gene mutations were identified in all patients who had unequivocal complementation studies, corresponding to 100% sensitivity. Complementation data was equivocal for 5 patients, all of which were found to carry no mutations in *MUT*. The clinical presentations of these patients were found to be atypical and the diagnoses for these patients were re-evaluated in light of the molecular findings. Relatively high baseline levels of propionate incorporation, which can interfere with

complementation studies, partly explain these unexpected findings. It is reasonable to suggest that patients with suspected *mut* MMA who present with atypical clinical findings and uncharacteristically high levels of propionate incorporation stand to benefit most from molecular analysis of the *MUT* gene.

Recently, we have also shown that the gene panel analysis has excellent specificity as well. Out of 131 patients who had MMA of unknown genetic origin, only one patient was found to have two variants in *MUT* (Pupavac et al. 2016a). One variant was predicted to be benign and the other was of uncertain clinical significance. The identification of two CNVs in this study highlights the usefulness of NGS-based gene panels with high overall depth of coverage. Other sequencing methods, such as Sanger sequencing or whole exome analysis, would be less likely to detect such mutations.

With the development of NGS technologies, the role of somatic cell studies in the diagnosis of inborn errors of cobalamin metabolism has become less clear. The outstanding sensitivity and specificity that we have shown for NGS-based gene panel analysis in detecting mutations in *MUT* suggests that gene panel analysis is a reasonable first-line diagnostic approach. Considering many mutations in *MUT* are private mutations that are found in a single family, it can be expected that a high rate of novel mutations and variants of uncertain pathogenicity will continue to be identified. Propionate incorporation has value in determining the pathogenicity of such sequencing findings by assessing whether the identified variants disturb functional enzymatic activity. Complementation analysis can be useful to confirm the diagnosis of *mut* in patients who have been found to carry *MUT* gene mutations that are known to be deleterious. The primary advantage of complementation analysis is to distinguish the different forms of MMA and assign patients to one of the known complementation groups. If the

genetic defect of a patient is already known and propionate incorporation has been found to be low, complementation studies are not necessary to make the diagnosis. Nevertheless, complementation analysis may be used as an independent confirmatory test.

Summary and conclusions

In the work presented in this thesis, it has been shown that a combination of NGS-analysis and somatic cell studies is able to provide optimal diagnoses for patients with suspected *mut* MMA. For 48/53 patients, NGS analysis confirmed the *mut* diagnosis made by somatic cell studies and identified the causal mutations. Fifty-four mutations in *MUT* were identified in total, 16 of which have not been previously reported in the literature. No mutations in *MUT* were identified in 5 patients. After reviewing the somatic cell complementation data used to diagnose these patients, the *mut* diagnosis was put into question. One patient was found to have two novel mutations in *SUCLG1* which appear to be responsible for the patient's disease. Another patient was found to have a heterozygous variant in *SUCLG2* and early evidence suggests that this variant contributes to the patient's phenotype. However, further studies are needed to evaluate the suspected existence of a second genetic defect in *SUCLG2* to support that deficiency in this gene is responsible for the patient's phenotype. Finally, 3 patients with apparent defects in propionyl-CoA metabolism remain undiagnosed. Genome-wide analyses such as whole genome or whole exome sequencing may prove fruitful in these patients for identifying novel genetic loci associated with propionyl-CoA or cobalamin metabolism.

Original contributions to science

The following are original contributions to the understanding of MMA.

1. Identification of 16 novel pathogenic mutations in the *MUT* gene which expand of spectrum of known mutations that cause *mut* MMA
2. Identification of 2 novel mutations in the *SUCLG1* gene that are associated with *SUCLG1* deficiency
3. Evidence that retroviral transduction of the *SUCLG2* open reading frame into fibroblasts derived from a patient with a putative mutation in *SUCLG2* partially corrected the cellular phenotype. This is the first observation in patient-derived cells that deficiency in *SUCLG2* may be associated with a disease phenotype.
4. Direct comparison of the relative efficacies of NGS-based gene panel analysis and somatic cell complementation analysis in assessing *mut* MMA.

Bibliography

Acquaviva C, Benoist J-F, Pereira S, Callebaut I, Koskas T, Porquet D, Elion J. 2005. Molecular basis of methylmalonyl-CoA mutase apoenzyme defect in 40 European patients affected by mut(o) and mut- forms of methylmalonic acidemia: identification of 29 novel mutations in the MUT gene. Hum. Mutat. 25: 167–76.

Acquaviva C, Benoist JF, Callebaut I, Guffon N, Ogier de Baulny H, Touati G, Aydin A, Porquet D, Elion J. 2001. N219Y, a new frequent mutation among mut0 forms of methylmalonic acidemia in Caucasian patients. Eur. J. Hum. Genet. 9: 577–82.

Baker EH, Sloan JL, Hauser NS, Gropman AL, Adams DR, Toro C, Manoli I, Venditti CP. 2015. MRI characteristics of globus pallidus infarcts in isolated methylmalonic acidemia. AJNR. Am. J. Neuroradiol. 36: 194–201.

Banerjee R, Gherasim C, Padovani D. 2009. The tinker, tailor, soldier in intracellular B12 trafficking. Curr. Opin. Chem. Biol. 13: 484–91.

Batshaw ML, MacArthur RB, Tuchman M. 2001. Alternative pathway therapy for urea cycle disorders: Twenty years later. J. Pediatr. 138: S46–S55.

Baumgartner MR, Hörster F, Dionisi-Vici C, Haliloglu G, Karall D, Chapman KA, Huemer M, Hochuli M, Assoun M, Ballhausen D, Burlina A, Fowler B, et al. 2014. Proposed guidelines for the diagnosis and management of methylmalonic and propionic acidemia. Orphanet J. Rare Dis. 9: 130.

Beedholm-Ebsen R, Wetering K van de, Hardlei T, Nexø E, Borst P, Moestrup SK. 2010. Identification of multidrug resistance protein 1 (MRP1/ABCC1) as a molecular gate for cellular export of cobalamin. Blood 115: 1632–9.

Bikker H, Bakker HD, Abeling NGGM, Poll-The BT, Kleijer WJ, Rosenblatt DS, Waterham HR, Wanders RJA, Duran M. 2006. A homozygous nonsense mutation in the methylmalonyl-CoA epimerase gene (MCEE) results in mild methylmalonic aciduria. Hum. Mutat. 27: 640–3.

Birn H, Fyfe JC, Jacobsen C, Mounier F, Verroust PJ, Orskov H, Willnow TE, Moestrup SK, Christensen EI. 2000. Cubilin is an albumin binding protein important for renal tubular albumin reabsorption. J. Clin. Invest. 105: 1353–61.

Bobik TA, Rasche ME. 2001. Identification of the human methylmalonyl-CoA racemase gene based on the analysis of prokaryotic gene arrangements. Implications for decoding the human genome. J. Biol. Chem. 276: 37194–8.

Bor M V., Nexø E, Hvas A-M. 2004. Holo-Transcobalamin Concentration and Transcobalamin Saturation Reflect Recent Vitamin B12 Absorption Better than Does Serum Vitamin B12. Clin. Chem. 50: 1043–1049.

Borths EL, Poolman B, Hvorup RN, Locher KP, Rees DC. 2005. In vitro functional characterization of BtuCD-F, the Escherichia coli ABC transporter for vitamin B12 uptake. Biochemistry 44: 16301–9.

Brasil S, Richard E, Jorge-Finnigan A, Leal F, Merinero B, Banerjee R, Desviat LR, Ugarte M, Pérez B. 2015. Methylmalonic aciduria cblB type: characterization of two novel mutations and mitochondrial dysfunction studies. Clin. Genet. 87: 576–81.

Brassier A, Boyer O, Valayannopoulos V, Ottolenghi C, Krug P, Cosson MA, Touati G, Arnoux JB, Barbier V, Bahi-Buisson N, Desguerre I, Charbit M, et al. 2013. Renal transplantation in 4 patients with methylmalonic aciduria: a cell therapy for metabolic disease. Mol. Genet. Metab. 110: 106–10.

Burger RL, Schneider RJ, Mehlman CS, Allen RH. 1975. Human plasma R-type vitamin B12-binding proteins. II. The role of transcobalamin I, transcobalamin III, and the normal granulocyte vitamin B12-binding protein in the plasma transport of vitamin B12. J. Biol. Chem. 250: 7707–13.

Calcar SC Van, Baker MW, Williams P, Jones SA, Xiong B, Thao MC, Lee S, Yang MK, Rice GM, Rhead W, Vockley J, Hoffman G, et al. 2013. Prevalence and mutation analysis of short/branched chain acyl- CoA dehydrogenase deficiency (SBCADD) detected on newborn screening in Wisconsin HHS Public Access. Mol Genet Metab 110: 111–115.

Carmel R. 1983. Gastric juice in congenital pernicious anemia contains no immunoreactive intrinsic factor molecule: study of three kindreds with variable ages at presentation, including a patient first diagnosed in adulthood. Am. J. Hum. Genet. 35: 67–77.

Carmel R. 2003. Mild transcobalamin I (haptocorrin) deficiency and low serum cobalamin concentrations. Clin. Chem. 49: 1367–74.

Carmel R, Parker J, Kelman Z. 2009. Genomic mutations associated with mild and severe deficiencies of transcobalamin I (haptocorrin) that cause mildly and severely low serum cobalamin levels. Br. J. Haematol. 147: 386–91.

Carrillo-Carrasco N, Venditti C. 1993. Propionic Acidemia. University of Washington, Seattle.

Carrozzo R, Dionisi-Vici C, Steuerwald U, Lucioli S, Deodato F, Giandomenico S Di, Bertini E, Franke B, Kluijtmans LAJ, Meschini MC, Rizzo C, Piemonte F, et al. 2007. SUCLA2 mutations are associated with mild methylmalonic aciduria, Leigh-like encephalomyopathy, dystonia and deafness. Brain 130: 862–74.

Carrozzo R, Verrigni D, Rasmussen M, Coo R de, Amartino H, Bianchi M, Buhas D, Mesli S, Naess K, Born AP, Woldseth B, Prontera P, et al. 2016. Succinate-CoA ligase deficiency due to mutations in SUCLA2 and SUCLG1: phenotype and genotype correlations in 71 patients. J. Inherit. Metab. Dis. 39: 243–52.

Chace DH, DiPerna JC, Kalas TA, Johnson RW, Naylor EW. 2001. Rapid diagnosis of methylmalonic and propionic acidemias: quantitative tandem mass spectrometric analysis of propionylcarnitine in filter-paper blood specimens obtained from newborns. Clin. Chem. 47: 2040–4.

Chakrapani A, Sivakumar P, McKiernan PJ, Leonard J V. 2002. Metabolic stroke in methylmalonic acidemia five years after liver transplantation. J. Pediatr. 140: 261–3.

Chery C, Hehn A, Mrabet N, Oussalah A, Jeannesson E, Besseau C, Alberto J-M, Gross I, Josse T, Gérard P, Guéant-Rodriguez RM, Freund J-N, et al. 2013. Gastric intrinsic factor deficiency with combined GIF heterozygous mutations and FUT2 secretor variant. Biochimie 95: 995–1001.

Chu J, Pupavac M, Watkins D, Tian X, Feng Y, Chen S, Fenter R, Zhang VW, Wang J, Wong L-J, Rosenblatt DS. 2016. Next generation sequencing of patients with mut methylmalonic aciduria: Validation of somatic cell studies and identification of 16 novel mutations. Mol. Genet. Metab.

Coelho D, Kim JC, Miousse IR, Fung S, Moulin M du, Buers I, Suormala T, Burda P, Frapolli M, Stucki M, Nürnberg P, Thiele H, et al. 2012. Mutations in ABCD4 cause a new inborn error of vitamin B12 metabolism. Nat. Genet. 44: 1152–5.

Cosson MA, Benoist JF, Touati G, Déchaux M, Royer N, Grandin L, Jais JP, Boddaert N, Barbier V, Desguerre I, Campeau PM, Rabier D, et al. 2009. Long-term outcome in methylmalonic aciduria: a series of 30 French patients. Mol. Genet. Metab. 97: 172–8.

Dejosez M, Levine SS, Frampton GM, Whyte WA, Stratton SA, Barton MC, Gunaratne PH, Young RA, Zwaka TP. 2010. Ronin/Hcf-1 binds to a hyperconserved enhancer element and regulates genes involved in the growth of embryonic stem cells. Genes Dev. 24: 1479–84.

Deme JC, Miousse IR, Plesa M, Kim JC, Hancock MA, Mah W, Rosenblatt DS, Coulton JW. 2012. Structural features of recombinant MMADHC isoforms and their interactions with MMACHC, proteins of mammalian vitamin B12 metabolism. Mol. Genet. Metab. 107: 352–62.

Deodato F, Boenzi S, Santorelli FM, Dionisi-Vici C. 2006. Methylmalonic and propionic aciduria. Am. J. Med. Genet. C. Semin. Med. Genet. 142C: 104–12.

Dobolyi A, Bagó AG, Gál A, Molnár MJ, Palkovits M, Adam-Vizi V, Chinopoulos C. 2015a. Localization of SUCLA2 and SUCLG2 subunits of succinyl CoA ligase within the cerebral cortex suggests the absence of matrix substrate-level phosphorylation in glial cells of the human brain. J. Bioenerg. Biomembr. 47: 33–41.

Dobolyi A, Ostergaard E, Bagó AG, Dóczi T, Palkovits M, Gál A, Molnár MJ, Adam-Vizi V, Chinopoulos C. 2015b. Exclusive neuronal expression of SUCLA2 in the human brain. Brain Struct. Funct. 220: 135–51.

Dobson CM, Gradinger A, Longo N, Wu X, Leclerc D, Lerner-Ellis J, Lemieux M, Belair C, Watkins D, Rosenblatt DS, Gravel RA. 2006. Homozygous nonsense mutation in the MCEE gene and siRNA suppression of methylmalonyl-CoA epimerase expression: a novel cause of mild methylmalonic aciduria. Mol. Genet. Metab. 88: 327–33.

Dobson CM, Wai T, Leclerc D, Wilson A, Wu X, Doré C, Hudson T, Rosenblatt DS, Gravel RA. 2002. Identification of the gene responsible for the cblA complementation group of vitamin B12-responsive methylmalonic acidemia based on analysis of prokaryotic gene arrangements. Proc. Natl. Acad. Sci. U. S. A. 99: 15554–9.

Dror DK, Allen LH. 2008. Effect of vitamin B12 deficiency on neurodevelopment in infants:

current knowledge and possible mechanisms. Nutr. Rev. 66: 250–5.

Farwell Gonzalez KD, Li X, Lu H-M, Lu H, Pellegrino JE, Miller RT, Zeng W, Chao EC. 2015. Diagnostic Exome Sequencing and Tailored Bioinformatics of the Parents of a Deceased Child with Cobalamin Deficiency Suggests Digenic Inheritance of the MTR and LMBRD1 Genes. JIMD Rep. 15: 29–37.

Fedosov SN, Fedosova NU, Berglund L, Moestrup SK, Nexø E, Petersen TE. 2005. Composite organization of the cobalamin binding and cubilin recognition sites of intrinsic factor. Biochemistry 44: 3604–14.

Fedosov SN, Fedosova NU, Kräutler B, Nexø E, Petersen TE. 2007. Mechanisms of discrimination between cobalamins and their natural analogues during their binding to the specific B12-transporting proteins. Biochemistry 46: 6446–58.

Feng Y, Chen D, Wang G-L, Zhang VW, Wong L-JC. 2015. Improved molecular diagnosis by the detection of exonic deletions with target gene capture and deep sequencing. Genet. Med. 17: 99–107.

Fenton W a, Gravel R a, Rosenblatt DS. 2001. Disorders of Propionate and Methylmalonate Metabolism. Online Metab. Mol. Bases Inherit. Dis. 2165–2194.

Fenton WA, Hack AM, Kraus JP, Rosenberg LE. 1987. Immunochemical studies of fibroblasts from patients with methylmalonyl-CoA mutase apoenzyme deficiency: detection of a mutation interfering with mitochondrial import. Proc. Natl. Acad. Sci. U. S. A. 84: 1421–4.

Ferrand A, Siu VM, Rupar CA, Napier MP, Al-Dirbashi OY, Chakraborty P, Prasad C. 2015. Biochemical and Hematologic Manifestations of Gastric Intrinsic Factor (GIF) Deficiency: A Treatable Cause of B12 Deficiency in the Old Order Mennonite Population of Southwestern Ontario. JIMD Rep. 18: 69–77.

Forny P, Schnellmann A-S, Buerer C, Lutz S, Fowler B, Froese DS, Baumgartner MR. 2016a. Molecular Genetic Characterization of 151 Mut-Type Methylmalonic Aciduria Patients and Identification of 41 Novel Mutations in MUT. Hum. Mutat.

Forny P, Schumann A, Mustedanagic M, Mathis D, Wulf M-A, Naegele N, Langhans C-D, Zhakupova A, Heeren J, Scheja L, Fingerhut R, Peters HL, et al. 2016b. Novel Mouse Models of Methylmalonic Aciduria Recapitulate Phenotypic Traits with a Genetic Dosage Effect. J. Biol. Chem. jbc.M116.747717.

Francalanci F, Davis NK, Fuller JQ, Murfitt D, Leadlay PF. 1986. The subunit structure of methylmalonyl-CoA mutase from Propionibacterium shermanii. Biochem. J. 236: 489–94.

Frank S, Brindley AA, Deery E, Heathcote P, Lawrence AD, Leech HK, Pickersgill RW, Warren MJ, Scott AI, Warren MJ, Raux E, Schubert HL, et al. 2005. Anaerobic synthesis of vitamin B12: characterization of the early steps in the pathway. Biochem. Soc. Trans. 33: 811–4.

Froese DS, Gravel RA. 2010. Genetic disorders of vitamin B_{12} metabolism: eight complementation groups--eight genes. Expert Rev. Mol. Med. 12: e37.

Froese DS, Kochan G, Muniz JRC, Wu X, Gileadi C, Ugochukwu E, Krysztofinska E, Gravel RA, Oppermann U, Yue WW. 2010. Structures of the human GTPase MMAA and vitamin B12-dependent methylmalonyl-CoA mutase and insight into their complex formation. J. Biol. Chem. 285: 38204–13.

Fyfe JC, Madsen M, Højrup P, Christensen EI, Tanner SM, la Chapelle A de, He Q, Moestrup SK. 2004. The functional cobalamin (vitamin B12)-intrinsic factor receptor is a novel complex of cubilin and amnionless. Blood 103: 1573–9.

Gailus S, Suormala T, Malerczyk-Aktas AG, Toliat MR, Wittkampf T, Stucki M, Nürnberg P, Fowler B, Hennermann JB, Rutsch F. 2010. A novel mutation in LMBRD1 causes the cblF defect of vitamin B(12) metabolism in a Turkish patient. J. Inherit. Metab. Dis. 33: 17–24.

Gherasim C, Hannibal L, Rajagopalan D, Jacobsen DW, Banerjee R. 2013a. The C-terminal domain of CblD interacts with CblC and influences intracellular cobalamin partitioning. Biochimie 95: 1023–32.

Gherasim C, Lofgren M, Banerjee R. 2013b. Navigating the B12 Road: Assimilation, Delivery, and Disorders of Cobalamin. J. Biol. Chem. 288: 13186–13193.

Gordon MM, Brada N, Remacha A, Badell I, Río E del, Baiget M, Santer R, Quadros E V, Rothenberg SP, Alpers DH. 2004. A genetic polymorphism in the coding region of the gastric intrinsic factor gene (GIF) is associated with congenital intrinsic factor deficiency. Hum. Mutat. 23: 85–91.

Gradinger AB, Bélair C, Worgan LC, Li CD, Lavallée J, Roquis D, Watkins D, Rosenblatt DS. 2007. Atypical methylmalonic aciduria: frequency of mutations in the methylmalonyl CoA epimerase gene (MCEE). Hum. Mutat. 28: 1045.

Grarup N, Sulem P, Sandholt CH, Thorleifsson G, Ahluwalia TS, Steinthorsdottir V, Bjarnason H, Gudbjartsson DF, Magnusson OT, Sparsø T, Albrechtsen A, Kong A, et al. 2013. Genetic Architecture of Vitamin B12 and Folate Levels Uncovered Applying Deeply Sequenced Large Datasets. PLoS Genet. 9: e1003530.

Gräsbeck R. 2006. Imerslund-Gräsbeck syndrome (selective vitamin B(12) malabsorption with proteinuria). Orphanet J. Rare Dis. 1: 17.

Gravel RA, Mahoney MJ, Ruddle FH, Rosenberg LE. 1975. Genetic complementation in heterokaryons of human fibroblasts defective in cobalamin metabolism. Proc. Natl. Acad. Sci. U. S. A. 72: 3181–5.

Guez S, Chiarelli G, Menni F, Salera S, Principi N, Esposito S, Ludwig M, Matthews R, Stabler S, Allen R, Savage D, Lindenbaum J, et al. 2012. Severe vitamin B12 deficiency in an exclusively breastfed 5-month-old Italian infant born to a mother receiving multivitamin supplementation during pregnancy. BMC Pediatr. 12: 85.

Hall CA, Colligan PD, Begley JA. 1987. Cyclic activity of the receptors of cobalamin bound to transcobalamin II. J. Cell. Physiol. 133: 187–91.

Hannibal L, Kim J, Brasch NE, Wang S, Rosenblatt DS, Banerjee R, Jacobsen DW. 2009.

Processing of alkylcobalamins in mammalian cells: A role for the MMACHC (cblC) gene product. Mol. Genet. Metab. 97: 260–6.

Hazra A, Kraft P, Lazarus R, Chen C, Chanock SJ, Jacques P, Selhub J, Hunter DJ. 2009. Genome-wide significant predictors of metabolites in the one-carbon metabolism pathway. Hum. Mol. Genet. 18: 4677–87.

Heldt D, Lawrence AD, Lindenmeyer M, Deery E, Heathcote P, Rigby SE, Warren MJ. 2005. Aerobic synthesis of vitamin B 12 : ring contraction and cobalt chelation.

Homolova K, Zavadakova P, Doktor TK, Schroeder LD, Kozich V, Andresen BS. 2010. The deep intronic c.903+469T>C mutation in the MTRR gene creates an SF2/ASF binding exonic splicing enhancer, which leads to pseudoexon activation and causes the cblE type of homocystinuria. Hum. Mutat. 31: 437–44.

Hörster F, Baumgartner MR, Viardot C, Suormala T, Burgard P, Fowler B, Hoffmann GF, Garbade SF, Kölker S, Baumgartner ER. 2007. Long-term outcome in methylmalonic acidurias is influenced by the underlying defect (mut0, mut-, cblA, cblB). Pediatr. Res. 62: 225–30.

Hove JLK Van, Saenz MS, Thomas JA, Gallagher RC, Lovell MA, Fenton LZ, Shanske S, Myers SM, Wanders RJA, Ruiter J, Turkenburg M, Waterham HR. 2010. Succinyl-CoA ligase deficiency: a mitochondrial hepatoencephalomyopathy. Pediatr. Res. 68: 159–64.

Huemer M, Bürer C, Ješina P, Kožich V, Landolt MA, Suormala T, Fowler B, Augoustides-Savvopoulou P, Blair E, Brennerova K, Broomfield A, Meirleir L De, et al. 2015. Clinical onset and course, response to treatment and outcome in 24 patients with the cblE or cblG remethylation defect complemented by genetic and in vitro enzyme study data. J. Inherit. Metab. Dis. 38: 957–67.

Institute of Medicine (US) Standing Committee on the Scientific Evaluation of Dietary Reference Intakes and its Panel on Folate, Other B Vitamins and C. 1998. Dietary Reference Intakes for Thiamin, Riboflavin, Niacin, Vitamin B6, Folate, Vitamin B12, Pantothenic Acid, Biotin, and Choline. National Academies Press (US).

Janata J, Kogekar N, Fenton WA. 1997. Expression and kinetic characterization of methylmalonyl-CoA mutase from patients with the mut- phenotype: evidence for naturally occurring interallelic complementation. Hum. Mol. Genet. 6: 1457–64.

Jansen R, Kalousek F, Fenton WA, Rosenberg LE, Ledley FD. 1989. Cloning of full-length methylmalonyl-CoA mutase from a cDNA library using the polymerase chain reaction. Genomics 4: 198–205.

Johnson JD, Mehus JG, Tews K, Milavetz BI, Lambeth DO. 1998. Genetic Evidence for the Expression of ATP- and GTP-specific Succinyl-CoA Synthetases in Multicellular Eucaryotes. J. Biol. Chem. 273: 27580–27586.

Jorge-Finnigan A, Aguado C, Sánchez-Alcudia R, Abia D, Richard E, Merinero B, Gámez A, Banerjee R, Desviat LR, Ugarte M, Pérez B. 2010. Functional and structural analysis of five mutations identified in methylmalonic aciduria cblB type. Hum. Mutat. 31: 1033–42.

Jusufi J, Suormala T, Burda P, Fowler B, Froese DS, Baumgartner MR. 2014. Characterization of functional domains of the cblD (MMADHC) gene product. J. Inherit. Metab. Dis. 37: 841–9.

Kacso G, Ravasz D, Doczi J, Nemeth B, Madgar O, Saada A, Ilin P, Miller C, Ostergaard E, Iordanov I, Adams D, Vargedo Z, et al. 2016. Two transgenic mouse models for beta subunit components of succinate-CoA ligase yielding pleiotropic metabolic alterations. Biochem. J.

Kaplan P, Ficicioglu C, Mazur AT, Palmieri MJ, Berry GT. 2006. Liver transplantation is not curative for methylmalonic acidopathy caused by methylmalonyl-CoA mutase deficiency. Mol. Genet. Metab. 88: 322–6.

Kawaguchi K, Okamoto T, Morita M, Imanaka T. 2016. Translocation of the ABC transporter ABCD4 from the endoplasmic reticulum to lysosomes requires the escort protein LMBD1. Sci. Rep. 6: 30183.

Kim JC, Lee N-C, Hwu PW-L, Chien Y-H, Fahiminiya S, Majewski J, Watkins D, Rosenblatt DS. 2012. Late onset of symptoms in an atypical patient with the cblJ inborn error of vitamin B12 metabolism: diagnosis and novel mutation revealed by exome sequencing. Mol. Genet. Metab. 107: 664–8.

Kolhouse JF, Utley C, Fenton WA, Rosenberg LE. 1981. Immunochemical studies on cultured fibroblasts from patients with inherited methylmalonic acidemia. Proc. Natl. Acad. Sci. U. S. A. 78: 7737–41.

Kowluru A, Tannous M, Chen H-Q. 2002. Localization and characterization of the mitochondrial isoform of the nucleoside diphosphate kinase in the pancreatic beta cell: evidence for its complexation with mitochondrial succinyl-CoA synthetase. Arch. Biochem. Biophys. 398: 160–9.

Kozyraki R, Fyfe J, Kristiansen M, Gerdes C, Jacobsen C, Cui S, Christensen EI, Aminoff M, la Chapelle A de, Krahe R, Verroust PJ, Moestrup SK. 1999. The intrinsic factor-vitamin B12 receptor, cubilin, is a high-affinity apolipoprotein A-I receptor facilitating endocytosis of high-density lipoprotein. Nat. Med. 5: 656–61.

Kristiansen M, Aminoff M, Jacobsen C, La Chapelle A de, Krahe R, Verroust PJ, Moestrup SK. 2000. Cubilin P1297L mutation associated with hereditary megaloblastic anemia 1 causes impaired recognition of intrinsic factor-vitamin B(12) by cubilin. Blood 96: 405–9.

Lai S-C, Nakayama Y, Sequeira JM, Wlodarczyk BJ, Cabrera RM, Finnell RH, Bottiglieri T, Quadros E V. 2013. The transcobalamin receptor knockout mouse: a model for vitamin B12 deficiency in the central nervous system. FASEB J. 27: 2468–75.

Leclerc D, Odièvre M, Wu Q, Wilson A, Huizenga JJ, Rozen R, Scherer SW, Gravel RA. 1999. Molecular cloning, expression and physical mapping of the human methionine synthase reductase gene. Gene 240: 75–88.

Ledley FD, Jansen R, Nham SU, Fenton WA, Rosenberg LE. 1990. Mutation eliminating mitochondrial leader sequence of methylmalonyl-CoA mutase causes muto methylmalonic acidemia. Proc. Natl. Acad. Sci. U. S. A. 87: 3147–50.

Ledley FD, Rosenblatt DS. 1997. Mutations in mut methylmalonic acidemia: clinical and enzymatic correlations. Hum. Mutat. 9: 1–6.

Lek M, Karczewski KJ, Minikel E V., Samocha KE, Banks E, Fennell T, O'Donnell-Luria AH, Ware JS, Hill AJ, Cummings BB, Tukiainen T, Birnbaum DP, et al. 2016. Analysis of protein-coding genetic variation in 60,706 humans. Nature 536: 285–291.

Lempp TJ, Suormala T, Siegenthaler R, Baumgartner ER, Fowler B, Steinmann B, Baumgartner MR. 2007. Mutation and biochemical analysis of 19 probands with mut0 and 13 with mut-methylmalonic aciduria: identification of seven novel mutations. Mol. Genet. Metab. 90: 284–90.

Lerner-Ellis JP, Anastasio N, Liu J, Coelho D, Suormala T, Stucki M, Loewy AD, Gurd S, Grundberg E, Morel CF, Watkins D, Baumgartner MR, et al. 2009. Spectrum of mutations in MMACHC, allelic expression, and evidence for genotype-phenotype correlations. Hum. Mutat. 30: 1072–81.

Lerner-Ellis JP, Dobson CM, Wai T, Watkins D, Tirone JC, Leclerc D, Doré C, Lepage P, Gravel RA, Rosenblatt DS. 2004. Mutations in the MMAA gene in patients with the cblA disorder of vitamin B12 metabolism. Hum. Mutat. 24: 509–16.

Lin X, Lu D, Gao Y, Tao S, Yang X, Feng J, Tan A, Zhang H, Hu Y, Qin X, Kim S-T, Peng T, et al. 2012. Genome-wide association study identifies novel loci associated with serum level of vitamin B12 in Chinese men. Hum. Mol. Genet. 21: 2610–7.

Liu M-Y, Liu T-T, Yang Y-L, Chang Y-C, Fan Y-L, Lee S-F, Teng Y-T, Chiang S-H, Niu D-M, Lin S-J, Chao M-C, Lin S-P, et al. 2012. Mutation Profile of the MUT Gene in Chinese Methylmalonic Aciduria Patients. JIMD Rep. 6: 55–64.

Lofgren M, Banerjee R. 2011. Loss of allostery and coenzyme B12 delivery by a pathogenic mutation in adenosyltransferase. Biochemistry 50: 5790–8.

Lowry OH, Rosebrough NJ, Farr AL, Randall RJ. 1951. Protein measurement with the Folin phenol reagent. J. Biol. Chem. 193: 265–75.

Lubrano R, Elli M, Rossi M, Travasso E, Raggi C, Barsotti P, Carducci C, Berloco P. 2007. Renal transplant in methylmalonic acidemia: could it be the best option? Report on a case at 10 years and review of the literature. Pediatr. Nephrol. 22: 1209–14.

Lyon RC, Johnston SM, Panopoulos A, Alzeer S, McGarvie G, Ellis EM. 2009. Enzymes involved in the metabolism of gamma-hydroxybutyrate in SH-SY5Y cells: identification of an iron-dependent alcohol dehydrogenase ADHFe1. Chem. Biol. Interact. 178: 283–7.

Mah W, Deme JC, Watkins D, Fung S, Janer A, Shoubridge EA, Rosenblatt DS, Coulton JW. 2013. Subcellular location of MMACHC and MMADHC, two human proteins central to intracellular vitamin B12 metabolism. Mol. Genet. Metab. 108: 112–118.

Manoli I, Sloan JL, Venditti CP. 1993. Isolated Methylmalonic Acidemia. University of Washington, Seattle.

Marcadier JL, Smith AM, Pohl D, Schwartzentruber J, Al-Dirbashi OY, FORGE Canada

Consortium, Majewski J, Ferdinandusse S, Wanders RJA, Bulman DE, Boycott KM, Chakraborty P, et al. 2013. Mutations in ALDH6A1 encoding methylmalonate semialdehyde dehydrogenase are associated with dysmyelination and transient methylmalonic aciduria. Orphanet J. Rare Dis. 8: 98.

Marsh EN, McKie N, Davis NK, Leadlay PF. 1989. Cloning and structural characterization of the genes coding for adenosylcobalamin-dependent methylmalonyl-CoA mutase from Propionibacterium shermanii. Biochem. J. 260: 345–52.

Martínez MA, Rincón A, Desviat LR, Merinero B, Ugarte M, Pérez B. 2005. Genetic analysis of three genes causing isolated methylmalonic acidemia: identification of 21 novel allelic variants. Mol. Genet. Metab. 84: 317–25.

Matsui SM, Mahoney MJ, Rosenberg LE. 1983. The natural history of the inherited methylmalonic acidemias. N. Engl. J. Med. 308: 857–61.

Matthews RG, Koutmos M, Datta S. 2008. Cobalamin-dependent and cobamide-dependent methyltransferases. Curr. Opin. Struct. Biol. 18: 658–66.

Mc Guire PJ, Lim-Melia E, Diaz GA, Raymond K, Larkin A, Wasserstein MP, Sansaricq C. 2008. Combined liver-kidney transplant for the management of methylmalonic aciduria: a case report and review of the literature. Mol. Genet. Metab. 93: 22–9.

Meer SB van der, Poggi F, Spada M, Bonnefont JP, Ogier H, Hubert P, Depondt E, Rapoport D, Rabier D, Charpentier C. 1994. Clinical outcome of long-term management of patients with vitamin B12-unresponsive methylmalonic acidemia. J. Pediatr. 125: 903–8.

Michaud J, Praz V, James Faresse N, Jnbaptiste CK, Tyagi S, Schütz F, Herr W. 2013. HCFC1 is a common component of active human CpG-island promoters and coincides with ZNF143, THAP11, YY1, and GABP transcription factor occupancy. Genome Res. 23: 907–16.

Miller C, Wang L, Ostergaard E, Dan P, Saada A. 2011. The interplay between SUCLA2, SUCLG2, and mitochondrial DNA depletion. Biochim. Biophys. Acta 1812: 625–9.

Miousse IR, Watkins D, Coelho D, Rupar T, Crombez EA, Vilain E, Bernstein JA, Cowan T, Lee-Messer C, Enns GM, Fowler B, Rosenblatt DS. 2009. Clinical and molecular heterogeneity in patients with the cblD inborn error of cobalamin metabolism. J. Pediatr. 154: 551–6.

Moestrup SK, Birn H, Fischer PB, Petersen CM, Verroust PJ, Sim RB, Christensen EI, Nexø E. 1996. Megalin-mediated endocytosis of transcobalamin-vitamin-B12 complexes suggests a role of the receptor in vitamin-B12 homeostasis. Proc. Natl. Acad. Sci. U. S. A. 93: 8612–7.

Muro S, Pérez B, Desviat LR, Rodríguez-Pombo P, Pérez-Cerdá C, Clavero S, Ugarte M. 2001. Effect of PCCB gene mutations on the heteromeric and homomeric assembly of propionyl-CoA carboxylase. Mol. Genet. Metab. 74: 476–83.

Nexo E, Hvas A-M, Bleie Ø, Refsum H, Fedosov SN, Vollset SE, Schneede J, Nordrehaug JE, Ueland PM, Nygard OK. 2002. Holo-transcobalamin is an early marker of changes in cobalamin homeostasis. A randomized placebo-controlled study. Clin. Chem. 48: 1768–71.

Nham SU, Wilkemeyer MF, Ledley FD. 1990. Structure of the human methylmalonyl-CoA mutase (MUT) locus. Genomics 8: 710–6.

Nielsen MJ, Rasmussen MR, Andersen CBF, Nexø E, Moestrup SK. 2012. Vitamin B12 transport from food to the body's cells--a sophisticated, multistep pathway. Nat. Rev. Gastroenterol. Hepatol. 9: 345–54.

Niemi A-K, Kim IK, Krueger CE, Cowan TM, Baugh N, Farrell R, Bonham CA, Concepcion W, Esquivel CO, Enns GM. 2015. Treatment of methylmalonic acidemia by liver or combined liver-kidney transplantation. J. Pediatr. 166: 1455–61.e1.

Nizon M, Ottolenghi C, Valayannopoulos V, Arnoux J-B, Barbier V, Habarou F, Desguerre I, Boddaert N, Bonnefont J-P, Acquaviva C, Benoist J-F, Rabier D, et al. 2013. Long-term neurological outcome of a cohort of 80 patients with classical organic acidurias. Orphanet J. Rare Dis. 8: 148.

O'Leary F, Samman S. 2010. Vitamin B12 in health and disease. Nutrients 2: 299–316.

O'Shea CJ, Sloan JL, Wiggs EA, Pao M, Gropman A, Baker EH, Manoli I, Venditti CP, Snow J. 2012. Neurocognitive phenotype of isolated methylmalonic acidemia. Pediatrics 129: e1541-51.

Ogasawara M, Matsubara Y, Mikami H, Narisawa K. 1994. Identification of two novel mutations in the methylmalonyl-CoA mutase gene with decreased levels of mutant mRNA in methylmalonic acidemia. Hum. Mol. Genet. 3: 867–72.

Otzen C, Bardl B, Jacobsen ID, Nett M, Brock M. 2014. Candida albicans utilizes a modified β-oxidation pathway for the degradation of toxic propionyl-CoA. J. Biol. Chem. 289: 8151–69.

Padovani D, Banerjee R. 2006. Assembly and protection of the radical enzyme, methylmalonyl-CoA mutase, by its chaperone. Biochemistry 45: 9300–6.

Padovani D, Labunska T, Palfey BA, Ballou DP, Banerjee R. 2008. Adenosyltransferase tailors and delivers coenzyme B12. Nat. Chem. Biol. 4: 194–6.

Pangilinan F, Mitchell A, VanderMeer J, Molloy AM, Troendle J, Conley M, Kirke PN, Sutton M, Sequeira JM, Quadros E V, Scott JM, Mills JL, et al. 2010. Transcobalamin II receptor polymorphisms are associated with increased risk for neural tube defects. J. Med. Genet. 47: 677–85.

Peters H, Ferdinandusse S, Ruiter JP, Wanders RJA, Boneh A, Pitt J. 2015. Metabolite studies in HIBCH and ECHS1 defects: Implications for screening. Mol. Genet. Metab. 115: 168–73.

Peters H, Nefedov M, Sarsero J, Pitt J, Fowler KJ, Gazeas S, Kahler SG, Ioannou PA. 2003. A knock-out mouse model for methylmalonic aciduria resulting in neonatal lethality. J. Biol. Chem. 278: 52909–13.

Pupavac M, Tian X, Chu J, Wang G, Feng Y, Chen S, Fenter R, Zhang VW, Wang J, Watkins D, Wong L-J, Rosenblatt DS. 2016a. Added value of next generation gene panel analysis for patients with elevated methylmalonic acid and no clinical diagnosis following functional studies of vitamin B12 metabolism. Mol. Genet. Metab. 117: 363–8.

Pupavac M, Watkins D, Petrella F, Fahiminiya S, Janer A, Cheung W, Gingras A-C, Pastinen T, Muenzer J, Majewski J, Shoubridge EA, Rosenblatt DS. 2016b. Inborn Error of Cobalamin Metabolism Associated with the Intracellular Accumulation of Transcobalamin-Bound Cobalamin and Mutations in ZNF143, Which Codes for a Transcriptional Activator. Hum. Mutat. 37: 976–82.

Quadros E V. 2010. Advances in the understanding of cobalamin assimilation and metabolism. Br. J. Haematol. 148: 195–204.

Quadros E V, Lai S-C, Nakayama Y, Sequeira JM, Hannibal L, Wang S, Jacobsen DW, Fedosov S, Wright E, Gallagher RC, Anastasio N, Watkins D, et al. 2010. Positive newborn screen for methylmalonic aciduria identifies the first mutation in TCblR/CD320, the gene for cellular uptake of transcobalamin-bound vitamin B(12). Hum. Mutat. 31: 924–9.

Quadros E V, Sequeira JM. 2013. Cellular uptake of cobalamin: transcobalamin and the TCblR/CD320 receptor. Biochimie 95: 1008–18.

Raff ML, Crane AM, Jansen R, Ledley FD, Rosenblatt DS. 1991. Genetic characterization of a MUT locus mutation discriminating heterogeneity in mut0 and mut- methylmalonic aciduria by interallelic complementation. J. Clin. Invest. 87: 203–7.

Ramirez AM, Demeestere K, Belie N De, Mäntylä T, Levänen E. 2010. Titanium dioxide coated cementitious materials for air purifying purposes: Preparation, characterization and toluene removal potential. Build. Environ. 45: 832–838.

Refsum H, Johnston C, Guttormsen AB, Nexo E. 2006. Holotranscobalamin and Total Transcobalamin in Human Plasma: Determination, Determinants, and Reference Values in Healthy Adults. Clin. Chem. 52: 129–137.

Rosenberg HFW and LE. 1980. Inherited Methylmalonyl CoA Mutase Apoenzyme Deficiency in Human Fibroblasts. 65:.

Rosenblatt DS, Aspler AL, Shevell MI, Pletcher BA, Fenton WA, Seashore MR. 1997. Clinical heterogeneity and prognosis in combined methylmalonic aciduria and homocystinuria (cblC). J. Inherit. Metab. Dis. 20: 528–38.

Rouzier C, Guédard-Méreuze S Le, Fragaki K, Serre V, Miro J, Tuffery-Giraud S, Chaussenot A, Bannwarth S, Caruba C, Ostergaard E, Pellissier J-F, Richelme C, et al. 2010. The severity of phenotype linked to SUCLG1 mutations could be correlated with residual amount of SUCLG1 protein. J. Med. Genet. 47: 670–6.

Rutsch F, Gailus S, Miousse IR, Suormala T, Sagné C, Toliat MR, Nürnberg G, Wittkampf T, Buers I, Sharifi A, Stucki M, Becker C, et al. 2009. Identification of a putative lysosomal cobalamin exporter altered in the cblF defect of vitamin B12 metabolism. Nat. Genet. 41: 234–9.

Schiff M, Ogier de Baulny H, Bard G, Barlogis V, Hamel C, Moat SJ, Odent S, Shortland G, Touati G, Giraudier S. 2010. Should transcobalamin deficiency be treated aggressively? J. Inherit. Metab. Dis. 33: 223–9.

Selhub J. 2008. Public health significance of elevated homocysteine. Food Nutr. Bull. 29: S116-

25.

Shah NP, Beech CM, Sturm AC, Tanner SM. 2011. Investigation of the ABC transporter MRP1 in selected patients with presumed defects in vitamin B12 absorption. Blood 117: 4397–8.

Shigematsu Y, Hirano S, Hata I, Tanaka Y, Sudo M, Sakura N, Tajima T, Yamaguchi S. 2002. Newborn mass screening and selective screening using electrospray tandem mass spectrometry in Japan. J. Chromatogr. B. Analyt. Technol. Biomed. Life Sci. 776: 39–48.

Stabler SP, Allen RH. 2004. Vitamin B12 Deficiency As a Worldwide Problem. Annu. Rev. Nutr 24: 299–326.

Strittmatter L, Li Y, Nakatsuka NJ, Calvo SE, Grabarek Z, Mootha VK. 2014. CLYBL is a polymorphic human enzyme with malate synthase and β-methylmalate synthase activity. Hum. Mol. Genet. 23: 2313–23.

Suormala T, Baumgartner MR, Coelho D, Zavadakova P, Kozich V, Koch HG, Berghaüser M, Wraith JE, Burlina A, Sewell A, Herwig J, Fowler B. 2004. The cblD defect causes either isolated or combined deficiency of methylcobalamin and adenosylcobalamin synthesis. J. Biol. Chem. 279: 42742–9.

Takahashi K, Tavassoli M, Jacobsen DW. 1980. Receptor binding and internalization of immobilized transcobalamin II by mouse leukaemia cells. Nature 288: 713–5.

Takeichi T, Hsu C-K, Yang H-S, Chen H-Y, Wong T-W, Tsai W-L, Chao S-C, Lee JY-Y, Akiyama M, Simpson MA, McGrath JA. 2015. Progressive hyperpigmentation in a Taiwanese child due to an inborn error of vitamin B12 metabolism (cblJ). Br. J. Dermatol. 172: 1111–5.

Tanaka T, Scheet P, Giusti B, Bandinelli S, Piras MG, Usala G, Lai S, Mulas A, Corsi AM, Vestrini A, Sofi F, Gori AM, et al. 2009. Genome-wide association study of vitamin B6, vitamin B12, folate, and homocysteine blood concentrations. Am. J. Hum. Genet. 84: 477–82.

Teplitsky V, Huminer D, Zoldan J, Pitlik S, Shohat M, Mittelman M. 2003. Hereditary partial transcobalamin II deficiency with neurologic, mental and hematologic abnormalities in children and adults. Isr. Med. Assoc. J. 5: 868–72.

Thomä NH, Leadlay PF. 1996. Homology modeling of human methylmalonyl-CoA mutase: a structural basis for point mutations causing methylmalonic aciduria. Protein Sci. 5: 1922–7.

Trakadis YJ, Alfares A, Bodamer OA, Buyukavci M, Christodoulou J, Connor P, Glamuzina E, Gonzalez-Fernandez F, Bibi H, Echenne B, Manoli I, Mitchell J, et al. 2014. Update on transcobalamin deficiency: clinical presentation, treatment and outcome. J. Inherit. Metab. Dis. 37: 461–73.

Valayannopoulos V, Haudry C, Serre V, Barth M, Boddaert N, Arnoux J-B, Cormier-Daire V, Rio M, Rabier D, Vassault A, Munnich A, Bonnefont J-P, et al. 2010. New SUCLG1 patients expanding the phenotypic spectrum of this rare cause of mild methylmalonic aciduria. Mitochondrion 10: 335–41.

Vinckevicius A, Parker JB, Chakravarti D. 2015. Genomic Determinants of

THAP11/ZNF143/HCFC1 Complex Recruitment to Chromatin. Mol. Cell. Biol. 35: 4135–46.

Warren MJ, Raux E, Schubert HL, Escalante-Semerena JC. 2002. The biosynthesis of adenosylcobalamin (vitamin B12). Nat. Prod. Rep. 19: 390–412.

Watanabe F. 2007. Vitamin B12 Sources and Bioavailability. Exp. Biol. Med. 232: 1266–1274.

Watson E, MacNeil LT, Ritter AD, Yilmaz LS, Rosebrock AP, Caudy AA, Walhout AJM. 2014. Interspecies systems biology uncovers metabolites affecting C. elegans gene expression and life history traits. Cell 156: 759–70.

Watson E, Olin-Sandoval V, Hoy MJ, Li C-H, Louisse T, Yao V, Mori A, Holdorf AD, Troyanskaya OG, Ralser M, Walhout AJ. 2016. Metabolic network rewiring of propionate flux compensates vitamin B12 deficiency in C. elegans. Elife 5:.

Willard HF, Rosenberg LE. 1977. Inherited deficiencies of human methylmalonyl CaA mutase activity: reduced affinity of mutant apoenzyme for adenosylcobalamin. Biochem. Biophys. Res. Commun. 78: 927–34.

Wilson A, Leclerc D, Rosenblatt DS, Gravel RA. 1999. Molecular basis for methionine synthase reductase deficiency in patients belonging to the cblE complementation group of disorders in folate/cobalamin metabolism. Hum. Mol. Genet. 8: 2009–16.

Worgan LC, Niles K, Tirone JC, Hofmann A, Verner A, Sammak A, Kucic T, Lepage P, Rosenblatt DS. 2006. Spectrum of mutations in mut methylmalonic acidemia and identification of a common Hispanic mutation and haplotype. Hum. Mutat. 27: 31–43.

Wuerges J, Geremia S, Fedosov SN, Randaccio L. 2007. Vitamin B12 transport proteins: crystallographic analysis of beta-axial ligand substitutions in cobalamin bound to transcobalamin. IUBMB Life 59: 722–9.

Yamanishi M, Vlasie M, Banerjee R. 2005. Adenosyltransferase: an enzyme and an escort for coenzyme B12? Trends Biochem. Sci. 30: 304–308.

Yu H-C, Sloan JL, Scharer G, Brebner A, Quintana AM, Achilly NP, Manoli I, Coughlin CR, Geiger EA, Schneck U, Watkins D, Suormala T, et al. 2013. An X-linked cobalamin disorder caused by mutations in transcriptional coregulator HCFC1. Am. J. Hum. Genet. 93: 506–14.

Zhai XY, Nielsen R, Birn H, Drumm K, Mildenberger S, Freudinger R, Moestrup SK, Verroust PJ, Christensen EI, Gekle M. 2000. Cubilin- and megalin-mediated uptake of albumin in cultured proximal tubule cells of opossum kidney. Kidney Int. 58: 1523–33.

Zhang J, Dobson CM, Wu X, Lerner-Ellis J, Rosenblatt DS, Gravel RA. 2006. Impact of cblB mutations on the function of ATP:cob(I)alamin adenosyltransferase in disorders of vitamin B12 metabolism. Mol. Genet. Metab. 87: 315–22.

APPENDIX A

Published article

Molecular Genetics and Metabolism, 118(4): 264-271 August 2016

Next generation sequencing of patients with *mut* methylmalonic aciduria: validation of somatic cell studies and identification of 16 novel mutations

Jordan Chu[1], Mihaela Pupavac[1], David Watkins[1], Xia Tian[2], Yanming Feng[2], Stella Chen[2], Remington Fenter[2], Victor W Zhang[2], Jing Wang[2], Lee-Jun Wong[2], David S Rosenblatt[1]

Affiliations:

[1]Department of Human Genetics, McGill University, Montreal, Quebec Canada

[2]Department of Molecular Genetics, Baylor College of Medicine, Houston, Texas, United States

Molecular Genetics and Metabolism 118 (2016) 264–271

Contents lists available at ScienceDirect

Molecular Genetics and Metabolism

journal homepage: www.elsevier.com/locate/ymgme

Next generation sequencing of patients with *mut* methylmalonic aciduria: Validation of somatic cell studies and identification of 16 novel mutations

Jordan Chu [a], Mihaela Pupavac [a], David Watkins [a], Xia Tian [b], Yanming Feng [b], Stella Chen [b], Remington Fenter [b], Victor W. Zhang [b], Jing Wang [b], Lee-Jun Wong [b], David S. Rosenblatt [a,*]

[a] Department of Human Genetics, McGill University, Montreal, Quebec, Canada
[b] Department of Molecular Genetics, Baylor College of Medicine, Houston, TX, United States

ARTICLE INFO

Article history:
Received 5 April 2016
Received in revised form 18 May 2016
Accepted 18 May 2016
Available online 20 May 2016

Keywords:
Next generation sequencing
mut
Methylmalonic aciduria
Methylmalonyl-CoA mutase
Vitamin B_{12}

ABSTRACT

Mutations in the *MUT* gene, which encodes the mitochondrial enzyme methylmalonyl-CoA mutase, are responsible for the *mut* form of methylmalonic aciduria (MMA). In this study, a next generation sequencing (NGS) based gene panel was used to analyze 53 patients that had been diagnosed with *mut* MMA by somatic cell complementation analysis. A total of 54 different mutations in *MUT* were identified in 48 patients; 16 novel mutations were identified, including 1 initiation site mutation (c.2T>C [p.M1?]), 1 missense mutation (c.566A>T [p.N189I]), 2 nonsense mutations (c.129G>A [p.W43*] and c.1975C>T [p.Q659*]), 2 mutations affecting splice sites (c.753 + 3A>G and c.754-2A>G), 8 small insertions, deletions, and duplications (c.29dupT [p.L10Ffs*39], c.55dupG [p.V19Gfs*30], c.631_633delGAG [p.E211del], c.795_796insT [p.M266Yfs*7], c.1061delCinsGGA [p.S354Wfs*20], c.1065_1068dupATGG [p.S357Mfs*5], c.1181dupT [p.L394Ffs*30], c.1240delG [p.E414Kfs*17]), a large insertion (c.146_147ins279), and a large deletion involving exon 13. Phenotypic rescue and cDNA analysis were used to confirm that the c.146_147ins279 and c.631_633delGAG mutations were associated with the decreased methylmalonyl-CoA mutase function observed in the patient fibroblasts. In five patients, the NGS panel did not confirm the diagnosis made by complementation analysis. One of these patients was found to carry 2 novel mutations (c.433G > A [p.E145K] and c.511A>C [p.N171H]) in the *SUCLG1* gene.

1. Introduction

Mutations in the *MUT* gene (MIM# 609058) resulting in deficient activity of the mitochondrial enzyme methylmalonyl-CoA mutase (MCM; EC 5.4.99.2) are responsible for the *mut* type of methylmalonic aciduria (*mut* MMA; MIM# 251000). MCM is responsible for the isomerization of L-methylmalonyl-CoA to succinyl-CoA, a key reaction in propionyl-CoA metabolism. Propionyl-CoA is generated during catabolism of certain branched chain amino acids (isoleucine, threonine, and valine), odd-chain fatty acids, methionine and cholesterol. In the presence of functioning MCM, it is converted to succinyl-CoA which can enter the TCA cycle. Isolated MMA is caused by a deficiency in either the MCM apoenzyme or the intracellular synthesis of its cofactor, adenosylcobalamin. The latter is secondary to mutations in the *MMAA* (MIM# 607481), *MMAB* (MIM# 607568), and *MMADHC* (MIM# 611935) genes, which are associated with the *cblA* (MIM# 251100), *cblB* (MIM# 251110), and *cblD*-variant 2 (MIM# 277410) disorders, respectively.

The *mut* form of MMA is a rare, autosomal recessive disorder characterized by elevated levels of methylmalonic acid in blood and urine. Patients often present symptoms of metabolic acidosis, failure to thrive, recurrent vomiting, lethargy, hypotonia, and dehydration in the newborn period [1]. Long-term complications include metabolic stroke affecting primarily the globus pallidus [2] and kidney disease, which may progress to end-stage renal failure requiring transplantation [3]. The disorder is divided into two subtypes; fibroblasts from patients with mut^0 have virtually undetectable levels of MCM activity, whereas mut^- cells have residual MCM activity that can be stimulated by hydroxocobalamin supplementation of culture medium. This has been shown to be caused by reduced affinity of the mutant MCM for adenosylcobalamin [4]. In general, mut^0 patients have earlier onset of symptoms, more severe clinical presentations and higher mortality than mut^- patients [1].

The human *MUT* gene is located on chromosome region 6p12.3 and spans 13 exons encompassing 35 kb of genomic DNA [5]. The *MUT* mRNA transcript encodes 750 amino acids which constitute the

* Corresponding author at: Research Institute of the McGill University Health Centre, Glen Site, 1001 Décarie Boulevard, Block E, M0.2220, Montreal, Quebec, H4A 3J1, Canada.
E-mail address: david.rosenblatt@mgcill.ca (D.S. Rosenblatt).

http://dx.doi.org/10.1016/j.ymgme.2016.05.014
1096-7192/

immature enzyme [6]. Upon entering the mitochondria, the mitochondrial leader sequence (residues 1–32) is cleaved from the immature MCM. MCM structure has been studied in both humans and the bacterium *Propionibacterium freudenreichi ssp shermanii*. The MCM α-subunit of this organism shares 65% of its amino acid sequence with human MCM, and X-ray crystallography has revealed highly conserved domain architecture between the human and bacterial enzymes [7,8]. Human MCM is a homodimer. Each subunit contains an N-terminal extended segment (residues 33–87) which is involved in subunit interaction and precedes the two functional domains of the protein. The N-terminal $(\beta\alpha)_8$ TIM barrel domain (residues 88–422) contains the substrate binding site and the C-terminal $(\beta\alpha)_5$ Rossmann domain (residues 578–750) is the adenosylcobalamin binding domain. The two functional domains are connected by a linker region (residues 423–577). The active MCM holoenzyme contains two adenosylcobalamin molecules, one bound to each subunit.

272 pathogenic mutations in the *MUT* gene have been identified, spanning the entire gene (human gene mutation database HGMD® Professional 2015.4 version as of March 2016). While the majority of the mutations have been reported in only a single family, recurrent mutations exist including c.281G>T (p.G94V), c.1867G>A (p.G623R), and c.2150G>T (p.G717V) in black patients [9], c.349G>T (p.E117*) in Japanese patients [10], c.655A>T (p.N219Y) in Caucasian patients [11], c.671_678dup (p.V227Nfs*2) in Spanish patients [12], c.280G>A (p.G94R), c.322C>T (p.R108C), and c.1022dupA (p.N341Kfs*20) in North American Hispanic patients [9], and c.729_730insT (p.D244Lfs*39), c.1280G>A (p.G427D), and c.1630_1631delGGinsTA (p.G544*) in Asian patients [13].

Somatic cell complementation analysis has been shown to be a reliable method to diagnose *mut* patients and to distinguish the *mut* disorder from the other causes of MMA. In the present study, 53 patients that had been diagnosed as *mut* by somatic cell complementation analysis were studied using a NGS panel targeting *MUT* and 23 other genes associated with cobalamin metabolism.

2. Materials and methods

2.1. Patients

Genomic DNA from 53 patients, diagnosed as *mut* by somatic cell complementation analysis, was extracted using the FlexiGene DNA Kit (Qiagen, Canada). All patient cell lines were referred to the Vitamin B_{12} Clinical Research Laboratory (Department of Medical Genetics, McGill University Health Centre) to rule out an inborn error of cobalamin metabolism. This study was approved by the Research Ethics Boards of the Royal Victoria Hospital, Montreal, Quebec, Canada.

2.2. Biochemical testing and diagnosis

Incorporation of label from [1-^{14}C] propionate into trichloroacetic acid-precipitable macromolecules by cultured patient fibroblasts was used as a measurement of MCM function in intact cells. Fibroblasts from all 53 patients had low baseline levels of [^{14}C] propionate incorporation characteristic of the *mut* phenotype. Additionally, fibroblasts from all 53 patients showed complementation with *cblA* and *cblB* fibroblasts, but not with *mut* fibroblasts. As a result, all 53 patients were diagnosed with *mut* MMA. 44 patients were classified as mut^0 and the remaining 9 as mut^- based upon the responsiveness of cellular MCM activity following the addition of hydroxocobalamin to culture medium. Detailed methods for [^{14}C] propionate incorporation and somatic cell complementation analysis are described in Watkins et al. 2000 [14].

2.3. Gene panel sequencing and data analysis

Genomic DNA from all 53 patients was analyzed with the "Cobalamin Metabolism Panel and Severe MTHFR Deficiency by Massively Parallel Sequencing" test developed at Baylor Miraca Genetics Laboratories. This clinically available NGS-based panel is comprised of *MUT* and 20 other genes associated with cobalamin metabolism or with elevated homocysteine levels. Three additional genes (*AMN*, *CUBN*, and *SLC46A1*) that are not currently included in the clinical test were analyzed in this study. Target sequences of all 24 genes (Table s1) were enriched using custom designed NimbleGen SeqCap probe hybridization (Roche NimbleGen Inc., Madison, WI, USA). The captured sequences include all exons and 20 bp of their flanking intronic regions. DNA template libraries were prepared according to the manufacturer's recommendation. Equal molar ratios of 10 indexed samples were pooled to be loaded onto each lane of the flow cells for sequencing on a HiSeq2000 (Illumina, San Diego, CA, USA) with 100 cycle single-end reads. Raw data in base call files (.bcl format) were converted to qseq files before demultiplexing with CAVAv1.7 software (Illumina Inc., San Diego, CA, USA). Demultiplexed data were processed further by NextGENe software for alignment (SoftGenetics, State College, PA, USA). Average depth of coverage of the NGS analysis was 500–1000×. All exons were covered at sufficient depth. The coverage-based depth analysis using NGS data has been previously reported [15].

2.4. Cellular phenotype rescue studies

Retroviral transduction of the wild-type *MUT* gene into immortalized fibroblasts from patients 7 and 17 was used to confirm that the mutations identified in the *MUT* gene were responsible for the MCM deficiency observed in fibroblasts from these patients. Fibroblasts from a *mut* patient with previously identified mutations, a *cblJ* patient and a healthy individual were used as controls. Wild type *MUT* (pDONR-*MUT* construct from GeneCopoeia, Rockville MD, USA) was cloned into the pBABE retroviral vector using Gateway® Technology (Life Technologies, Burlington, ON). The pBABE-*MUT* retroviral vector was subsequently transiently transfected into a Phoenix amphoteric cell line using the HEPES-buffered saline/$Ca_3(PO_4)_2$ protocol and supernatant was collected (https://web.stanford.edu/group/nolan/_OldWebsite/protocols/pro_helper_dep.html). Patient and control fibroblasts were exposed to the retroviral supernatant in the presence of 4 μg/mL polybrene and incubated in media containing 1 μg/mL puromycin for 4 to 5 days to select for cells that had incorporated the vector. [^{14}C] propionate incorporation was then assessed in the transduced and untransduced cell lines.

2.5. cDNA analysis

Total RNA was extracted from cultured skin fibroblasts from patients 7 and 17 using TRI-Reagent (Sigma-Aldrich, Oakville, ON) according to the manufacturer's protocol. The Superscript III First Strand Synthesis System for RT-PCR (Life Technologies) was used to generate cDNA. PCR amplification of 3 overlapping segments encompassing the entire *MUT* open reading frame was performed using the primers *MUT*-c1F (5′-CGGGGGACGCAGAAGTGCAG-3′), *MUT*-c1R (5′-GGCATCAGCCCTGCTTCCTG-3′), *MUT*-c2F (5′-AACCCTCGACTTCGTGGTGATG-3′), *MUT*-c2R (5′-CAATCTGCCTGTTTCGCACTGAA-3′), *MUT*-c3F (5′-ATGTGCTGCCCGAAGACAAGC-3′), and *MUT*-c3R (5′-CAAGCACCTGAACGGCAGCCT-3′).

3. Results

3.1. Sequencing

Mutations in *MUT* were detected in 48 of 53 (91%) patients. 29 patients had two heterozygous mutations (Table 1), 19 had homozygous mutations (Table 2) and no *MUT* mutations were detected in the remaining 5 (Table 3). A total of 54 different *MUT* gene mutations were identified, including 16 that have not been previously reported in the literature (Fig. 1). The 16 novel mutations include 1 initiation site

Table 1
Patients with heterozygous mutations in *MUT*.

Patient	Ethnicity	Age at biopsy	*mut* class	Prop. Inc	Prop. Inc. + OHCbl	Gene	Mutation	Protein change	Protein domain
1	NR	13 months	mut^-	2.4	4.7	*MUT*	c.1A>G	p.M1?	MLS
						MUT	c.2150G>T	p.G717 V	Cbl
2	Palestinian	1 month	mut^0	1.5	1.5	*MUT*	**c.2T>C**	p.M1?	MLS
						MUT	c.1630_1631delGGinsTA	p.G544*	Link
						CD320	c.658G>A	p.G220R	
3	Irish/Scottish/Polish	19 years	mut^0	1.2	1.2	*MUT*	**c.29dupT**	p.L10Ffs*39	MLS
						MUT	c.1658delT	p.V553Gfs*17	Link
4	Black	2 years	mut^-	2.1	3.1	*MUT*	c.91C>T	p.R31*	MLS
						MUT	c.323G>A	p.R108H	TIM
						TCN2	c.89T>G	p.L30R	
5	Korean	1 year 9 months	mut^0	0.7	0.7	*MUT*	c.91C>T	p.R31*	MLS
						MUT	c.349G>T	p.E117*	TIM
6	White	2 months	mut^-	1.1	3.0	*MUT*	**c.129G>A**	p.W43*	NES
						MUT	c.299A>G	p.Y100C	TIM
7	White	10 days	mut^0	0.4	0.5	*MUT*	**c.146_147ins279**	mRNA not detected	NES
						MUT	c.372_374dupGGA	p.K124_D125insE	TIM
8	White/Mexican	12 days	mut^0	0.8	1.0	*MUT*	c.322C>T	p.R108C	TIM
						MUT	c.654A>C	p.Q218H	TIM
9	Hispanic	46 days	mut^0	0.8	1.2	*MUT*	c.322C>T	p.R108C	TIM
						MUT	c.654A>C	p.Q218H	TIM
10	Northern European/Filipino	6 days	mut^0	1.4	1.5	*MUT*	c.322C>T	p.R108C	TIM
						MUT	c.682C>T	p.R228*	TIM
11	White/Hispanic	6 years	mut^-	2.6	7.0	*MUT*	**c.566A>T**	p.N189I	TIM
						MUT	c.655A>T	p.N219Y	TIM
12	NR	6 years	mut^-	0.5	1.3	*MUT*	c.556A>G	p.M186 V	TIM
						MUT	c.1106G>A	p.R369H	TIM
13	English/Irish	21 years	mut^0	1.5	1.5	*MUT*	c.572C>A	p.A191E	TIM
						MUT	c.682C>T	p.R228*	TIM
14	White/Australian	3 months	mut^0	0.5	0.5	*MUT*	c.572C>A	p.A191E	TIM
						MUT	c.682C>T	p.R228*	TIM
15	White	3 weeks	mut^0	0.5	0.7	*MUT*	c.572C>A	p.A191E	TIM
						MUT	**c.754-2A>G**	Splice	N/A
16	Lao/Thai/Mexican/Portugese	5 days	mut^0	0.6	0.5	*MUT*	c.581C>T	p.P194L	TIM
						MUT	c.682C>T	p.R228*	TIM
17	Black	6 years	mut^0	0.6	0.6	*MUT*	**c.631_633delGAG**	p.E211del	TIM
						MUT	c.682C>T	p.R228*	TIM
						MCEE	c.428G>A	p.R143H	TIM
18	French Canadian	2 months	mut^0	0.7	0.7	*MUT*	c.655A>T	p.N219Y	TIM
						MUT	**c.1240delG**	p.E414Kfs*17	TIM
19	White	1 month	mut^0	1.2	1.0	*MUT*	c.655A>T	p.N219Y	TIM
						MUT	c.1332+1delG	Splice	N/A
20	White	5 days	mut^0	2.1	1.9	*MUT*	c.682C>T	p.R228*	TIM
						MUT	c.1106G>A	p.R369H	TIM
21	White	2 months	mut^0	0.6	0.6	*MUT*	c.682C>T	p.R228*	TIM
						MUT	c.1287C>G	p.Y429*	Link
22	Korean	28 months	mut^0	0.8	0.8	*MUT*	c.682C>T	p.R228*	TIM
						MUT	c.1481T>A	p.L494*	Link
23	French Canadian	3 months	mut^0	1.4	1.3	*MUT*	**c.753+3A>G**	Splice	N/A
						MUT	c.1332+1delG	Splice	N/A
24	NR	NR	mut^0	0.4	0.4	*MUT*	**c.795_796insT**	p.M266Yfs*7	TIM
						MUT	c.1207C>T	p.R403*	TIM
25	White	25 years	mut^0	1.3	1.2	*MUT*	c.935G>T	p.G312 V	TIM
						MUT	c.1909G>A	p.G637R	Cbl
26	Hispanic	7 years	mut^-	4.5	7.2	*MUT*	c.970G>A	p.A324 T	TIM
						MUT	c.1846C>T	p.P649L	Cbl
27	NR	NR	mut^0	0.4	0.4	*MUT*	**c.1061delCinsGGA**	p.S354Wfs*20	TIM
						MUT	**c.1065_1068dupATGG**	p.S357Mfs*5	TIM
28	European	1 year, 1 month	mut^0	1.1	1.2	*MUT*	**c.1181dupT**	p.L394Ffs*30	TIM
						MUT	**c.1975C>T**	p.Q659*	Cbl
29	Chinese	3 months	mut^0	0.3	0.6	*MUT*	c.1280G>A	p.G427D	Link
						MUT	**Exon 13 deletion**		Cbl
						TCN2	c.509G>A	p.R170Q	

Novel mutations are in **bold** font. DNA nucleotide +1 is the A of the ATG translation initiation codon in the reference sequence (*MUT*: NM_000255.3, *TCN2*: NM_000355.3, *CD320*: NM_016579.3, *MCEE*: NM_032601.3). Prop. Inc. = [^{14}C]-labeled propionate incorporation; values are given in nmol/mg protein/18 h (reference [mean ± SD]: 13.1 ± 4.1, n = 217; *mut*: 0.9 ± 0.7, n = 190). Prop. Inc. + OHCb = [^{14}C]-labeled propionate incorporation with hydroxocobalamin supplementation. FS = translational frameshift. NR = no record. N/A = not applicable. MLS = mitochondrial leader sequence. NES = N-terminal extended segment. Link = linker region. TIM = N-terminal $(\beta\alpha)_8$ TIM barrel domain. Cbl = C-terminal $(\beta\alpha)_5$ cobalamin-binding domain. To maintain consistency with our previous study [9], tables are ordered by the location of the mutations, starting with the most 5′ mutation.

mutation, c.2T>C (p.M1?), 1 missense mutation, c.566A>T (p.N189I), 2 nonsense mutations, c.1975C>T (p.Q659*) and c.129G>A (p.W43*), 2 mutations affecting splice-sites, c.753 + 3A>G and c.754 − 2A>G, 8 small insertions, deletions, and duplications, c.795_796insT (p.M266Yfs*7), c.1240delG (p.E414Kfs*17), c.1061delCinsGGA (p.S354Wfs*20), c.631_633delGAG (p.E211del), c.29dupT (p.L10Ffs*39), c.1065_1068dupATGG (p.S357Mfs*5), c.1181dupT (p.L394Ffs*30), and c.55dupG (p.V19Gfs*30), one large insertion (c.146_147ins279), and a large deletion encompassing exon 13 (Fig. 1). Allele-specific PCR (Fig. 2B) was used to validate the presence of the c.146_147ins279 insertion in patient 7. The exon 13 deletion, identified in patient 29, was confirmed by microarray-based comparative genomic hybridization [16].

Table 2
Patients with homozygous mutations in *MUT*.

Patient	Ethnicity	Age at biopsy	*mut* class	Prop. Inc.	Prop. Inc. + OHCbl	Gene	Mutation	Protein change	Protein domain
30	Pakistani	6 weeks	mut^0	0.8	0.7	*MUT*	**c.55dupG**	p.V19Gfs*39	MLS
31[a]	Indian	2 months	mut^-	0.7	1.9	*MUT*	c.257C>T	p.P86L	NES
32[a]	Arab	10 years	mut^0	1.0	1.0	*MUT*	c.278G>A	p.R93H	TIM
33	Hispanic	9 months	mut^0	1.0	1.3	*MUT*	c.322C>T	p.R108C	TIM
34	White/Hispanic	3.5 weeks	mut^0	1.6	1.8	*MUT*	c.322C>T	p.R108C	TIM
35	Hispanic	5 years	mut^0	0.5	0.7	*MUT*	c.322C>T	p.R108C	TIM
36[a]	Hispanic	14 months	mut^0	0.7	0.8	*MUT*	c.406G>T	p.V136F	TIM
37	Moroccan	18 months	mut^0	0.5	0.5	*MUT*	c.683G>A	p.R228Q	TIM
38	German/Polish	9 years	mut^0	0.5	0.5	*MUT*	c.1106G>A	p.R369H	TIM
39[b]	Asian	1 year	mut^0	1.4	1.5	*MUT*	c.1280G>A	p.G427D	Link
40[a]	Middle Eastern	NR	mut^0	1.8	1.6	*MUT*	c.1420C>T	p.R474*	Link
41	Pakistani	6 months	mut^0	0.6	0.6	*MUT*	c.1560G>C	p.K520 N	Link
42	Hmong	1 year, 7 months	mut^-	4.5	9.0	*MUT*	c.1663G>A	p.A555 T	Link
						CUBN	c.3500G>T (het)	p.G1167 V	
						CUBN	c.6211A>G (het)	p.I2071V	
43	Lebanese	20 years	mut^0	1.4	1.1	*MUT*	c.1741C>T	p.R581*	Cbl
44	Arab	13 years	mut^0	0.8	1.1	*MUT*	c.1871A>G	p.Q624R	Cbl
45	NR	NR	mut^0	1.5	1.6	*MUT*	c.1891delG	p.A631Qfs*17	Cbl
46	White	1 year	mut^0	1.0	0.9	*MUT*	c.1962_1963delTC	p.P654Pfs*2	Cbl
47[b]	Barbadian	2 years, 7 months	mut^-	0.4	1.3	*MUT*	c.2150G>T	p.G717 V	Cbl
48	Indian	8 months	mut^0	1.1	1.1	*MUT*	c.2179C>T	p.R727*	Cbl

Novel mutations are in **bold** font. DNA nucleotide +1 is the A of the ATG translation initiation codon in the reference sequence (*MUT*: NM_000255.3, *CUBN*: NM_001081.3). Prop. Inc. = [^{14}C]-labeled propionate incorporation; values are given in nmol/mg protein/18 h (reference [mean ± SD]: 13.1 ± 4.1, n = 217; *mut*: 0.9 ± 0.7, n = 190). Prop. Inc. + OHCbl = [^{14}C]-labeled propionate incorporation with hydroxocobalamin supplementation. FS = translational frameshift. Het = heterozygous. MLS = mitochondrial leader sequence. NR = no record. NES = N-terminal extended segment. Link = linker region. TIM = N-terminal $(\beta\alpha)_8$ TIM barrel domain. Cbl = C-terminal $(\beta\alpha)_5$ cobalamin-binding domain. To maintain consistency with our previous study [9], tables are ordered by the location of the mutations, starting with the most 5′ mutation.

[a] Documented consanguinity.

[b] Reportedly non-consanguineous.

Homozygous mutations in *MUT* were identified in 19 patients (Table 2). In total, 17 different homozygous mutations were seen, including 11 missense mutations, 3 nonsense mutations, and 3 indels leading to a translational frameshift and a subsequent premature termination codon. Among the latter was the novel c.55dupG (p.V19Gfs*39) mutation identified in a Pakistani patient (patient 30) with a mut^0 biochemical phenotype. 4 patients (patients 31, 32, 36, and 40) had documented parental consanguinity. The high incidence of homozygosity is partly explained by the prevalence of ethnicity-specific recurrent mutations. 3 patients (patients 33, 34, and 35) were found to have the common c.322C>T (p.R108C) Hispanic mutation, 1 patient (patient 39) was found to have the common c.1280G>A (p.G427D) Asian mutation, and 1 patient (patient 47) was found to have the common c.2150G>T (p.G717V) black mutation. Since the capture-based NGS panel is able to detect major exonic deletions, homozygosity could be distinguished from autosomal hemizygosity resulting from large deletions in the other allele.

No mutations in the *MUT* gene were identified in 5 (9%) patients. In patients 49 and 50, no mutations in any of the genes targeted by the NGS panel were detected. Patient 51 was found to harbor two novel variants (c.433G>A [p.E145K] and c.511A>C [p.N171H]) in the succinate-CoA ligase, GDP-forming, α-subunit gene (*SUCLG1*; MIM# 611224). A single novel heterozygous c.273A>T (p.R91S) variant in the succinate-CoA ligase, GDP-forming, β-subunit gene (*SUCLG2*; MIM# 603922) was identified in patient 52. Female patient 53 was found to carry a single novel heterozygous c.4475C>T (p.P1492L) variant in the host cell factor C1 gene (*HCFC1*; MIM# 300019).

3.2. Functional analysis

Functional studies were conducted on fibroblasts from patient 7 to further characterize the large insertion and patient 17, who was found to have a heterozygous variant in the methylmalonyl-CoA epimerase gene (*MCEE*; MIM# 608419), to confirm that a *MUT* gene defect was responsible for the MMA phenotype. Retroviral transduction of the wild-type *MUT* gene into fibroblasts from patients 7 and 17 resulted in correction of MCM function to within the reference range (Fig. 2C). Following transduction, propionate incorporation increased 6-fold in fibroblasts from patient 7 and 9-fold in fibroblasts from patient 17. Propionate incorporation of fibroblasts from a previously reported *mut* patient with known pathogenic mutations increased 7-fold following retroviral transduction. RT-PCR amplification of RNA from patient 7 identified loss of heterozygosity for the c.372_374dupGGA mutation and the c.636G>A, c.1595G>A, and c.2011A>G common polymorphisms, which were heterozygous in genomic DNA (Fig. 2D). Loss of heterozygosity for the c.631_633delGAG mutation was seen in cDNA from patient 17.

Table 3
Patients with no mutations in *MUT*.

Patient	Ethnicity	Age at biopsy	Initial diagnosis	Prop. Inc.	Prop. Inc. + OHCbl	Gene	Mutation	Protein change
49	White	13 years	mut^0	3.1	3.4	N/A	N/A	N/A
50	German/Dutch	5 months	mut^0	3.0	2.8	N/A	N/A	N/A
51	Irish/Italian	3 weeks	mut^0	1.0	0.9	*SUCLG1*	**c.433G**>**A** (het)	p.E145K
						SUCLG1	**c.511A**>**C** (het)	p.N171H
52	White	3 months	mut^0	2.0	2.3	*SUCLG2*	**c.273A**>**T** (het)	p.R91S
53 (female)	Arab/Turkish	4 months	mut^0	1.0	0.8	*HCFC1*	**c.4475C**>**T** (het)	p.P1492L

Novel variants are in **bold** font. DNA nucleotide +1 is the A of the ATG translation initiation codon in the reference sequence (*SUCLG1*: NM_003849.3, *SUCLG2*: NM_001177599.1, *HCFC1*: NM_005334.2). Prop. Inc. = [^{14}C]-labeled propionate incorporation; values are given in nmol/mg protein/18 h (reference [mean ± SD]: 13.1 ± 4.1, n = 217; *mut*: 0.9 ± 0.7, n = 190). Prop. Inc. + OHCbl = [^{14}C]-labeled propionate incorporation with hydroxocobalamin supplementation. Het = heterozygous. N/A = not applicable.

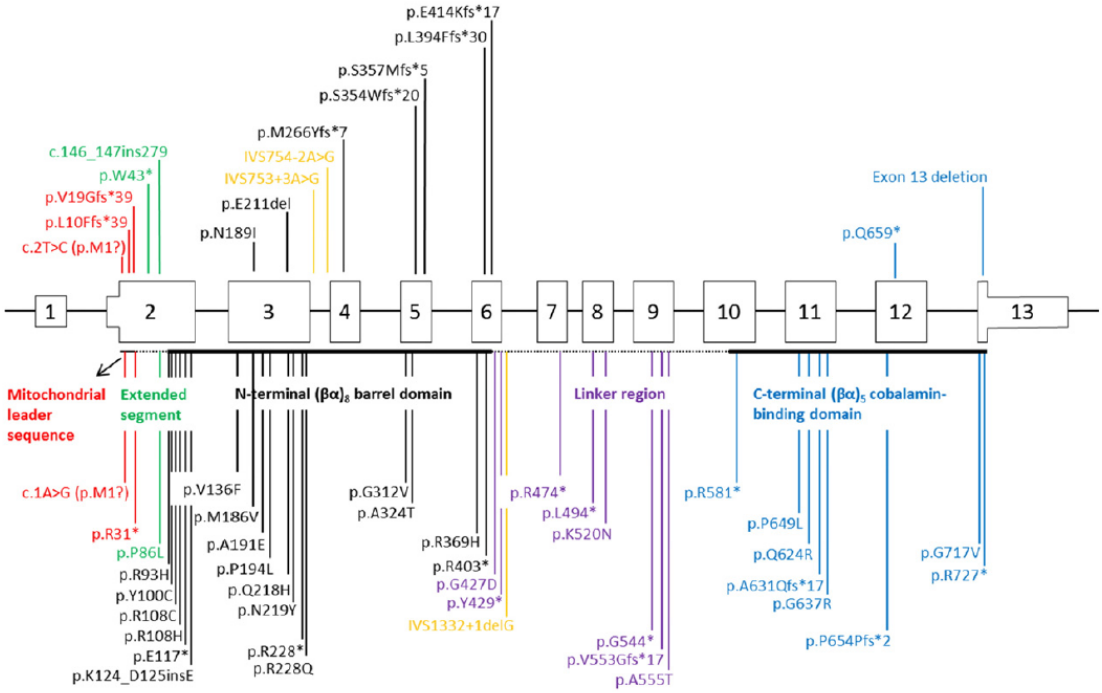

Fig. 1. Distribution of mutations identified in the MUT locus. The distribution of mutations identified in the mitochondrial leader sequence (red), the N-terminal extended segment (green), the N-terminal $(\beta\alpha)_8$ barrel domain (black), splicing junctions (gold), the linker region (purple), and the C-terminal $(\beta\alpha)_5$ cobalamin-binding domain are shown. Novel mutations are shown above the schematic and previously reported mutations are shown below.

4. Discussion

In this study, the molecular basis of *mut* MMA in 53 patients diagnosed by somatic cell complementation analysis was investigated with a NGS based targeted panel. Homozygous or compound heterozygous mutations in the *MUT* gene were detected in 91% (48/53) of patients. Sixteen mutations that have not been previously reported in the literature were identified. None of the novel mutations identified in this study, except for the c.1240delG and c.753 + 3A>G mutations, is documented in the Exome Aggregation Consortium (ExAC) database. The c.1240delG and c.753 + 3A>G mutations each exist as singletons in the database (MAF = 0.000008244).

4.1. Novel initiation site mutation

Patient 2, who was diagnosed as mut^0, was heterozygous for a novel c.2T>C (p.M1?) mutation and a previously reported c.1630_1631delGGinsTA (p.G544*) nonsense mutation. The c.2T>C mutation is predicted to abolish the translation initiation site. The nearest in-frame AUG codon following the c.2T>C mutation is located 78 amino acids downstream of the variant and would produce a protein lacking a mitochondrial targeting sequence, should this second methionine serve as a new initiation codon. Such mutations have been associated with non-functional MCM [17].

4.2. Novel missense mutation

The novel c.566A>T (p.N189I) mutation was identified in patient 11 (mut^-), who also carried the common c.655A>T (p.N219Y) mutation. The c.566A>T mutation, located in the TIM barrel domain, results in the substitution of an isoleucine residue for an asparagine. This change alters the polarity of the original amino acid and is predicted to be pathogenic by three damage-prediction algorithms (SIFT, PolyPhen2, and Mutation Taster).

4.3. Novel nonsense mutations

Two novel nonsense mutations, c.1975C>T (p.Q659*) and c.129G>A (p.W43*), were identified as heterozygous changes. Patient 6 (mut^-) carried the c.129G>A (p.W43*) and c.299A>G (p.Y100C) mutations. The c.129G>A mutation introduces a premature termination codon in the N-terminal extended segment. The c.1975C>T mutation, identified in patient 28, is predicted to produce a truncated polypeptide that lacks the cobalamin binding domain. This patient exhibited a mut^0 biochemical phenotype and was also found to have a novel heterozygous c.1181dupT (p.L394Ffs*30) frameshift mutation, which introduces a premature termination codon 30 amino acids downstream of the mutation.

4.4. Novel consensus splice-site mutations

Novel mutations (c.753 + 3A>G and c.754-2A>G) involving nucleotides in splice-site sequences were identified as heterozygous changes. Both mutations affect the splicing junctions of intron 3 and are associated with a mut^0 phenotype. The c.753 + 3A>G mutation, identified in patient 23, is predicted to eliminate the 5′ donor site of intron 3 and the c.754-2A>G mutation, found in patient 15, is predicted to have the same effect on the 3′ acceptor site (Berkeley Drosophila Genome Project, www.fruitfly.org/seq_tools/splice.html).

4.5. Novel small insertions, deletions, and duplications

Eight of the novel mutations identified in this study were indels consisting of: one single nucleotide insertion, c.795_796insT (p.M266Yfs*7); three small deletions, c.1240delG (p.E414Kfs*17),

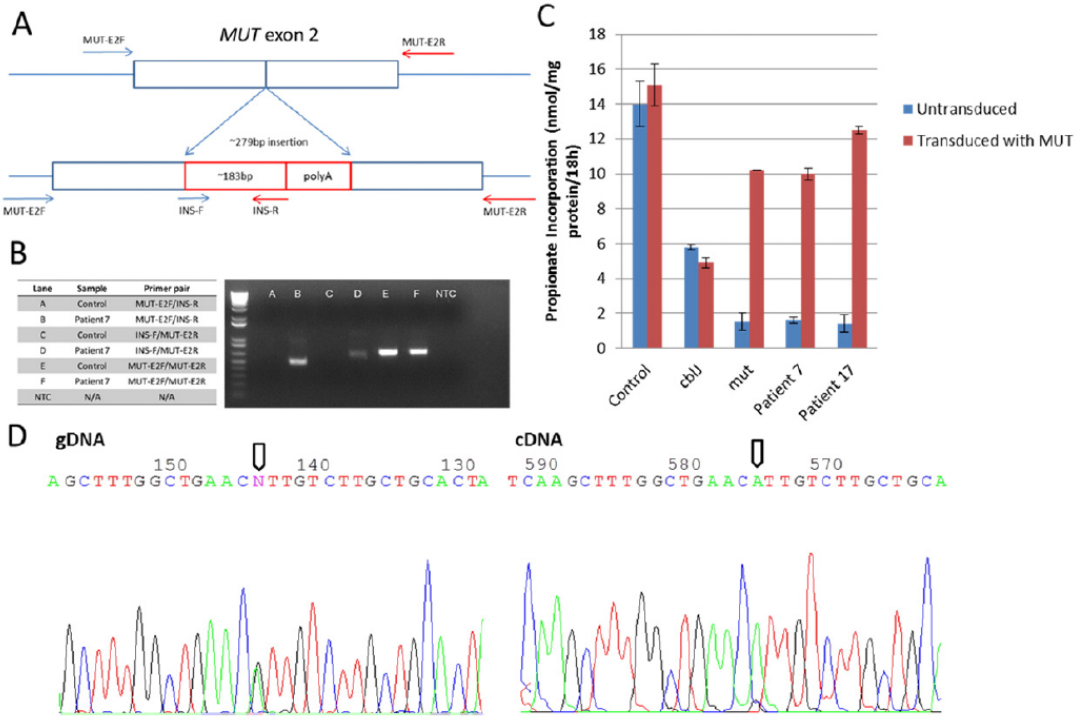

Fig. 2. Analysis of c.146_147ins279 mutation and phenotypic rescue experiments. A: Schematic of the c.146_147ins279 mutation in patient 7. Forward (blue) and reverse (red) primers are shown as arrows. B: PCR amplification of DNA from patient 7 using primers specifically designed to amplify the c.146_147ins279 mutation. NTC = no template control. N/A = not applicable. C: Propionate incorporation in fibroblasts from patients 7 and 17, a *cblJ* patient, a *mut* patient with known mutations, and a healthy individual following transduction with the wild-type *MUT* gene. D: Sanger sequencing of gDNA (left) and cDNA (right) from patient 7 identified loss of heterozygosity for the c.1595G > A common polymorphism (arrows).

c.1061delCinsGGA (p.S354Wfs*20), and c.631_633delGAG (p.E211del); and four small duplications, c.29dupT (p.L10Ffs*39), c.1065_1068dupATGG (p.S357Mfs*5), c.1181dupT (p.L394Ffs*30), and c.55dupG (p.V19Gfs*30). Seven of the eight novel indels result in translational frameshift and a subsequent premature termination codon. The c.1061delCinsGGA and c.1065_1068dupATGG mutations were each identified in patient 27. Since these two mutations are in close proximity with each other, an examination of the NGS reads was able to determine that the mutations are in *trans*. This region of the gene appears to be a mutation hotspot. All of the novel small insertions, deletions, and duplications identified in this study were associated with a mut^0 phenotype.

Patient 17 was heterozygous for the novel c.631_633delGAG (p.E211del) mutation, in combination with the c.682C>T (p.R228*) nonsense mutation. The c.631_633delGAG is an in-frame deletion that eliminates a glutamic acid residue from the TIM barrel domain. RT-PCR of mRNA from patient 17 showed monoallelic expression of the *MUT* allele carrying the deletion with no expression of the allele carrying the c.682C>T mutation, demonstrating that the mutations are in *trans* (data not shown). It is possible that dropout of the allele carrying the c.682C>T nonsense mutation reflects instability of the mutant transcript. Retroviral transduction of the wild-type *MUT* gene into fibroblasts from this patient corrected MCM function to within the reference range (Fig. 2C), suggesting that the c.631_633delGAG mutation in *MUT* is responsible for the patient's clinical presentation. A heterozygous c.428G>A (p.R143H) variant in the *MCEE* gene was also identified in this patient. *MCEE* catalyzes the interconversion of D- to L-methylmalonyl-CoA, the step in propionyl-CoA metabolism preceding that catalyzed by MCM; biallelic mutations in this gene have been seen in patients with mild MMA [18]. Considering the phenotypic rescue findings, this variant is not likely to be associated with the patient's MMA.

4.6. Novel copy number variants (CNVs)

A novel large deletion encompassing exon 13 was identified in patient 29.This patient also carries the heterozygous c.1280G>A (p.G427D) mutation and exhibits a mut^0 biochemical phenotype. NGS analysis of genomic DNA from this patient revealed that the normalized mean coverage of exon 13 was half that of all other exons, indicating a heterozygous deletion (Fig. s1). Microarray-based comparative genomic hybridization confirmed the presence of the deletion. Furthermore, the copy number of a marker located 401 kb downstream of the *MUT* gene did not significantly deviate from the reference sample value, suggesting that the deletion does not extend beyond this marker. The precise breakpoints of the deletion were not determined.

Patient 7 was found to have a novel ~279-bp insertion (c.146_147ins279) in exon 2, the largest identified insertion mutation in the *MUT* gene to date. The insertion was detected in the heterozygous state associated with the c.372_374dupGGA (p.K124_D125insE) mutation. The c.372_374dupGGA duplication has not been previously published as a mutation but has been reported in the ClinVar database as a "likely pathogenic" variant. The ~279-bp insertion consists of a 183-bp segment that aligns to the 3′ UTR of the alpha enolase gene (*ENO1*; MIM#172430) located on chr1:8861004-8861186 plus a ~96-bp polyA repeat (Fig. 2A). PCR amplification of genomic DNA from this patient using primer pairs designed specifically for the insertion-containing *MUT* allele confirmed presence of the insertion (Fig. 2B). PCR amplification of DNA from a control subject yielded no product when using the same primers under the same conditions (Fig. 2B). The allele

carrying the ~279-bp insertion did not amplify from the patient's genomic DNA when using two separate pairs of primers that targeted exon 2. Analysis of cDNA identified loss of heterozygosity of polymorphisms (Fig. 2D) and the c.372_374dupGGA mutation, suggesting monoallelic expression of the allele carrying the duplication and providing evidence that the ~279-bp insertion and the c.372_374dupGGA mutation are *in trans*. It is possible that the presence of the large insertion produces an unstable transcript. Correction of MCM activity following transduction of wild-type *MUT* into fibroblasts from this patient (Fig. 2C) supports the likelihood that the large insertion is associated with the patient's MMA.

4.7. Patients with no mutations in MUT

A review of the somatic cell complementation data for the 5 patients with no identified mutations in *MUT* (patients 49, 50, 51, 52, and 53) found the results to be equivocal (Table s2). In some cases, this likely reflects the relatively high levels of baseline propionate incorporation which can make the test results difficult to interpret. Considering the unconvincing complementation analyses and the lack of identified mutations in *MUT*, and in some cases the presence of variants in other genes known to cause MMA, these patients are likely to have been misdiagnosed as *mut*. It is possible that clinical phenotypes in some of these patients are associated with novel genetic defects.

No potentially causal sequence variants in genes in the panel were identified in patients 49 and 50. Both patients were initially diagnosed as "atypical" mut^0 patients and had clinical presentations not typically associated with *mut* MMA. Patient 49 had moderate mental retardation and a history of nonspecific neonatal problems. Urine organic acids were normal. Patient 50 experienced symptoms of developmental delay, failure to thrive, abnormal posturing, and crystals in urine. Elevated fat metabolites were detected in urine, which is not typical for patients with *mut* MMA. It is unlikely that these patients have *mut* MMA and, as sequencing analysis was negative for all of the genes examined, no alternative diagnosis is suggested.

Two novel heterozygous variants (c.433G>A [p.E145K] and c.511A>C [p.N171H]) in *SUCLG1*, both predicted to be damaging by prediction algorithms, were identified in patient 51. Mutations in *SUCLG1* cause mitochondrial DNA depletion syndrome 9 (MIM# 245400), which is characterized by mild MMA and can produce results that are difficult to interpret when complemented with fibroblasts from patients with inborn errors affecting MCM function (Table s2). The patient presented with severe metabolic acidosis, mildly elevated levels of methylmalonic acid, elevated levels of lactic acid and sensorineural hearing loss, consistent with the clinical presentations of previously published patients with *SUCLG1* deficiency [19,20]. The *SUCLG1* mutations identified in this patient are likely causative of the patient's phenotype.

A single heterozygous variant in *SUCLG2* was identified in patient 52. This patient was reported to have elevated methylmalonic acid and SIDS. Post-mortem blood spot analysis revealed a substantial elevation in C3 carnitine levels. As mutations in *SUCLG2* have not been previously associated with disease, the relevance of this variant to the patient's phenotype is unknown. A heterozygous variant in *HCFC1* was detected in female patient 53. Mutations affecting the kelch domain of HCFC1 have been associated with the X-linked *cblX* inborn error of cobalamin metabolism (MIM# 309541) [21]. The variant in this patient lies outside the kelch domain. Clinical presentation did not include metabolic acidosis or homocystinuria and fibroblast studies showed normal synthesis of both adenosylcobalamin and methylcobalamin, suggesting that the patient does not have the *cblX* disease. It is therefore unlikely that the identified variant is related to the patient's MMA.

4.8. Spectrum of MUT gene mutations

Twenty-nine patients were found to carry two heterozygous mutations in *MUT* and 19 carried homozygous mutations. Due to the inaccessibility of parental DNA, the phase of heterozygous mutations was not determined for the majority of patients. However, given that the somatic cell findings and clinical presentations of these patients were consistent with the *mut* phenotype, it is expected that the identified mutations are in *trans*. 54 different mutations in *MUT* were identified spanning the entire *MUT* gene (Fig. 1). At least one mutation was identified in all coding exons (exons 2–13). The distribution of *MUT* mutations identified by this study favored the N-terminal TIM barrel domain, with nearly half (25/54) of the mutations located in this region. Ten out of 54 (19%) of the identified mutations reside in the C-terminal cobalamin-binding Rossman domain. This uneven distribution may be explained by the low number of mut^- patients studied as the mut^- phenotype is known to be associated with mutations in the Rossman domain. Nine percent (5/54) of the identified *MUT* gene mutations affect the mitochondrial leader sequence, 6% (3/54) affect the N-terminal extended segment and 15% (8/54) are located in the linker region. The distribution of mutations identified by this study is consistent with the distribution of all previously reported mutations in *MUT*. No mutations were detected in exon 1, which is entirely untranslated and consists of only 36 nucleotides. Mutations in exon 1 of *MUT* have not been previously reported in the literature. Further research is needed to elucidate the physiological role of this exon, which is conserved in species ranging from bacteria to humans.

The 16 novel mutations in *MUT* identified in this study add to the spectrum of mutations that are associated with *mut* MMA (Table s3). Most interesting was the identification of a complex ~279-bp insertion in patient 7. Identification of this insertion highlights the unique utility of NGS panel testing in simultaneous detection of both single nucleotide variants (SNVs) and CNVs [15], as standard PCR analysis of both genomic DNA and cDNA did not detect the insertion. The panel was able to identify both insertion and deletion CNVs, as demonstrated by the molecular findings of patients 7 and 29. Previously, we analyzed the *MUT* gene by Sanger sequencing in 160 patients diagnosed with *mut* MMA by complementation analysis [9]. Mutations in *MUT* were identified in 156/160 patients (97.5%). In 4 patients no mutations were found. One of these patients was subsequently re-diagnosed with the *cblA* disorder and the remaining 3 patients were included in this study. No mutations in *MUT* were found in these patients following NGS analysis.

4.9. Genotype-phenotype associations

14 of the 16 novel mutations were associated with a mut^0 phenotype. The novel c.566A>T (p.N189I) mutation was found in the heterozygous state in a mut^- patient (patient 11) who also carried a heterozygous recurrent mutation (c.655A>T [p.N219Y]). The latter has been previously shown to be associated with a mut^0 phenotype by transfection studies [11]. These findings support the suggestion that mut^- mutations have a dominant effect on the biochemical phenotype of the cell [22]. The novel c.129G>A (p.W43*) mutation was found in a mut^- patient as a heterozygous change in association with the c.299A>G (p.Y100C) mutation. The c.299A>G mutation has been previously shown to be associated with a mut^- phenotype [23]. It is therefore not possible, in this instance, to determine whether the c.129G > A mutation is associated with a mut^0 or mut^- phenotype.

4.10. Comparison of somatic cell complementation and NGS panel

In this study, 53 patients that had been diagnosed with *mut* MMA by somatic cell complementation analysis were studied with a NGS based panel. *MUT* gene mutations were identified in all patients who had unequivocal complementation findings. The panel also had value in

re-evaluating the diagnosis in 5 patients in whom the complementation analysis was not clear.

Overall, the NGS panel displayed 100% sensitivity in detecting *MUT* gene mutations in patients with *mut* MMA. We have recently shown that the panel has exceptional specificity for detecting mutations in *MUT* as well [24]. In 131 patients with MMA and no diagnosis after somatic cell studies, the panel identified two *MUT* gene variants in only one patient. One variant was likely benign and the second was of uncertain significance.

Sequencing and somatic cell studies are two distinct, clinically available tests that are commonly used to diagnose patients with elevated methylmalonic acid levels. Considering the outstanding sensitivity of *MUT* gene mutation detection displayed in this study and the extensive spectrum of known pathogenic mutations, NGS based gene panel analysis is a reasonable first-line approach in diagnosing the *mut* disorder in patients with reported MMA. However, given that a large proportion of mutations in *MUT* are detected only in a single family, it is expected that variants of unknown significance and novel mutations will frequently be identified. Somatic cell studies, including complementation analysis, are valuable in determining the functional significance of these occurrences. Thus, an approach whereby somatic cell studies follow molecular analysis may be an effective diagnostic strategy for *mut* MMA.

Addendum

Since acceptance of this manuscript, 41 novel *MUT* mutations have been identified in Forny et al., 2016 [25]. Six of the 16 novel mutations identified in this study overlap (c.2T>C, c.55dupG, c.129G>A, c.566A>T, c.1181dupT, and c.1975C>T). These mutations and 3 mutations in ClinVar bring the total number of identified mutations in *MUT* to 326.

Acknowledgements

The authors would like to thank all patients and their families for their contributions to the study. We also thank the physicians who referred patient samples and provided clinical information. This work was supported by the Canadian Institutes of Health Research (CIHR-M08-15078).

Appendix A. Supplementary data

Supplementary data to this article can be found online at http://dx.doi.org/10.1016/j.ymgme.2016.05.014.

References

[1] F. Hörster, M.R. Baumgartner, C. Viardot, T. Suormala, P. Burgard, B. Fowler, et al., Long-term outcome in methylmalonic acidurias is influenced by the underlying defect (mut^0, mut$^-$, cblA, cblB), Pediatr. Res. 62 (2007) 225–230, http://dx.doi.org/10.1203/PDR.0b013e3180a0325f.

[2] E.H. Baker, J.L. Sloan, N.S. Hauser, A.L. Gropman, D.R. Adams, C. Toro, et al., MRI characteristics of globus pallidus infarcts in isolated methylmalonic acidemia, AJNR Am. J. Neuroradiol. 36 (2015) 194–201, http://dx.doi.org/10.3174/ajnr.A4087.

[3] M.A. Cosson, J.F. Benoist, G. Touati, M. Déchaux, N. Royer, L. Grandin, et al., Long-term outcome in methylmalonic aciduria: a series of 30 French patients, Mol. Genet. Metab. 97 (2009) 172–178, http://dx.doi.org/10.1016/j.ymgme.2009.03.006.

[4] H.F. Willard, L.E. Rosenberg, Inherited deficiencies of human methylmalonyl CaA mutase activity: reduced affinity of mutant apoenzyme for adenosylcobalamin, Biochem. Biophys. Res. Commun. 78 (1977) 927–934 (http://www.ncbi.nlm.nih.gov/pubmed/20894 accessed February 2, 2016).

[5] S.U. Nham, M.F. Wilkemeyer, F.D. Ledley, Structure of the human methylmalonyl-CoA mutase (MUT) locus, Genomics 8 (1990) 710–716 (http://www.ncbi.nlm.nih.gov/pubmed/1980486 accessed February 2, 2016).

[6] R. Jansen, F. Kalousek, W.A. Fenton, L.E. Rosenberg, F.D. Ledley, Cloning of full-length methylmalonyl-CoA mutase from a cDNA library using the polymerase chain reaction, Genomics 4 (1989) 198–205 (http://www.ncbi.nlm.nih.gov/pubmed/2567699 accessed February 2, 2016).

[7] N.H. Thomä, P.F. Leadlay, Homology modeling of human methylmalonyl-CoA mutase: a structural basis for point mutations causing methylmalonic aciduria, Protein Sci. 5 (1996) 1922–1927, http://dx.doi.org/10.1002/pro.5560050919.

[8] D.S. Froese, G. Kochan, J.R.C. Muniz, X. Wu, C. Gileadi, E. Ugochukwu, et al., Structures of the human GTPase MMAA and vitamin B12-dependent methylmalonyl-CoA mutase and insight into their complex formation, J. Biol. Chem. 285 (2010) 38204–38213, http://dx.doi.org/10.1074/jbc.M110.177717.

[9] L.C. Worgan, K. Niles, J.C. Tirone, A. Hofmann, A. Verner, A. Sammak, et al., Spectrum of mutations in mut methylmalonic acidemia and identification of a common Hispanic mutation and haplotype, Hum. Mutat. 27 (2006) 31–43, http://dx.doi.org/10.1002/humu.20258.

[10] M. Ogasawara, Y. Matsubara, H. Mikami, K. Narisawa, Identification of two novel mutations in the methylmalonyl-CoA mutase gene with decreased levels of mutant mRNA in methylmalonic acidemia, Hum. Mol. Genet. 3 (1994) 867–872 (http://www.ncbi.nlm.nih.gov/pubmed/7951229 accessed February 3, 2016).

[11] C. Acquaviva, J.F. Benoist, I. Callebaut, N. Guffon, H. Ogier de Baulny, G. Touati, et al., N219Y, a new frequent mutation among mut^0 forms of methylmalonic acidemia in Caucasian patients, Eur. J. Hum. Genet. 9 (2001) 577–582, http://dx.doi.org/10.1038/sj.ejhg.5200675.

[12] M.A. Martínez, A. Rincón, L.R. Desviat, B. Merinero, M. Ugarte, B. Pérez, Genetic analysis of three genes causing isolated methylmalonic acidemia: identification of 21 novel allelic variants, Mol. Genet. Metab. 84 (2005) 317–325, http://dx.doi.org/10.1016/j.ymgme.2004.11.011.

[13] M.-Y. Liu, T.-T. Liu, Y.-L. Yang, Y.-C. Chang, Y.-L. Fan, S.-F. Lee, et al., Mutation Profile of the MUT Gene in Chinese Methylmalonic Aciduria Patients., JIMD Rep. 62012 55–64, http://dx.doi.org/10.1007/8904_2011_117.

[14] D. Watkins, N. Matiaszuk, D.S. Rosenblatt, Complementation studies in the cblA class of inborn error of cobalamin metabolism: evidence for interallelic complementation and for a new complementation class (cblH), J. Med. Genet. 37 (2000) 510–513 (http://www.pubmedcentral.nih.gov/articlerender.fcgi?artid=1734625&tool=pmcentrez&rendertype=abstract accessed February 3, 2016).

[15] Y. Feng, D. Chen, G.-L. Wang, V.W. Zhang, L.-J.C. Wong, Improved molecular diagnosis by the detection of exonic deletions with target gene capture and deep sequencing, Genet. Med. 17 (2015) 99–107, http://dx.doi.org/10.1038/gim.2014.80.

[16] J. Wang, H. Zhan, F.-Y. Li, A.N. Pursley, E.S. Schmitt, L.-J. Wong, Targeted array CGH as a valuable molecular diagnostic approach: experience in the diagnosis of mitochondrial and metabolic disorders, Mol. Genet. Metab. 106 (2012) 221–230, http://dx.doi.org/10.1016/j.ymgme.2012.03.005.

[17] F.D. Ledley, R. Jansen, S.U. Nham, W.A. Fenton, L.E. Rosenberg, Mutation eliminating mitochondrial leader sequence of methylmalonyl-CoA mutase causes muto methylmalonic acidemia, Proc. Natl. Acad. Sci. U. S. A. 87 (1990) 3147–3150 (http://www.pubmedcentral.nih.gov/articlerender.fcgi?artid=53851&tool=pmcentrez&rendertype=abstract accessed March 2, 2016).

[18] A.B. Gradinger, C. Bélair, L.C. Worgan, C.D. Li, J. Lavallée, D. Roquis, et al., Atypical methylmalonic aciduria: frequency of mutations in the methylmalonyl CoA epimerase gene (MCEE), Hum. Mutat. 28 (2007) 1045, http://dx.doi.org/10.1002/humu.9507.

[19] E. Ostergaard, E. Christensen, E. Kristensen, B. Mogensen, M. Duno, E.A. Shoubridge, et al., Deficiency of the alpha subunit of succinate-coenzyme A ligase causes fatal infantile lactic acidosis with mitochondrial DNA depletion, Am. J. Hum. Genet. 81 (2007) 383–387, http://dx.doi.org/10.1086/519222.

[20] J.L.K. Van Hove, M.S. Saenz, J.A. Thomas, R.C. Gallagher, M.A. Lovell, L.Z. Fenton, et al., Succinyl-CoA ligase deficiency: a mitochondrial hepatoencephalomyopathy, Pediatr. Res. 68 (2010) 159–164, http://dx.doi.org/10.1203/PDR.0b013e3181e5c3a4.

[21] H.-C. Yu, J.L. Sloan, G. Scharer, A. Brebner, A.M. Quintana, N.P. Achilly, et al., An X-linked cobalamin disorder caused by mutations in transcriptional coregulator HCFC1, Am. J. Hum. Genet. 93 (2013) 506–514, http://dx.doi.org/10.1016/j.ajhg.2013.07.022.

[22] C. Acquaviva, J.-F. Benoist, S. Pereira, I. Callebaut, T. Koskas, D. Porquet, et al., Molecular basis of methylmalonyl-CoA mutase apoenzyme defect in 40 European patients affected by mut(o) and mut-forms of methylmalonic acidemia: identification of 29 novel mutations in the MUT gene, Hum. Mutat. 25 (2005) 167–176, http://dx.doi.org/10.1002/humu.20128.

[23] T.J. Lempp, T. Suormala, R. Siegenthaler, E.R. Baumgartner, B. Fowler, B. Steinmann, et al., Mutation and biochemical analysis of 19 probands with mut^0 and 13 with mut$^-$ methylmalonic aciduria: identification of seven novel mutations, Mol. Genet. Metab. 90 (2007) 284–290, http://dx.doi.org/10.1016/j.ymgme.2006.10.002.

[24] M. Pupavac, X. Tian, J. Chu, G. Wang, Y. Feng, S. Chen, et al., Added value of next generation gene panel analysis for patients with elevated methylmalonic acid and no clinical diagnosis following functional studies of vitamin B12 metabolism, Mol. Genet. Metab. 117 (2016) 363–368, http://dx.doi.org/10.1016/j.ymgme.2016.01.008.

[25] P. Forny, A.-S. Schnellmann, C. Buerer, S. Lutz, B. Fowler, D.S. Froese, et al., Molecular genetic characterization of 151 mut-type methylmalonic aciduria patients and identification of 41 novel mutations in MUT, Hum. Mutat. (2016) http://dx.doi.org/10.1002/humu.23013.

Contribution of Authors

Chu J: Writing, mutation analysis, cell culture, DNA extraction, RNA extraction, PCR, RT-PCR, propionate incorporation, correction studies

Pupavac M: mutation analysis, DNA extraction, cloning

Watkins D: editing

Tian X, Feng Y, Chen S, Fenter R, Zhang VW, Wang J, Wong LJ: NGS analysis

Rosenblatt DS: principal investigator